



Universidade de Évora - Escola de Ciências e Tecnologia

Mestrado Integrado em Medicina Veterinária

Dissertação

**Targeted gene editing in *Neospora caninum* using
CRISPR/Cas9**

Maria Cristina Ferreira de Sousa

Orientador(es) | Helder Carola Cortes
Andrew Hemphill

Évora 2021





Universidade de Évora - Escola de Ciências e Tecnologia

Mestrado Integrado em Medicina Veterinária

Dissertação

**Targeted gene editing in *Neospora caninum* using
CRISPR/Cas9**

Maria Cristina Ferreira de Sousa

Orientador(es) | Helder Carola Cortes
Andrew Hemphill

Évora 2021



A dissertação foi objeto de apreciação e discussão pública pelo seguinte júri nomeado pelo Diretor da Escola de Ciências e Tecnologia:

Presidente | Margarida Simões (Universidade de Évora)

Vogais | Helder Carola Cortes (Universidade de Évora) (Orientador)
Liliana Machado Ribeiro da Silva (Universitaet Giessen) (Arguente)

Acknowledgments

I would like to express my deepest gratitude and appreciation to those who were part of this accomplishment. Thank you:

To Prof. Helder, my supervisor, for challenging me with this wonderful internship, and for all the advice given in the writing of this thesis.

To Prof. Andrew, my supervisor, for welcoming me with friendship and kindness and providing me an amazing experience for learning and improving during the internship, and for his valuable help in the development of this work.

To all the team of the Parasitology department at the University of Bern, especially to Naja and Vreni for teaching me and accompanying me during the beginning and ending of my journey respectively.

To my friends Patrícia, Isabel and Pina, for the support and friendship over five incredible college years, and which with whom it is a pleasure to become a veterinarian.

To Inês, for growing and thriving with me, and being my best friend. Thank you for all the adventures along the journey. O resto é paisagem.

To all the friends I met in Tscharnergut that made Bern feel like home for six months and made me very happy, every day. Thank you Jatin, Bia, Perwin, Raphy, Enrico, Jamal, and Marius.

To my parents, for everything that they have taught me without realizing it. It is a pleasure to become your colleague.

Targeted gene editing in *Neospora caninum* using CRISPR/Cas9

Abstract

Apicomplexa are amongst the most prevalent and morbidity-causing pathogen agents worldwide, representing serious challenges to animal and public health. *Neospora caninum* and *Besnoitia besnoiti* are causing agents of neosporosis and besnoitiosis. Until today, there are no effective treatment options against these parasitosis. Therefore, it is urgent to invest in the development of methods for diagnosis, prevention, control, and treatment against these protozoan pathogens.

The present dissertation is divided in two parts. The first part summarizes three assays on drug development, testing the *in vitro* efficacy of selected endochin-like quinolones (ELQs) against *B. besnoiti* and *N. caninum* tachyzoites on a 3-day proliferation inhibition assay, long-term experiment with the duration of 20 days, and ultrastructural changes induced by ELQs were evaluated in *N. caninum*. The second part of the report consists of a monography reviewing the CRISPR/Cas9 gene editing technology applied to a targeted *sag1* gene knock-out in *N. caninum* assay.

Keywords: CRISPR/Cas9; *Benoitia besnoiti*; *Neospora caninum*; endochin-like-quinolones; electron microscopy

Edição genómica em *Neospora caninum* usando CRISPR/Cas9

Resumo

Os parasitas do filo Apicomplexa estão entre os agentes patogénicos causadores de morbilidade mais prevalentes no mundo, representando sérios desafios para a saúde pública e animal. *Neospora caninum* e *Besnoitia besnoiti* são agentes etiológicos da neosporose e besnoitose. Até hoje, não existem opções de tratamento e prevenção disponíveis para estas parasitoses, tornando-se urgente investir no desenvolvimento de métodos para o diagnóstico, prevenção e tratamento destes protozoários.

A presente dissertação está dividido em duas partes. A primeira parte relativa a três ensaios focados no desenvolvimento de medicamentos, testa a eficácia *in vitro* de endoquinas tipo quinolonas contra taquizoítos de *B. besnoiti* e *N. caninum* num ensaio inibição-proliferação de três dias, numa experiência de tratamento de longo-curso e através de microscopia de transmissão de electrões para avaliar alterações ultraestruturais. A segunda parte consiste numa monografia sobre a tecnologia de edição genómica CRISPR/Cas9 aplicada ao knock-out do gene *sag1* em *N. caninum*.

Palavras-chave: CRISPR/Cas9; *B. besnoiti*; *N. caninum*; endoquinas tipo quinolonas; microscopia de electrões

Index

Acknowledgments	I
Abstract.....	II
Resumo	III
Index	IV
Index of tables	VIII
Index of figures.....	IX
Abbreviation List.....	XIV
Preamble	1
I. Introduction	2
1. Apicomplexan parasites.....	2
1.1. Morphology of apicomplexan parasites.....	2
1.2. The lytic cycle.....	3
2. <i>Neospora caninum</i>	4
2.1. <i>N. caninum</i> life cycle	4
2.2. <i>N. caninum</i> epidemiology	6
2.3. Bovine neosporosis	7
2.4. Treatment	7
2.5. Prevention	8
3. <i>Besnoitia besnoiti</i>	9
3.1. <i>B. besnoiti</i> life cycle.....	9
3.2. <i>B. besnoiti</i> epidemiology	10
3.3. Bovine besnoitiosis	11
3.3.1. Acute phase of disease	11
3.3.2. Chronic phase of disease	12
3.4. Treatment	13
3.5. Prevention of <i>B. Besnoiti</i> infection	13
II. Internship Report.....	15
1. Research for novel drugs.....	15
1.1. Endochin-like quinolones	16

1.2. The mitochondrion of apicomplexan parasites as a drug target	17
1.2.1. The cytochrome bc1 complex	18
1.2.2. Q-cycle of mitochondria.....	19
1.2.3. Mechanism of action of endochin-like quinolones	21
2. Assessment of half-maximal inhibitory concentration (IC ₅₀ assay).....	21
2.1. Methods for IC ₅₀ Assay	24
2.1.1. Cell culture of human foreskin fibroblasts.....	24
2.1.2. Counting human foreskin fibroblasts	25
2.1.3. Addition of the ELQs on test.....	26
2.1.4. Controls for the <i>in vitro</i> trials.....	27
2.1.5. Infection of the seeded cells with <i>B. besnoiti</i>	27
2.1.6. DNA extraction from the cells in each well of the <i>in vitro</i> trial.....	28
2.1.7. Real-Time PCR for quantification of <i>B. besnoiti</i>	30
2.1.8. Real-Time PCR setup.....	32
2.2. Results.....	33
2.3. Discussion and Conclusion	35
3. Long Treatment Assay	39
3.1. Methods for Long Treatment Assay	40
3.1.1. Culture of HFF cells.....	40
3.1.2. Infection of the seeded cells	40
3.1.3. Positive controls	40
3.1.4. Addition of the compound ELQ-121	40
3.1.5. Renewing the treatment with the compound ELQ-121.....	41
3.1.6. Treatment with increased concentrations of ELQ-121	41
3.1.7. Splitting confluent cells.....	43
3.2. Results of long-term treatment with ELQ-121	43
3.2.1. Day-0 (11.09.18)	43
3.2.2. Day-3 (14.09.18)	44
3.2.3. Day-6 (17.09.18)	45
3.2.4. Day-9 (20.09.18)	46
3.2.5. Day-12 (23.09.18)	46

3.2.6. Day-15 (26.09.18)	47
3.2.7. Day-20 (01.10.18)	48
3.3. Discussion and Conclusion	51
4. Transmission Electron Microscopy Assay	54
4.1. Methods for TEM Assay	55
4.1.1. Embedding samples	55
4.1.2. Sectioning of embedded samples in EPON	56
4.1.3. Stretching the samples on the surface of the water	57
4.1.4. Collection of samples to the grids	57
4.1.5. Staining of samples for TEM	58
4.2. Results of TEM evaluation	58
4.2.1. <i>N. caninum</i> tachyzoites treated with ELQ-316 after 12h	59
4.2.2. <i>N. caninum</i> tachyzoites treated with ELQ-316 after 24h	61
4.2.3. <i>N. caninum</i> tachyzoites treated with ELQ-316 after 48h	62
4.3. Discussion and Conclusion	64
III. Monography: “ <i>sag1</i> gene knock-out on <i>Neospora caninum</i> using CRISPR/Cas9” ..	67
1. Introduction	67
1.1. Identification of targets	67
1.1.1. The CRISPR/Cas system	68
1.2. Operation and classification of CRISPR systems	69
1.3. Type II Crispr/Cas9 System	70
1.4. Gene editing on apicomplexan parasites of veterinary importance	72
2. <i>Sag1</i> gene knock-out in <i>Neospora caninum</i> using CRISPR/Cas9	74
2.1. <i>Sag1</i> as the targeted gene	76
2.2. Construction of the plasmid with repair template	76
2.3. Transfection by electroporation	78
2.4. Pyrimethamine selection	79
2.5. Identification of positive clones	79
2.6. PCR confirmation of the knock-out	80
2.6.1. PCR with primers targeting <i>sag1</i>	80
2.6.2. PCR with primers targeting <i>dhfr</i> gene	83

2.6.3. Selection of possible knock-out clones	84
2.6.4. Confirmation of <i>dhfr</i> gene's position on clone genome.....	85
2.6.5. Repetition of PCR with primers targeting <i>sagI</i>	87
3. Discussion	89
4. Future prospects	91
5. Ethical issues associated with genome editing.....	91
6. Conclusion.....	94
7. Final considerations.....	95
IV. References	96
Appendix	i
Materials	i
1. Materials for IC ₅₀ Assay	i
2. Materials for Long Treatment Assay	vi
3. Materials for Electron Microscopy Assay	ix
4. Materials for <i>sagI</i> knock-out using CRISPR/Cas9 Assay.....	xi

Index of tables

Table 1. Relative growth of <i>B. besnoiti</i> tachyzoites treated with ELQs at 0.01, 0.1 and 1 μ M	22
Table 2. Assessed values for cell culture.....	24
Table 3. Master Mix composition.....	32
Table 4. IC ₅₀ values for ELQ-316 and ELQ-334 against <i>B. besnoiti</i> and <i>N. caninum</i>	35
Table 5. Master Mix composition.....	80
Table 6. Summary of PCR results of 70 clones.....	84
Table 7. PCR primers for knock-out confirmation.....	85
Table 8. PCR results of possible knock-out clones	86

Index of figures

Figure 1. The morphology of apicomplexan parasites (Morrissette and Sibley, 2002).	2
Figure 2. Schematic illustration of <i>N. caninum</i> life cycle.	5
Figure 3. Schematic illustration of <i>B. besnoiti</i> life cycle.....	10
Figure 4. Chemical structures of endochin (a) (Doggett et al.,2012) and general 4-(1H)-quinolones with numbered chemical positions (b) (Stickles et al., 2015).....	16
Figure 5. Schematic representation of the Q- Cycle. Red arrows represent the first electron pathway unto the final receptor cytochrome c. Green arrows represent the recycling pathway of the second electron unto its storage in a semi quinone radical ion and its later reduction into ubiquinol, upon receiving another electron (product of the oxidation of a second Ubiquinol in Qo) and 2 protons. A - external surface of inner mitochondrial membrane; B - luminal side of the inner mitochondrial membrane; H ⁺ - released proton; e ⁻ - released electron.	20
Figure 6. Synthesis and metabolization of the prodrug ELQ-334. (Lawres et al., 2016).....	21
Figure 7. Schematic representation of the method for determining IC ₅₀ values of a compound in a three-day proliferation inhibition assay.	23
Figure 8. Schematic illustration of Neubauer counting chamber used to count cells and parasites. A) Each blue square includes 16 small squares (green). B) The cells/parasites inside the squares of the chamber are counted except for those touching the border lines marked in red. C) Formula for calculating the number of items per ml.	25
Figure 9. Plate design for testing the compounds. A) 6-well plate carrying the highest concentrations of the compound; B) 6-well plate carrying the lowest concentrations - because of possible edge effects, on this plate the lowest concentration is placed in the middle (red arrow).	26
Figure 10. NucleoSpin® DNA RapidLyse protocol for purifying DNA. Materials are from MACHINERY-NAGEL Rapid Lyse DNA isolation kit	29
Figure 11. Serial dilutions of standard sample. Starting with 10µl of the initial aliquot, 1µl is diluted in 9µl of water producing the first dilution (1:10). Sequentially, 1µl of the previous	

dilution (red arrows) is diluted again in 9µl of water to produce 1:100 dilution and the process is repeated to achieve a final 1:1000 dilution of the initial aliquot.	31
Figure 12. Dose-response curve for ELQ-334 relating the concentration of the compound with the concentration of <i>B. besnoiti</i> DNA measured. Each curve is identified by the calculated IC ₅₀ value calculated through a logarithmic function.	34
Figure 13. Dose-response curve for ELQ-316 relating the concentration of the compound with the concentration of <i>B. besnoiti</i> DNA measured. Each curve is identified by the calculated IC ₅₀ value calculated through a logarithmic function.	34
Figure 14. Methods for Long Treatment Experiment. Regrowth of parasites was monitored on daily basis by light microscope for a maximum period of three weeks.	39
Figure 15. Long treatment experiment since day-0 to day-9. ELQ-121 concentration was increased on day 9; two flasks continued to be exposed to 2.5µM of the compound and three flasks were exposed to 5µM, 7.5µM and 10µM.	42
Figure 16. <i>B. besnoiti</i> on day-1 (12.09.18). A) ELQ-121 at 2.5µM concentration. Extracellular parasites can be observed; B) Control flask, presenting rosette shaped parasitophorous vacuoles (PV)(red arrows).	44
Figure 17. A) <i>B. besnoiti</i> after three days of treatment with ELQ-121 at 2.5 µM concentration with living parasites; B) Control flask, showing big PVs formed by <i>B. besnoiti</i> and lysed cell layer with extracellular parasites.	44
Figure 18. <i>B. besnoiti</i> after removal of drug pressure on day-3 (a,b) and after six days of treatment with ELQ-121 with 2.5 µM. (c,d) a) parasite inside a round structure; b, c) parasitophorous vacuoles with a rosette shape; d) abnormal structures resembling bubbles.	45
Figure 19. a) <i>B. besnoiti</i> after drug removal on day-3. PV and living parasites can be observed; b) <i>B. besnoiti</i> after drug removal on day-6. Living parasites and parasites inside a round structure can be observed; c) <i>B. besnoiti</i> after nine days of treatment with ELQ-121, 2,5 µM. Living parasites and deformed PVs can be observed.	46
Figure 20. A) <i>B. besnoiti</i> treated with ELQ-121 at 5 µM (concentration increased on day-9), a destroyed PV can be observed; B) <i>B. besnoiti</i> treated with ELQ-121 at 10µM (concentration increased on day-9), cell lysis and living parasites were observed.	47

Figure 21. <i>B. besnoiti</i> treated with ELQ-121 at 2.5µM on day-15. A) After 15 days of treatment, parasites still proliferate although some present abnormal shape. B) Several PVs and alive parasites were observed.	47
Figure 22. <i>Besnoitia besnoiti</i> after 20 days of treatment with ELQ-121 in different concentrations. A, B, C) Living parasites; D - Dead parasites.	48
Figure 23. <i>B. besnoiti</i> on day-20, treatment with ELQ-121 at 2.5 µM was interrupted on day-3. A) Non confluent cell layer (flask splitted on day-15) with living parasites. B) Confluent cell layer (non splitted) with living and dead parasites.	49
Figure 24. <i>B. besnoiti</i> on day-27. Large round parasites and abnormal PVs can be observed.	50
Figure 25. General layout of a TEM describing the path of electron beam. Electrons enter the condenser system, composed by one or two lenses creating a magnetic field that focuses and constricts electrons into a thin beam. The beam of electrons produced is transmitted through the sample and into another series of electromagnetic lenses that focus the electrons onto a fluorescent screen at the bottom of the microscope e to create the image. Generally, the images produced by TEM are grey scale: the lighter areas correspond to the higher number of electrons transmitted and the darker areas represent lower number of electrons transmitted - dense areas on the sample. (Marturi, 2015).	54
Figure 26. Trapezoid cut on the EPON block.	56
Figure 27. Ultramicrotome. 1) EPON block; 2) Diamond knife; 3) Water; 4) Ultra-thin cut sections. Sections show different colours, since the light reflects in different ways depending on the sample's thickness. The colours corresponding to the aimed thickness are yellow and gold.	57
Figure 28. TEM picture of control. A) <i>N. caninum</i> tachyzoite non-treated with normal internal structures. cri: cristae; gran: dense granules; mic: micronemes; con: conoid; mit: mitochondria; rop: rhoptries; B) Tachyzoites within a parasitophorous vacuole delineated by a parasitophorous vacuole membrane (pvm).	59
Figure 29. <i>N. caninum</i> tachyzoites treated with ELQ-316 at 12h. nuc: nucleous; gran: dense granules; mic: micronemes; con: conoid; mit: mitochondria; rop: rhoptries	60

Figure 30. *N. caninum* tachyzoite treated with ELQ-316 at 24h. mit: mitochondria; inc: inclusion; ves: intracellular vesicular structures..... 61

Figure 31. *N. caninum* tachyzoite treated with ELQ-316 at 24h. The encircled are indicates the mitochondria. inc: inclusion; ves: intracellular vesicular structures; nuc: nucleous. 62

Figure 32. a, b, c) *N. caninum* tachyzoites treated with ELQ-316 at 48h. Alterations in the mitochondria (a,b) and dead parasites (c) can be observed. nuc: nucleous; gran: dense granules; mit: mitochondria; rop: rhoptries; D: dead parasite..... 63

Figure 33. CRISPR/Cas9 System; A – Cluster of Cas genes; B – Short palindromic repeat; C – Spacer: short DNA sequences of exogenous genetic materials..... 69

Figure 34. Representative operons for CRISPR System Types. Genes involved in the interference stage are coloured red, genes involved in crRNA biogenesis stage are coloured yellow, and those involved in adaptation are coloured blue (Wright et al., 2016)..... 70

Figure 35. CRISPR-Cas9 mediated gene-editing mechanisms. A guide RNA (gRNA) recognizes a genomic region followed by PAM sequence, recruiting the Cas9 DNA endonuclease. A double stranded break is created, being repaired by (i) non-homologous end joining (NHEJ) or (ii) homology directed repair (HDR) in the presence of a donor template (Ding et al., 2016)..... 71

Figure 36. Illustration of resistance gene dhfr knock-in on sag1. 75

Figure 37. pUC19 plasmid construct with the pyrimethamine-resistance selectable marker (dhfr) and an ampicillin resistance gene (ampR). The targeting sequence of the sag1 sgRNA is highlighted. Adapted from Norrander et al., 1983; Sidik et al. 2014. 77

Figure 38. Agarose gel scheme. The gel carries 18 probe wells (P), three empty wells (E) and a positive control well (C). 81

Figure 39. First gel carrying clones 1 – 18, two ladders (L), three empty wells (E) and a positive control (C). Bands of DNA stained with ethidium bromide visualized under UV light represent positive PCR results..... 81

Figure 40. Second gel carrying clones 19 – 36, two ladders (L), three empty wells (E) and a positive control (C)..... 82

Figure 41. Fourth gel carrying clones 55 – 70, two ladders (L), five empty wells (E) and a positive control (C)..... 82

Figure 42. Third gel carrying clones 37 – 54, two ladders (L), three empty wells (E) and a positive control (C)..... 82

Figure 43. Electrophoresis result. A) First gel, carrying clones 1-18; B) Second gel, carrying clones 19-36; C)Third gel, carrying clones 37-54; D)Fourth gel, carrying clones 55-70; L – Ladder; E – Empty well; C - PCR positive control. 83

Figure 44. Schematic illustration of target sites for different primers used on PCR 1 – 4... 85

Figure 45. Gel electrophoresis result obtained from four different PCR reactions on clones 30, 35, 37, 44, 46, 52, 69 and 70. L – ladder, E – Empty well, C – PCR positive control... 86

Figure 46. Gel electrophoresis result obtained by PCR reactions using sag1 primers on PCR negative for sag1. L – ladder, E – Empty well, C – PCR positive control. 87

Figure 47. Gel electrophoresis result obtained by PCR reactions using sag1 primers on three clones. L – ladder, E – Empty well, C – PCR positive control. 88

Abbreviation List

IMC	Inner Membrane Complex
PV	Parasitophorous Vacuole
pvm	Parasitophorous vacuole membrane
CNS	Central Nervous System
P.i.	Post infection
PCR	Polymerase Chain Reaction
IC ₅₀	Half-maximal Inhibitory Concentration
MIC	Minimum Inhibitory Concentration
ELQ	Endochin Like Quinolone
ETC	Electron transport chain
ATP	Adenosine triphosphate
ROS	Toxic Reactive Oxygen Species
DNA	Deoxyribonucleic Acid
Cyt bc1	Cytochrome bc1 Complex
Q _o	Oxidative site
Q _i	Reductive site
QH ₂	Ubiquinol
ISP	Rieske iron sulfur protein
H ⁺	proton
e ⁻	electron
Q	Ubiquinone
nM	nanomolar
HFF	Human foreskin fibroblasts
RG	Relative growth
qPCR	Real-time quantitative polymerase chain reaction
DMSO	Dimethyl sulfoxide
PBS	Phosphate-buffered saline

EDTA	Ethylenediamine tetraacetic acid
DMEM	Dulbecco's Modified Eagle Medium
FCS	Foetal Calf Serum
C+	Positive Control
C-	Negative Control
W/o	Control without host cells seeded
rpm	Rotations per minute
MM	Master Mix
Neg	Internal negative control
Primer F	Primer Forward
Primer R	Primer Reverse
HBSS	Hank's Balanced Salt Solution
RNA	Ribonucleic acid
CRISPR	Clustered regularly interspaced short palindromic repeats
crRNA	CRISPR RNA
sgRNA	Single guide RNA
tracrRNA	Trans-activating RNA
DBS	Double strand break
PAM	Protospacer Adjacent Motif
NHEJ	Non-homologous End Joining
HDR	Homologous Direct Repair
KO	knock-out
KI	knock-in
Pyr	Pyrimethamine
<i>dhfr</i>	Dihydrofolate reductase-thymidylate synthase
MCS	Multiple Cloning Site
<i>ampR</i>	Ampicillin resistance gene
L	Ladder

Preamble

The present thesis, on behalf of the Master's degree in Veterinary Medicine of the University of Évora, reports on the curricular internship.

The internship started on September 3rd 2018 until February 28th 2019, and lasted over a period of six months. It took place at the Institute of Parasitology, Vetsuisse Faculty of University of Bern, Switzerland, under the supervision of Prof. Dr. Andrew Hemphill. The Institute focuses on parasitosis of domestic and farm animals, as well as zoonotic parasites. Its mission includes teaching, research, and service to the community – offering diagnostic examinations for hospitals, private veterinarians, and public health offices.

The main research areas of the Institute of Parasitology are focused on pathogenic protozoan of cattle diseases (neosporosis, besnoitiosis, toxoplasmosis, tritrichomonosis), immunology and chemotherapy of alveolar echinococcosis, and giardiasis.

The internship focused on the research in pathogenetic processes during the infection of *Neospora caninum* and *Besnoitia besnoiti*, thus contributing for a better knowledge, and the development of new therapeutic approaches and the identification of targets. The present report summarizes three assays developed during the internship, and a monography reviewing the CRISPR/Cas9 technique.

I. Introduction

1. Apicomplexan parasites

Apicomplexan parasites are the causative agents of many important diseases in farm animals, leading to serious economic losses in the production of cattle, pork, sheep, goats, and poultry. Therefore, methods for detection, prevention, control and treatment of these parasites have become of great economic importance and need to be improved (Hemphill et al., 2017).

The most relevant apicomplexan parasites in the field of veterinary and human medicine are *Neospora* spp., *Toxoplasma* spp., *Cryptosporidium* spp., *Eimeria* spp., *Plasmodium* spp. and *Theileria* spp. (Müller et al., 2017). The genus *Besnoitia*, that includes more than ten distinct species, is closely related to *Toxoplasma gondii* and *Neospora caninum* (Cortes et al., 2014). *Neospora caninum* and *Besnoitia besnoiti* will be discussed in more detail throughout the present report.

1.1. Morphology of apicomplexan parasites

Apicomplexan parasites share a variety of morphological traits that are considered characteristic of this phylum (Morrisette and Sibley, 2002) (Figure 1) such as micronemes, rhoptries, conoid and the apical polar ring – contained in the apical complex (Santos et al., 2009).

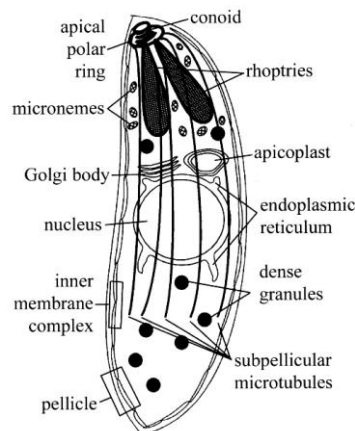


Figure 1. The morphology of apicomplexan parasites (Morrisette and Sibley, 2002).

These obligatory intracellular parasites have co-evolved with hosts to be able to invade their cells and proliferate. In order to do so, specific molecular parasite-host cell interactions must be established to manipulate its immune system, the host cell structures, mechanisms and pathways. The apical complex is an exclusive structure of this group of parasites (Santos et al., 2009) and it is involved in host-cell invasion (Cardoso et al., 2014). Its composition differs depending on the members of the phylum. All apicomplexan parasites display specialized secretory organelles - micronemes, rhoptries, dense granules. Coccidia, such as *Besnoitia*, *Toxoplasma* and *Neospora*, also possess an apical polar ring and a structure named conoid. Other organelles include the endoplasmic reticulum, Golgi, nucleus, apicoplast and a single mitochondrion (Santos et al., 2009). The apicoplast is a remnant of a secondary endosymbiosis with photosynthesizing bacteria and green algae, and contains DNA that codes for a variety of essential plant like enzymes involved in signalling and metabolic processes of these parasites, which do not occur in mammalian cells, and are therefore potential drug targets of high interest (Hemphill et al., 2017).

The pellicle consists of the plasma membrane and the inner membrane complex (IMC). The IMC extends itself throughout the body of the parasite and it is the support for the gliding machinery, which is crucial for migration across biological barriers and active penetration of host cells - since these processes rely on the parasite's ability to glide (Santos et al., 2009). The term gliding motility refers to the advance upon a target host cell for invasion, playing a key role in the apicomplexan life cycle. (Wetzel et al., 2005)

1.2. The lytic cycle

These parasites have complex multi-stage life cycles including obligate intracellular stages (Suarez et al., 2017) and undergo a lytic cycle whereby a single zoite – the invasive stage of apicomplexan parasites – invades a host cell, multiplies to differentiate into a new zoite generation, which undergoes egress to restart a new cycle (Santos et al., 2009).

The structures involved in host cell invasion are the secretory organelles micronemes, rhoptries and dense granules (Cortes, et al. 2014). Intracellular parasites are located within a specialized compartment, the parasitophorous vacuole (PV), which is surrounded by a

parasitophorous vacuole membrane (pvm) that is essentially host cell surface membrane-driven and modified by secretory parasite components. Proliferation of intracellular parasites will result in lethal lysis of the host cells by a mechanism termed egress, leading to the exit of infective parasites from their PVs (Santos et al., 2009). Since parasites released by host cell lysis do not grow or undergo cell division extracellularly, the parasites must rapidly reinvade other host cells to survive (Morrissette and Sibley, 2002).

2. *Neospora caninum*

Neospora caninum is an obligate intracellular parasite and a member of the phylum Apicomplexa (Ellis et al., 1994). It was first described in 1984 as an unidentified protozoan parasite associated with lesions in the central nervous system (CNS) and skeletal muscles found on six Norwegian dogs (Bjerkås et al., 1984).

N. caninum was misdiagnosed as *Toxoplasma gondii* until 1988, since the infective stages (tachyzoites) and tissue cysts of these two parasites are almost identical morphologically. Slight differences in the structure of the tachyzoite's rhoptries have been detected and these provided a method for distinguishing *N. caninum* from *T. gondii* by electron microscopy (Ellis et al., 1994). In 1988, the parasite was identified as a novel species and named *Neospora caninum* by Dubey et al. (Dubey et al., 1988).

2.1. *N. caninum* life cycle

N. caninum is a major pathogen for cattle and dogs and it occasionally causes clinical infections in horses, goats, sheep, and deer (Dubey, 2005). It has a heteroxenous life cycle (Figure 2) involving three infectious stages: the rapidly proliferating tachyzoite, the slowly proliferating bradyzoite and the sporozoite resulting from sexual reproduction (Monney and Hemphill, 2014). Tachyzoites and tissue cysts can be found in the intermediate hosts, occurring intracellularly (Dubey et al., 2002).

The definitive hosts of *N. caninum* are dogs and related canids, such as coyotes and dingoes, whereas cattle is the most relevant intermediate host (Dubey et al., 2007). The definitive host excretes faeces infected with oocysts in an unsporulated form to the environment. Within 24 hours the sporozoites will be developed, leading to the contamination of food, water and soil by sporulated oocysts ready to infect the intermediate host (Reichel et al., 2007). After ingestion, by a competent intermediate host, sporozoites are released from the oocysts in the small intestine, invading the epithelial cells. Sporozoites will develop into tachyzoites, the rapid proliferating form of the parasite. It is believed that this phase occurs in the mesenteric lymph nodes, which provides access of the parasites to the bloodstream. Tachyzoites divide rapidly inside the cells and may infect many cell types including neural cells, vascular endothelial cells, myocytes, hepatocytes, renal cells, alveolar macrophages and placental trophoblasts (Dubey et al., 2006).

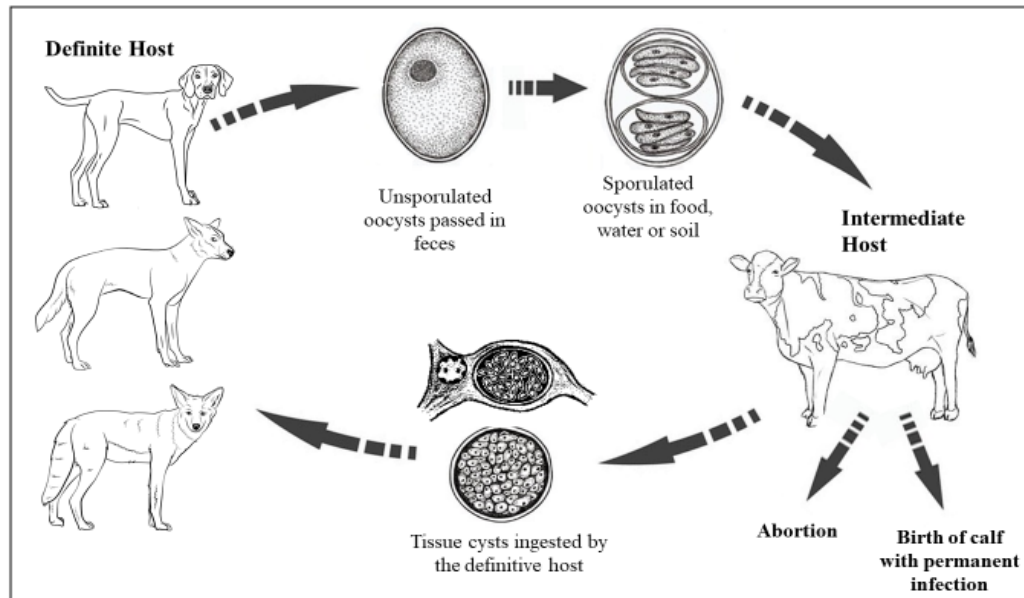


Figure 2. Schematic illustration of *N. caninum* life cycle.

Transmission of *N. caninum* to an uninfected individual can occur via two different paths named horizontal and vertical transmission (Monney and Hemphill, 2014). Horizontal transmission occurs when carnivores are infected by ingesting tissues containing encysted

bradyzoites, and when herbivores are infected by the ingestion of food or drinking water contaminated with *N. caninum* sporulated oocyst. Vertical or transplacental, infection can occur when tachyzoites are transmitted during pregnancy, resulting in the infection of the foetus (Dubey et al., 2007). Tissue cysts containing bradyzoites are more frequently observed in the CNS (Dubey et al., 2006) but they can also be found in skeletal muscle (Peters et al., 2001). The presence of *N. caninum* bradyzoites in skeletal muscles of definitive hosts indicates that they could be easily infected through the ingestion of infected carcasses or butchered meat without the need of access to infective CNS tissue that is protected by the cranium and the vertebrae (Peters et al., 2001).

2.2. *N. caninum* epidemiology

Since *N. caninum* was identified in 1988, bovine neosporosis has emerged as a serious disease of cattle and dogs worldwide. It affects dogs, cattle, cats, camels, pigs, sheep, goats, wolves, foxes (Dubey et al., 2007). It is transmitted very efficiently in cattle, and both horizontal and vertical transmission routes of infection are vital for the parasite survival (Dubey et al., 2006). *N. caninum* point-source infections are most likely the cause for abortion outbreaks in cattle and dogs, whereas vertical transmission leads to an increased annual abortion rate (Björkman et al., 2003).

Neospora caninum follows three main epidemic patterns of disease: sporadic, endemic and epidemic abortions (Reichel et al., 2013). Abortion outbreaks can be defined as epidemic if it is temporary and if 15% of the cows abort in four weeks, 12.5% of the cows abort in eight weeks, and if 10% of the cows abort in six weeks. On the other hand, an abortion outbreak is considered endemic if it persists in the herd for several months or years (Dubey et al., 2007).

Although antibody titres have been observed in humans, there is no evidence of its zoonotic potential, neither the parasite has been isolated (Dubey et al., 2007).

2.3. Bovine neosporosis

N. caninum is the causing agent of bovine neosporosis, being considered an important veterinary health problem with high economic significance (Monney and Hemphill, 2014) especially in the dairy industry, representing an impact up to approximately 1.3 billion US dollars per year (Reichel et al., 2013).

The main clinical manifestation of bovine neosporosis in both dairy and beef cattle is abortion (Dubey et al., 2006). In cattle, the gestation period is approximately 280 days. Abortions can occur from the third gestational month to term, although the rate increases during mid-gestation at five to six months (Buxton et al., 2002). In rare occasions, neurological signs can be observed in congenitally infected calves with less than one month of age. Such calves may have a below average birthweight and are unable to rise (Dubey et al., 2006). The majority of calves born from seropositive cows show no abnormalities, being apparently healthy, but they can transmit the infection (Buxton et al., 2002).

The diagnosis of *N. caninum* infection has been commonly based on the presence of pathognomonic foetal lesions (Thurmond et al., 1999) such as multifocal necrosis and widespread mononuclear infiltrations in various tissues (Dubey et al., 2006).

2.4. Treatment

Up to date, there is no effective vaccine or drug for neosporosis commercially available, which increases the relevance of studies on the development of a successful treatment (Aguado-Martínez et al., 2017). Chemotherapeutic treatment of seropositive animals is not an economically viable option given that there are no effective and safe drugs available (Dubey et al., 2007). Essentially, there are several drugs available for the treatment of clinically affected dogs, resulting in the therapeutical management of symptoms. Treatment must be initiated as early as possible before clinical symptoms become irreversible (Reichel and Ellis, 2009).

An effective treatment against neosporosis has to not only protect against the disease and cure the disease, but also be safe to administer during gestation (Aguado-Martínez et al., 2017). Since there is no available treatment, as stated before, methods of control have become of great importance to avoid economic losses and promote animal welfare.

Current recommendations for controlling neosporosis englobe the identification and elimination of infected animals (Reichel and Ellis, 2009), reducing seropositive animals by non-breeding of the infected (Müller and Hemphill, 2016), quarantine of animals (Weston et al., 2012), prevention of the transmission between dogs and cattle at the farm level through increased biosecurity (fences, testing of all incoming stock) and vaccination of all susceptible stock, when an appropriate vaccine will be available, including both seropositive and seronegative cattle present in a herd (Reichel and Ellis, 2009). In spite of all these control options, infection rates cannot be reduced to zero, since horizontal transmission cannot be entirely prevented, and the control of vertical transmission does not eliminate the parasite (Hemphill et al., 2016).

2.5. Prevention

The costs related to the control of neosporosis indicate that the most efficient intervention strategy could be vaccination (Reichel and Ellis, 2009). The vaccine Bovilis Neoguard™ based on tachyzoites lysate (Monney and Hemphill, 2014) was the only commercially available treatment against neosporosis, but due to questionable efficacy, it was removed from the market. To date, there is no effective treatment against *N. caninum* infection available (Aguado-Martínez et al., 2017) which leads to an urgent necessity on developing new means of neosporosis prevention (Monney and Hemphill, 2014).

3. *Besnoitia besnoiti*

The genus *Besnoitia* represents mandatory intracellular protozoan parasites that belong to the phylum Apicomplexa. The species of this genus are closely related to *Neospora caninum* (Cortes et al., 2014).

The disease was first described by C adeac in 1884 as elephantiasis, a skin disease in cattle. Many years later, in 1912, its parasitic nature was identified, and its causative agent and pathogenicity were determined (Besnoit and Robin, 1912). Few years later, a deeper description of the disease and its epidemiology, as well as the genus and species name were given by Franco and Borges (Franco and Borges, 1915). Even though this parasite has shown to be non-infective to humans (Cortes et al., 2014), it affects cattle of all breeds and ages, leading to considerable economic losses due to decreased milk and meat production, infertility of bulls and skin damage (Basso et al., 2013).

3.1. *B. besnoiti* life cycle

Although its complete lifecycle and transmission pathways are still unclear, it is known that *B. besnoiti* has a largely intracellular lifestyle (Cortes et al., 2014). A heteroxenous life cycle is suspected for *B. besnoiti* but the assumed definitive host which sheds oocysts after ingestion of infected tissues remains unknown (Basso et al., 2011).

The most relevant intermediate hosts are cattle and antelopes, where two different asexual parasitic stages can occur: tachyzoites and bradyzoites – responsible for the acute and chronic stages of the disease, respectively (reviewed in  lvarez-Garc a et al., 2013). *Besnoitia* species have been also recognised worldwide in rabbits, marsupials and micro mammals presenting internal cysts, mainly in the mesenterium – being the cat the definitive host (Cortes et al., 2014).

Moreover, it has been shown that wild animals such as red deer, roe deer (Gutiérrez-Expósito et al., 2017) and rodents (Basso et al., 2011) could represent intermediate hosts of some other *Besnoitia* species as well, being considered reservoirs of the parasite (Figure 3).

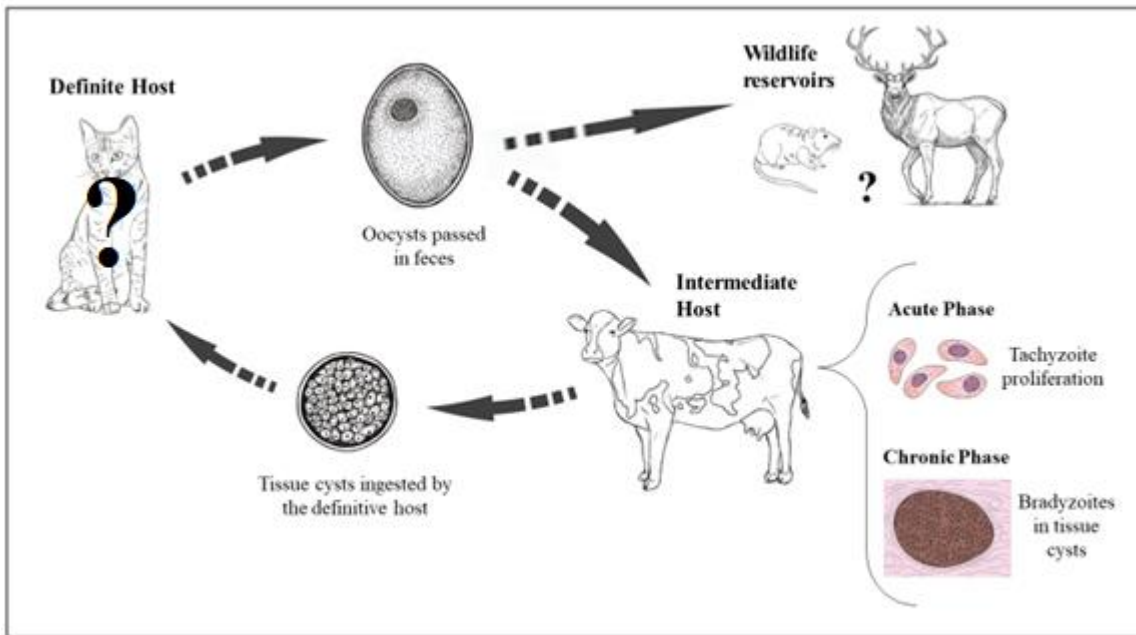


Figure 3. Schematic illustration of *B. besnoiti* life cycle.

3.2. *B. besnoiti* epidemiology

Bovine besnoitiosis is distributed across sub-Saharan Africa and Asia (Cortes et al., 2014). In Europe, the disease emerged in a few restricted areas in France and Portugal in the early 20th century (reviewed in Álvarez-García et al., 2013), being also detected in Spain, Germany, Italy and Switzerland (Olias et al., 2011).

Since 2010, bovine besnoitiosis is considered by the European Food Safety Authority to be a re-emerging disease due to the increasing number of cases and its geographic expansion. This expansion may be explained by animal trade and management practices introducing infected animals into the herd (reviewed in Álvarez-García, et al. 2013) and climate changes that influence arthropod population distribution and survival, favouring the

mechanical transmission of the disease by vectors such as tabanids and *Stomoxys calcitrans* – biting flies (Liénard et al., 2015).

3.3. Bovine besnoitiosis

The disease caused by *B. besnoiti* is named bovine besnoitiosis, given that the intermediate host is represented by cattle (Frey et al., 2016). Bovine besnoitiosis is characterised by local and systemic clinical signs of variable severity (Álvarez-García et al., 2013). In general, it leads to severe economic losses due to definitive or transient sterility in bulls, abortion, decreased milk production and low body condition resulting in depreciating slaughter value and skin quality (Cortes et al., 2005). Even though the disease has an important economic impact, mortality rates are low (Álvarez-García et al., 2013).

Bovine besnoitiosis has two presentations: an acute phase occurring 11-13 days after infection and a chronic phase, developed while the animal is recovering from the acute phase of the infection (Pols, 1960). The incubation period of the parasite in infected cattle ranges from two weeks up to two months (Álvarez-García et al., 2013).

3.3.1. Acute phase of disease

The acute or febrile phase occurs more often in adults. This phase includes the proliferative stage of the obligate intracellular parasite, represented by the fast replicating tachyzoites (Cortes et al., 2005). They mostly invade endothelial cells of blood vessels although monocytes and neutrophilic granulocytes may also be affected (Álvarez-García et al., 2013). They proliferate rapidly inside the host cell within a parasitophorous vacuole membrane. This rapid growth of tachyzoites leads to the rupture of the vacuole and lysis of the host cell (Cortes et al., 2014). The released tachyzoites enter the blood and are disseminated by its circulation, being able to invade new cells and repeat their lytic cycle.

These proliferative tachyzoites can be observed in the blood of infected animals from day-3 post infection (p.i.) up to day-12 from beginning of the acute phase (Álvarez-García et al., 2014).

Clinical signs such as fever, anorexia, nasal and ocular discharge, tachycardia, tachypnoea, salivation, subcutaneous edemas and orchitis may occur during the acute stage (Basso et al., 2013). Inspiratory dyspnoea may also occur from the inflammation of the upper respiratory mucosae. Diarrhoea and abortion – happening when a cow develops the disease while pregnant - are less common manifestations (Pols, 1960).

3.3.2. Chronic phase of disease

While the acute phase consists of the effects of *B. besnoiti* tachyzoites, this phase is characterized by tissue cysts containing the bradyzoites stage and skin lesions (Álvarez-García et al., 2014). These macroscopic thick-walled tissue cysts can be found predominantly in the mucosa of the upper respiratory tract, on the lower genital tract, in the scleral conjunctiva of the eyes and in the dermis and tendons of the lower limbs (Frey et al., 2016). Skin lesions may include thickening, hardening and folding of the skin (Basso et al., 2013), especially around the neck, shoulders and rump, accompanied by hyperpigmentation and alopecia. There may also be pronounced thickening of the limbs, and locomotion may be difficult and painful (Pols, 1960). The anorexia and weight loss present in the acute phase may continue (Cortes et al., 2005).

Animals showing clinical signs represent a small percentage of the infected animals, given that the higher portion of cattle is considered sub-clinically infected yet seropositive (Álvarez-García et al., 2014) – being epidemiologically relevant since they are able to introduce the parasite unnoticed into healthy herds (Basso et al., 2013). Most deaths occur during the chronic stage of the disease (Pols, 1960).

3.4. Treatment

There are no effective pharmaceutical or chemotherapeutics agents available to treat bovine besnoitiosis and no vaccines are licensed in Europe (Cortes et al., 2005; Álvarez-García et al., 2013).

The first reported attempts for the treatment of bovine besnoitiosis are from Herin in 1952 and include an intravenous injection of 30 mL of a 1% solution of formalin during the acute stage of the disease and administering 30–40 mL Lugol's iodine solutions five times intravenously at intervals of four to seven days for the chronic stage. Since such treatments exhibited obvious adverse effects and no positive results, these options were no further developed (Cortes et al., 2014). Other treatment approaches like the administration of pentamidine, aureomycin, formalin, sodium iodide, sulfamerazine, mycostatin and terramycin were investigated in rabbits, but were also discarded for not being successful against the disease (Pols, 1960).

Nitro-thiazolide nitazoxanide and bromo-derivatives have proven to be potent inhibitors of *B. besnoiti* tachyzoite proliferation *in vitro*. Both agents seemed to be effective. However, nitro groups can be harmful so bromo-derivatives could represent safer alternatives (Cortes, et al. 2014). More recent studies demonstrated the efficacy, at least *in vitro*, of commercially available anti-coccidial drugs against *B. besnoiti* including bumped kinase inhibitors (Jiménez-Meléndez et al., 2017), diclazuril and decoquinate (Jiménez-Meléndez et al., 2018), and naphto-quinone buparvaquone (Müller et al., 2019).

3.5. Prevention of *B. Besnoiti* infection

Live vaccines have been used for the prevention of bovine besnoitiosis in South Africa and in Israel. In South Africa, the vaccine is based on tachyzoites of an isolate from blue wildebeest, which passed through rabbits and was later grown in cell cultures, being recommended for use in weaners and older animals. Although it protects cattle against clinical besnoitiosis, it does not entirely prevent sub-clinical infection. In Israel, the vaccine

in use contains live attenuated parasites derived from the isolation in infected cattle, inoculated into gerbils and later cultivated in cell lines. In addition, live attenuated vaccines carry risks of introducing the parasite into uninfected herds (Cortes, et al. 2014).

Due to the economic negative impact of bovine besnoitiosis, it becomes fundamental to invest in disease control. A global strategy to control bovine besnoitiosis is based on management measures such as mandatory testing new entries into a herd – requiring that all newly introduced animals should be tested prior to entrance into the herd (Álvarez-García et al., 2013). Serological examination of cattle and culling of confirmed positive animals are also relevant prophylactic and control measures to avoid the introduction of infected animals from endemic to non-endemic areas (Basso et al., 2013).

II. Internship Report

1. Research for novel drugs

Protozoan parasites represent major challenges to public and animal health. Until today there are no effective treatment options against neosporosis or besnoitiosis. Therefore, it is urgent to invest in drug development, testing new compounds and their activities against protozoan infections. Generally, drug development can have two different lines of action: screening of novel compound libraries in high-throughput systems and using a target-based drug design with additional genomic and proteomic analysis (Müller and Hemphill, 2016).

In apicomplexan parasites, there is a significant potential for cross-species approaches, given that many members of this phylum exhibit common biological hallmarks that could be explored for the development of preventive measures and/or novel therapeutic approaches. Furthermore, some of these particularities - such as the need to invade and modify their host cells in order to survive, the need to undergo sexual and/or asexual proliferation, and the expression of enzymes encoded by the apicoplast - have no counterparts in mammalian cells, thus rendering these features the perfect targets for the development of novel intervention tools (Hemphill et al., 2017).

The first step to test drug effectiveness is a whole-organism screening for antiparasitic compounds *in vitro* using an appropriate system. This way, parameters such as parasite proliferation and growth inhibition, as well as alterations in morphology, shape and mobility can be monitored and evaluated. Nevertheless, this represents a subjective method, being necessary the support of quantitative methods, such as colorimetry, immunofluorescence, real-time quantitative Polymerase Chain Reaction (qPCR) or using transgenic parasites expressing reporter genes under a strong promoter. After a first round of drug screening, the effects of the compounds must be assessed by a quantitative parameter to allow comparison to other compounds. The half-maximal inhibitory concentration (IC₅₀) and minimum inhibitory concentration (MIC) are commonly used (Müller and Hemphill, 2013).

1.1. Endochin-like quinolones

Endochin (Figure 4) is a 4-(1H)-quinolone initially investigated in 1948 by Salzer et al. as an experimental anti-malarial drug. It became a compound of great interest because of its efficacy against *Plasmodium falciparum* (etiologic agent of malaria) in an avian malaria model (Salzer et al., 1948). In 1951, it was found that endochin was also active against avian and murine toxoplasmosis (Doggett et al., 2012) and more recent studies have shown endochin-like quinolones (ELQs) to be active against *Neospora caninum in vitro* (Anghel et al., 2018).

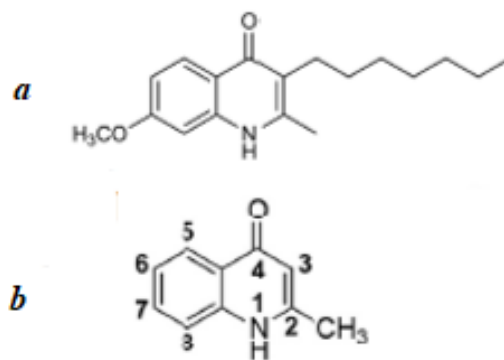


Figure 4. Chemical structures of endochin (a) (Doggett et al., 2012) and general 4-(1H)-quinolones with numbered chemical positions (b) (Stickles et al., 2015).

Despite of revealing potent activity against *Plasmodium falciparum* and *Toxoplasma gondii in vitro*, the 4-(1H)-quinolone derivatives, named ELQs have shown to be poorly soluble in water and unstable in the presence of mammalian (rat and human) microsomes (Doggett et al., 2012). Because of low aqueous solubility and high crystallinity, ELQ analogues have limited oral absorption (Miley et al., 2015), and are difficult to be administrated to animals (Winter et al., 2011). To face this difficulty, prodrugs for the most effective compounds *in vitro* were produced, presenting improved water-solubility and consequentially higher oral bioavailability. These prodrugs were designed to be metabolized

after administration and release the active compound, increasing the drug efficacy by increasing its exposure (Winter et al., 2011; Miley et al., 2015).

The proven efficacy of these drugs against protozoan parasites such as *Plasmodium* spp., *Toxoplasma gondii* and *Neospora caninum* (Doggett et al., 2012; Anghel et al., 2018) opened the window for the construction of a library of 4(1H)-quinolone-3-diarylethers to facilitate the improvement of its properties (Doggett et al., 2012). Two important modifications of the original series of ELQs were made in order to enhance stability and bioavailability. The incorporation of aromatic side chains (diarylether group) at the third position led to higher metabolic stability (Ortiz et al., 2016) and the integration of various heterocycles into the quinolone side chain increased aqueous solubility (Biagini et al., 2012).

1.2. The mitochondrion of apicomplexan parasites as a drug target

Twenty years ago, the discovery of the effects of atovaquone on the mitochondrial electron transport chain (ETC) of *Plasmodium falciparum* turned the mechanisms involved in oxidative phosphorylation into potential targets for antiparasitic therapies. Atovaquone targets the ETC inhibiting proton pumping leading to loss of mitochondrial membrane potential and organelle dysfunction which disrupts the pyrimidine synthesis (Biagini et al., 2012). The cell growth and division of *P. falciparum* requires robust purine and pyrimidine supplies (Belen Cassera et al., 2011). Thus, the disruption of pyrimidine metabolic pathways caused by the collapse of mitochondrial function leads to the death of the parasite (Biagini et al., 2012).

The mitochondrial transport of the electron chain is therefore considered an important target for the development of novel therapeutic strategies since its activity is essential for parasitic survival. In addition to its role in the synthesis of metabolically essential pyrimidines in *Plasmodium* spp, the ETC generates cellular ATP (adenosine triphosphate) – the source of energy for eukaryotic cells (Ortiz et al., 2016).

The ETC mediates the transport of electrons via multiprotein complexes present in the inner mitochondrial membrane named Complexes I-IV. So, blocking this reactive chain results in deficiency of essential molecules and can generate reactive oxygen species (ROS) such as superoxide anion (O_2^-), given that the Complex III of the mitochondria respiratory chain (also known as bc1 Complex) is the main source for ROS generation (Ortiz et al., 2016). ROS causes damage to the deoxyribonucleic acid (DNA) and proteins, resulting in cellular aging (Crofts, 2004). Hence, the inhibit of the ETC activity - specifically the cytochrome bc1 complex – in parasites exerts toxicity (Stickles et al., 2015).

1.2.1. The cytochrome bc1 complex

The Cytochrome bc1 Complex (cyt bc1) (also known as cytochrome c oxidoreductase and Complex III) is the third component of the mitochondrial electron transport chain (Stickles et al., 2015). It is present in all metazoan, many fungi and protozoa, and it catalyses the electrons transfer in order to maintain the membrane potential of mitochondria (Barton et al., 2010).

The transfer of electrons is coupled to the translocation of protons across the inner mitochondrial membrane that leads to the synthesis of ATP, using the electrochemical gradient produced. The complex cytochrome bc1 catalytic core is composed by three subunits: the cytochrome b, the cytochrome c1 and the Riske iron-sulphur protein (2Fe-2S). All three subunits participate directly in the electron transfer pathway (Barton et al., 2010). Cyt bc1 facilitates the electron transfer from ubiquinol to cytochrome c1 via catalytic reactions, operating through a mechanism known as the Q- Cycle (Stickles et al., 2015).

1.2.2. Q-cycle of mitochondria

The catalytic cycle of cyt bc1 is essentially explained (Figure 5) by Mitchell's Q-cycle hypothesis from 1975 (Barton et al., 2010). Structurally, this complex contains two catalytic sites susceptible to small-molecule inhibition: a reductive site (Qi) oriented to the luminal side of the inner mitochondrial membrane, and an oxidative site (Qo) oriented to the external surface of that membrane. The blocking of either site is sufficient to disrupt the entire cycle (Stickles et al., 2015; Ortiz et al., 2016).

As stated before, the cyt bc1 promotes the transfer of electrons from ubiquinol (QH₂) to cytochrome c, requiring two binding sites located on opposite sides of the mitochondrial membrane and connected by a transmembrane electron transfer pathway (Barton et al., 2010). This electron transfer is paired to the transfer of one proton (H⁺) per electron across the membrane (Crofts, 2004).

Ubiquinol (produced by dehydrogenases on complex II) binds to the Qo site and is oxidized, releasing two protons and two electrons. In a bifurcated reaction at this point, each electron follows two different reaction chains. The initial acceptor of the first electron from ubiquinol is the [2Fe-2S] cluster of the Rieske iron sulfur protein (ISP), that is reduced and goes through a conformational shift that leads to a close contact of the IPS to the heme group of cytochrome c1, facilitating the electron transfer. The reduced cytochrome c1 transfers the electron to cytochrome c, a mobile electron carrier protein, that is water soluble and transports the electron to complex IV (Barton et al., 2010).

The second electron follows a recycling pathway thus conserving energy. It is passed through the heme groups of cytochrome b and onto an extra ubiquinone (Q), present on complex III, forming a partially reduced species called a semiquinone radical ion. This species will store the electron until another electron completes the reduction of ubiquinone into ubiquinol on the Qi reduction site. Because this reaction requires two electrons, the Qo site must turn over twice, oxidizing two QH₂, releasing four H⁺, and delivering two electrons

successively to each chain. The ubiquinol formed in the Qi site can be used again in the cycle to generate the proton gradient needed to synthesize ATP (Crofts, 2004; Barton et al., 2010).

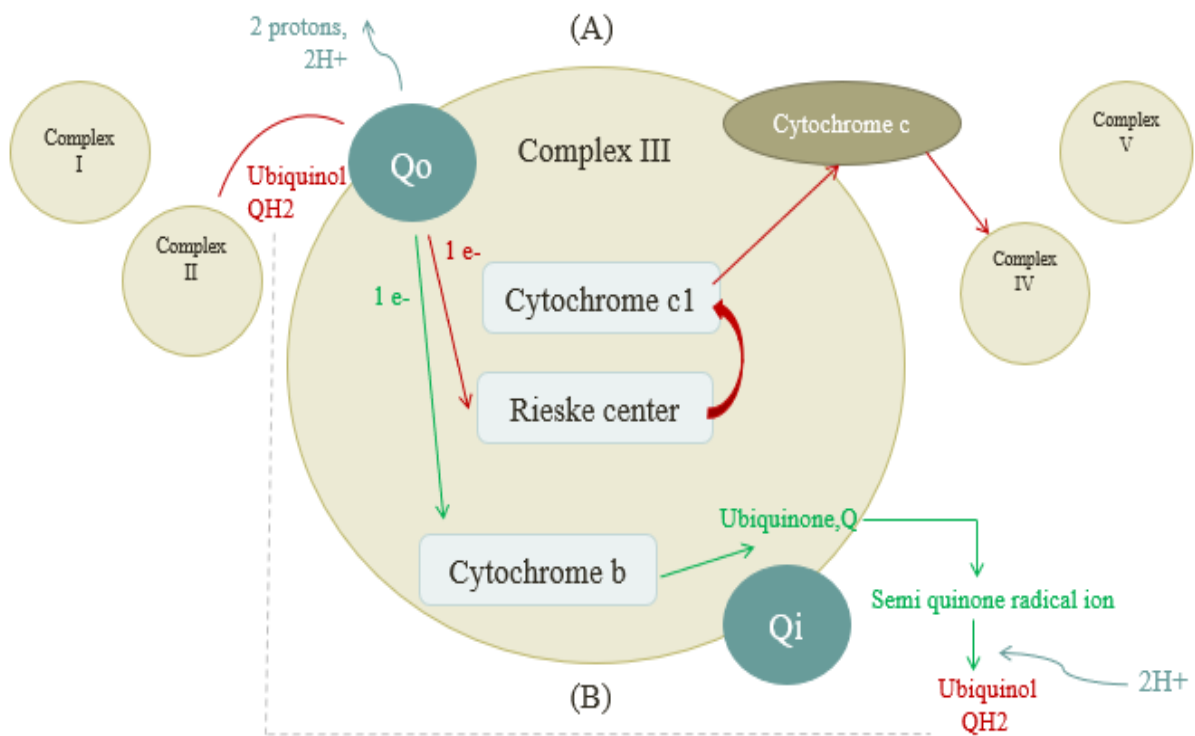


Figure 5. Schematic representation of the Q- Cycle. Red arrows represent the first electron pathway unto the final receptor cytochrome c. Green arrows represent the recycling pathway of the second electron unto its storage in a semi quinone radical ion, and its later reduction into ubiquinol, upon receiving another electron (product of the oxidation of a second Ubiquinol in Q_o) and 2 protons. A - external surface of inner mitochondrial membrane; B - luminal side of the inner mitochondrial membrane; H⁺ - released proton; e⁻ - released electron.

1.2.3. Mechanism of action of endochin-like quinolones

ELQs are ubiquinol analogues, so they can act as competitive inhibitors of *cyt bc1* by binding to Qo and/or Qi sites (Ortiz et al., 2016), disrupting pyrimidine biosynthesis and oxidative phosphorylation (Doggett et al., 2012). It was shown that single atom changes such as substitutions at different positions of the quinolone ring of ELQs control whether quinolones bind to Qo site or Qi site of cytochrome b on *Plasmodium falciparum* and *Toxoplasma gondii*. ELQs are currently among the most effective preclinical compounds against acute and chronic toxoplasmosis (Stickles et al., 2015; McConnell et al., 2018).

ELQ-316 has proven to be very effective against *T. gondii*, exhibiting *in vitro* IC₅₀ values below one nanomolar (nM), and being effective *in vivo* against not only tachyzoites, but also tissue cysts (Doggett et al., 2012). Because of poor bioavailability of ELQ compounds, a prodrug of ELQ-316, named ELQ-334 (Figure 6) was synthesized to face this difficulty (Lawres et al., 2016).

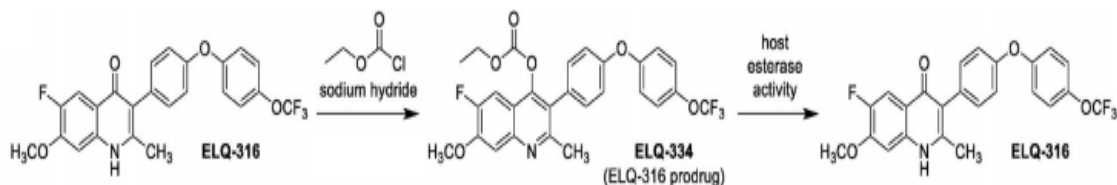


Figure 6. Synthesis and metabolization of the prodrug ELQ-334. (Lawres et al., 2016).

2. Assessment of half-maximal inhibitory concentration (IC₅₀ assay)

In this assay, the half-maximal inhibitory concentration (IC₅₀) of different compounds against *B. besnoiti* was determined to evaluate their activity and efficacy. The ELQ analogs used were synthesized at the Health & Science University Department of Medicine in Oregon US. For *in vitro* studies, the compounds were received as dry powders or stored as stock

solutions of 5 mM or 10 mM in dimethyl sulfoxide (DMSO) at -20°C. All materials used are listed in the appendix (1. Materials for IC₅₀ Assay).

Fourteen compounds were primarily screened against a strain of *B. besnoiti* Bb Lisbon tachyzoites: ELQ-100, ELQ-121, ELQ-127, ELQ-136, ELQ-271, ELQ-300, ELQ-316, ELQ-334, ELQ-400, ELQ433, ELQ-434, ELQ-435, ELQ-346 and ELQ-347. In a 3-day proliferation assay, *B. besnoiti* cultures were exposed to each ELQ at three different concentrations and parasite proliferation was quantified by qPCR. In summary, human foreskin fibroblasts (HFF) were the host cells infected with the strain and the compounds were added at 0.01, 0.1 and 1 μM. Infected cultures were incubated at 37°C and 5% CO₂. Three days later, qPCR was performed to quantify and evaluate ELQ activity in terms of growth inhibition of the tachyzoites. Table 1 reports on the relative growth (RG) of treated *B. besnoiti* tachyzoites in relation to untreated cultures (Eberhard et al., 2020).

Table 1. Relative growth of *B. besnoiti* tachyzoites treated with ELQs at 0.01, 0.1 and 1 μM

ELQ	100	121	127	136	271	300	316	334	400	433	434	435	436	437
RG (%) at 0.01μM	100	10	100	11	100	100	42	45	24	12	70	62	74	21
RG (%) at 0.1 μM	93	0	10	0	21	67	12	7	0	5	ND	9	6	0
RG (%) at 1μM	3	0	0	0	1	8	5	0	0	0	25	8	0	0

Table 1. Primary screening of fourteen ELQs and assessed relative growth (RG) values at three different concentrations - 0.01, 0.1 and 1 μM.

All compounds revealed to be active against *B. besnoiti* tachyzoites. Parasite proliferation decreased under drug pressure, being inhibited at 100% (maximum growth inhibition) by ELQ-121, ELQ-136, ELQ-400 and ELQ-437 at 0.1 μM. ELQ-121 and ELQ-136 proved to be more effective proliferation inhibitors exhibiting ≈10% relative growth at 0.01 μM, while ELQ-400 and ELQ-437 treatments resulted in >20% relative growth. ELQ-

121 exhibit the lowest relative growth value at 0.01 μ M, thus being the most potent inhibitor of *B. besnoiti* tachyzoite proliferation. For this reason, it was interesting to select ELQ-121 to study in more detail its effect on a long-term treatment experiment to be described further on in the present report.

The effects of ELQ-316 and ELQ-334 on *in vitro* proliferation of *N. caninum* tachyzoites were studied by Anghel, presenting IC₅₀ values of 0.66 nM and 3.33 nM respectively (Anghel et al., 2018). Given that *Besnoitia besnoiti* is closely related to *Neospora caninum*, these ELQs were selected to be further analysed by determining the IC₅₀ with more accuracy using qPCR and nine different concentrations of the compounds.

The aim of this assay was the evaluation of *in vitro* efficacy of ELQ-316 and its prodrug ELQ-334 against *B. besnoiti* tachyzoites (Figure 7).

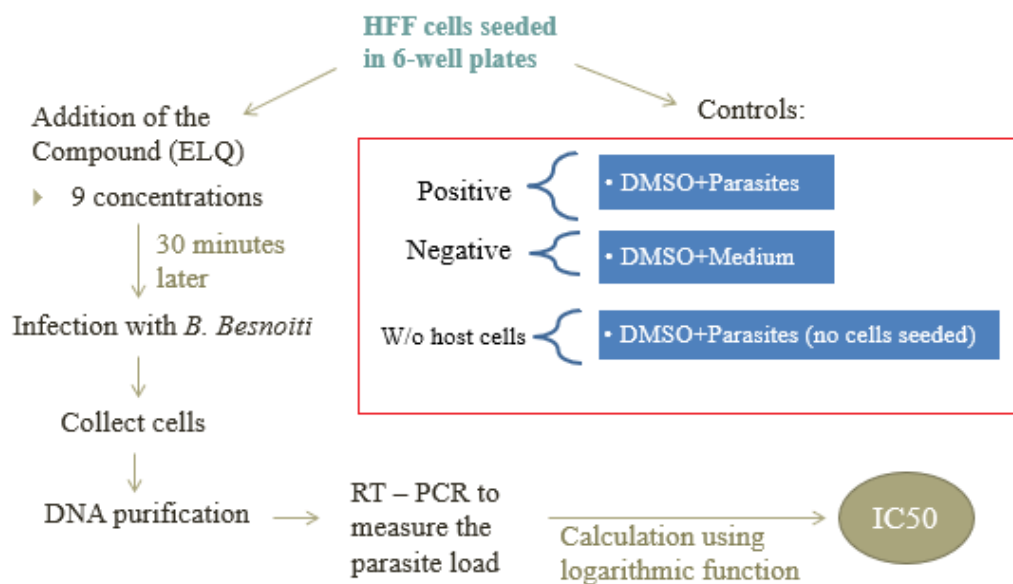


Figure 7. Schematic representation of the method for determining IC₅₀ values of a compound in a three-day proliferation inhibition assay.

2.1. Methods for IC₅₀ Assay

To avoid redundancy, the following protocols are cross-referenced to previously described methods where appropriate.

2.1.1. Cell culture of human foreskin fibroblasts

HFF (human foreskin fibroblasts) cells were maintained at 37 °C and 5% CO₂ in DMEM (Dulbecco's Modified Eagle Medium) with 10% foetal calf serum (FCS) and supplemented with antibiotics and antimycotics (10'000 units/ml penicillin, 10'000 µg/ml streptomycin and 25 µg/ml amphotericin B). For this assay, 1.2x10⁵ HFF cells were seeded on each well of the 6-well plates. The first step for seeding the cells is to split and count them. For splitting HFF cells, culture medium was discarded using aspiration pipettes and cells were washed with PBS (phosphate-buffered saline) – a physiological buffer solution. After washing the cells, trypsin with ethylenediamine tetraacetic acid (EDTA) was added to detach them from the container's wall. Cells and trypsin-EDTA were incubated for 5 minutes at 37 °C and 5% CO₂. The amount of trypsin-EDTA added depends on the volume of the flask containing the cells (Table 2). After incubation, the reaction was stopped by adding medium with serum - using at least the same volume of trypsin previously used. Finally, cells were suspended by pipetting up and down and a small volume was collected for cell counting.

Table 2. Assessed values for cell culture

	Medium per flask/well (ml)	PBS (ml)	Trypsin-EDTA (ml)	Amount of HFF cells to be infected in three days
Small T25	5	3	1.5	5 x 10 ⁵
Medium T75	20	5	4	1.5 x 10 ⁶
Large T175	40	10	7	3.5 x 10 ⁶
6-well plate	4	-	-	1.2 x 10 ⁵

Table 2. Volumes of culture medium, PBS, Trypsin-EDTA and HFF cells for cell culture process.

2.1.2. Counting human foreskin fibroblasts

To properly infect the seeded cells on 6-well plates after three days, 1.2×10^5 cells must be seeded on each well (Table 2). To count the cells, a dilution 1:2 using PBS was prepared and 10 μ l of this solution collected for loading the Neubauer counting chamber (Figure 8).

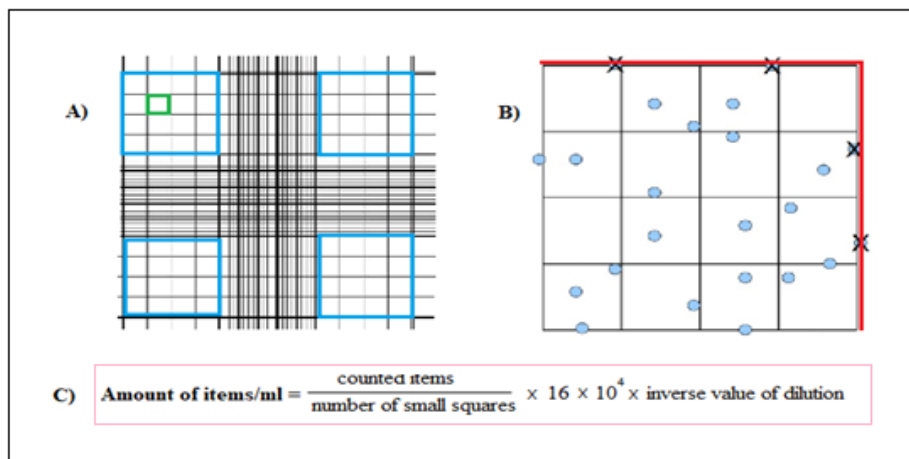


Figure 8. Schematic illustration of Neubauer counting chamber used to count cells and parasites. A) Each blue square includes 16 small squares (green). B) The cells/parasites inside the squares of the chamber are counted except for those touching the border lines marked in red. C) Formula for calculating the number of items per ml.

Once the cells were counted, they were transferred into each well (except for two wells that were the controls, having parasites and the compound but no host cells). Each well received 4 ml of DMEM containing 1.2×10^5 cells. The cells were incubated at 37 °C and 5% CO₂ for three days to reach an almost confluent layer, set for infection. This technique can also be used to count parasites, using a 1:10 dilution with PBS.

2.1.3. Addition of the ELQs on test

After three days of incubation, the compound was added to the seeded cells. For this assay, two ELQs were tested: ELQ-316 and ELQ-334. Each well of the 6-well plates carried 2 ml of suspension with compound in variable concentrations and 2 ml of suspension with parasites, representing a ratio 1:1.

The compound was added at nine different concentrations, calculated starting from the compound stock concentration of 10 mM in DMSO. Using DMEM, serial dilutions were prepared in the following concentrations: 25 μM , 5 μM , 0.75 μM , 0.25 μM , 0.1 μM , 0.05 μM , 0.01 μM , 0.005 μM , 0.001 μM . Both the ELQ stock solution and the medium were previously heated up to 37°C in a water bath. Each concentration had a duplicate, so each 6-well plate carried three different concentrations (Figure 9).

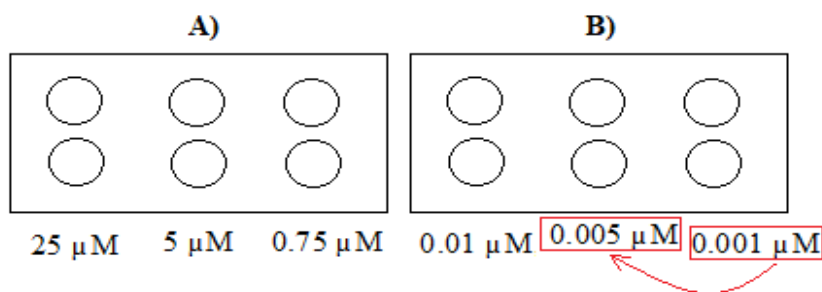


Figure 9. Plate design for testing the compounds. A) 6-well plate carrying the highest concentrations of the compound; B) 6-well plate carrying the lowest concentrations - because of possible edge effects, on this plate the lowest concentration is placed in the middle (red arrow).

2.1.4. Controls for the *in vitro* trials

One of the 6-well plates was used to carry the controls: a positive control (C+), a negative control (C-) and a control without host cells seeded (w/o) – in duplicates. None of the control wells contained the compound. A stock solution of DMSO was diluted in medium (DMEM) and used at the same concentration as the highest concentration of the compound (25 μ M). The C+ wells with host cells seeded carried medium and parasites; the C- wells carried host cells seeded, medium and DMSO; and the w/o wells was filled with the suspension of parasites and DMSO with no host cells seeded.

2.1.5. Infection of the seeded cells with *B. besnoiti*

After 30 minutes of adding the compound, cells were infected with 2 ml of suspension containing the parasites. *B. besnoiti* was cultivated in HFF cells and incubated at 37 °C and 5% CO₂. Parasites were passed over to new host cells twice a week to avoid lysis of the host cells and guarantee their survival. It also improves parasite growth since a highly confluent host cell monolayer reduces the invasion surface.

HFF cells infected with *B. besnoiti* were taken from the incubator and medium was discarded and renewed using fresh medium or PBS (suitable volumes depending on the container are stipulated on Table 2). Parasites were scraped from the flask and transferred to a tube. Using a syringe and 25G needle to pump the suspension up and down, the cells were broken to release the parasites. A small amount of this suspension was collected to an Eppendorf tube. Parasites were counted using the Neubauer chamber as previously described on “2.1.2. Counting human foreskin fibroblasts”.

HFF cells seeded on each well were infected with 2.5×10^4 parasites suspended in 2 ml of medium. The control plate was loaded first. The C- wells were filled with medium and DMSO, C+ and w/o wells were filled with 2 ml of suspension containing the parasites. The

remaining wells containing host cells and a dilution of the compound were infected with 2 ml of this suspension and incubated for three days at 37 °C and 5% CO₂. The 6-well plates containing the samples were observed by light microscope throughout the incubation time and after three days of infection, positive control wells presented numerous vacuoles on the monolayer, and signs of initial lysis.

2.1.6. DNA extraction from the cells in each well of the *in vitro* trial

The total amount of *B. besnoiti* DNA contained in a well can be measured using Real-Time PCR. In order to do so, DNA in each sample must be isolated first.

i) Collection of samples

Using the scraper, cells were removed from each well (containing 4ml: 2ml of parasite suspension and 2 ml of medium) and they were transferred into 15 ml tubes previously identified with the corresponding ELQ concentration. Each well was washed with 1 ml of PBS and this amount was added to the corresponding 15 ml tube.

The tubes were centrifuged at 4°C and 1200rpm (rotations per minute) for 10 minutes. After the centrifugation, the supernatant was discarded with an aspiration pipette, leaving the pellet in the tube. The pellet was re-suspended by adding 90 µl of PBS to each tube and pipetted up and down. After suspension, 1 ml of the liquid was transferred to Eppendorf tubes. The process should begin with the negative control well to reduce the risk of contamination.

Collected samples were centrifuged again at room temperature (22/24°C) for 10 minutes at 5000rpm. The supernatant was carefully discarded using a 1 ml pipette at first and 20 µl pipette for more precision.

ii) DNA Extraction

The DNA was purified following the NucleoSpin® DNA RapidLyse protocol using the Rapid Lyse DNA isolation kit (Figure 10).











NucleoSpin® DNA RapidLyse		
1 Lyse sample		Up to 40 mg wet weight sample or 1 x 10 ⁹ cells in a 2 mL tube 150 µL RLY 10 µL Liquid Proteinase K 56 °C, 1 h, thermomixer at maximum speed
2 Adjust DNA binding conditions		440 µL RLB Vortex 5 s
3 Bind DNA	 	Load 640 µL lysate on a NucleoSpin® DNA RapidLyse Column 11,000 x g, 1 min
4 Wash silica membrane	 	1st 500 µL RLW 11,000 x g, 1 min 2nd 500 µL RLW 11,000 x g, 1 min
5 Dry silica membrane	 	11,000 x g, 1 min
6 Elute DNA	 	100 µL RLE 11,000 x g, 1 min

Figure 10. NucleoSpin® DNA RapidLyse protocol for purifying DNA. Materials are from MACHINERY-NAGEL Rapid Lyse DNA isolation kit.

For lysing each sample, it was necessary to add 150 µl of Lysis Buffer RLY plus 10 µl of Liquid Proteinase K. For this assay, the total number of samples was 24 (18 wells containing duplicates for each of the nine concentrations and the control plate with 6 wells containing C+, C- and w/o samples in duplicate). The samples were incubated at 56°C on the Thermomixer at maximum speed, 1400 rpm for 30 minutes.

To adjust DNA binding conditions, 440 µl of Binding Buffer RLB were added to the samples and each sample was mixed in the vortex for three seconds. The lysate mixture was

then loaded onto the NucleoSpin® DNA RapidLyse column placed inside a 2 ml collection tube and centrifuged at full speed for one minute. After centrifugation, the liquid inside the column was discarded and the silica membrane was washed with 500 µl of Wash Buffer RLW twice. RLW was added and samples were centrifuged for one minute at maximum speed. The liquid was then discarded, and the process was repeated for the second wash. To dry the silica membrane and remove residual wash buffer, samples were centrifuged again for one minute at full speed.

After centrifugation, the column was placed into a 1.5 ml nuclease-free tube and the collection tube was discarded. The last step was to elute DNA by adding 100 µl of Elution Buffer RLE into each column. The samples were centrifuged at full speed for one minute. The column was discarded, and each collection tube holds purified DNA corresponding to each well.

2.1.7. Real-Time PCR for quantification of *B. besnoiti*

To quantify the amount of *B. besnoiti* DNA on each sample, real-Time PCR using a LightCycler® with primers on *B. besnoiti* genome sequence in a final reaction volume of 4 µl of template DNA and 6 µl of Master Mix were performed. Through interpolation of a standard curve with DNA from a cell culture of a known number of tachyzoites included in each run (10, 100, 1000 and 10 000), the parasite load on each sample could be determined.

i) Standard dilutions for qPCR

To correctly calculate the amount of DNA template, a standard curve was calculated from samples of known tachyzoite quantity. For this assay, three standard samples were produced by serial dilutions of *B. besnoiti* DNA obtained from cell culture with a known number of tachyzoites - 1×10^4 tachyzoites/ml (undiluted sample). Each standard sample was

carried out in duplicate. For this purpose, a 6-well plate was seeded with 1.2×10^5 HFF cells per well following the procedure described on “2.1.1. Cell culture of human foreskin fibroblasts”. Seeded cells were incubated at 37°C and 5% CO_2 for three days.

After this incubation time, cells were infected with 2.5×10^4 parasites per well and incubated at the same conditions. Three days later, cells were collected to a 50 ml falcon tube and centrifuged for 20 minutes at 4°C , 1200 rpm. The supernatant was discarded and using 5 ml of PBS, the pellet was re-suspended. After carefully counting the parasites using the Neubauer counting chamber (Figure 7), the DNA was isolated as described on “2.1.6. ii. DNA extraction”. This way, aliquots containing 1×10^4 tachyzoites per ml were produced, diluted in PBS, and stored at -20°C . To produce four standard samples, a stock of $10 \mu\text{l}$ of the aliquot was diluted through three simple serial dilutions using a dilution factor of 10 as illustrated on Figure 11.

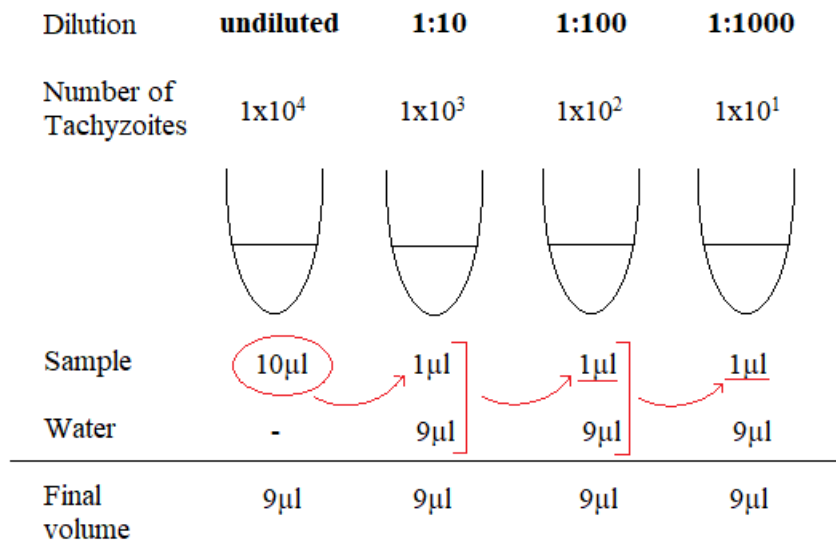


Figure 11. Serial dilutions of standard sample. Starting with $10 \mu\text{l}$ of the initial aliquot, $1 \mu\text{l}$ is diluted in $9 \mu\text{l}$ of water producing the first dilution (1:10). Sequentially, $1 \mu\text{l}$ of the previous dilution (red arrows) is diluted again in $9 \mu\text{l}$ of water to produce 1:100 dilution and the process is repeated to achieve a final 1:1000 dilution of the initial aliquot.

ii) Master Mix (MM)

PCR reactions were performed in glass capillaries containing 6 μl of Master Mix and 4 μl of 1:10 diluted DNA template. For this assay, the total amount of samples was 32: 23 DNA templates (duplicates of nine ELQ concentrations, duplicates of three controls except for one sample of C- that is discarded), eight standard samples (each standard carried a duplicate) and one internal negative control (neg) with RNase free water. For a total of 32 samples to be tested, it is recommended to prepare a volume of Master Mix for at least five more samples. The Master Mix composition is specified on Table 3 as well as the final volume calculated for 38 samples.

Table 3. Master Mix composition

<i>Reagent</i>	<i>Volume per sample (μl)</i>	<i>Volume for 38 samples (μl)</i>
Water	0.3	11.4
SybrGreen	5	190
Primer F (Forward)	0.25	9.5
Primer R (Reverse)	0.25	9.5
MgCl ₂	1.2	45.6
Total volume	7	266

Table 3- Master Mix for B. besnoiti qPCR is composed by water, a fluorescent dye (SybrGreen), Primers Forward and Reverse and magnesium chloride (MgCl₂).

2.1.8. Real-Time PCR setup

The total volume for a sample in a capillary for qPCR was 6 μl of Master Mix and 4 μl of the 1:10 diluted DNA template. To dilute the DNA samples, 23 tubes filled with 45 μl of water were prepared. Each tube was correctly identified and 5 μl of the respective DNA sample was added, attaining a 1:10 dilution of each template and duplicate. Additionally to these 23 templates, one negative control containing water and four standard samples (in duplicate) were loaded into capillaries – making a total of 32 samples.

To load the capillaries, 6 µl of Master Mix was carefully pipetted into each one of the 32 capillaries. The first capillary was the internal negative control, pipetted with 4 µl of water. The remaining capillaries were pipetted with 4 µl of the corresponding sample. The correspondence between each capillary number and sample was carefully annotated to facilitate the interpretation of the results.

Reactions were performed in a thermal cycle. The initial step corresponds to a denaturation at 95°C for 15 minutes in one cycle. The amplification for 15 seconds at 95°C was completed in one cycle and is followed by 15 seconds annealing at 56°C and 30 seconds extension at 72°C in a total of 50 cycles completed. If a sample shows a higher value comparing to the control without host cells, it is considered positive.

2.2. Results

The value for 50% parasite growth inhibition, using nine ELQ concentrations, was calculated using a logit-log-transformation (Joachim Müller, IPB). The relative growth (RG) of the control was determined as 1. The logit-log-transformation formula $\ln[\text{RG}/(1-\text{RG})] = a \times \ln(\text{drug concentration}) + b$ was completed and a following regression analysis by an Excel software package “Analysis Tool Pack” (Microsoft, Seattle, WA) was performed to calculate IC₅₀ values. For both ELQs tested, qPCR was run in triplicates. Results are displayed on Figures 12 and 13 and Table 4.

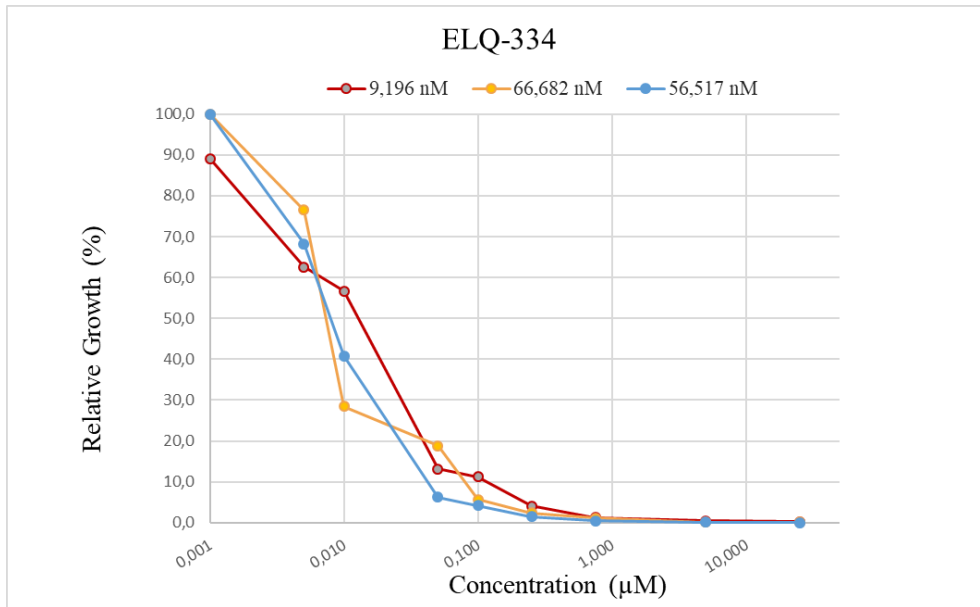


Figure 12. Dose-response curve for ELQ-334 relating the concentration of the compound with the concentration of *B. besnoiti* DNA measured. Each curve is identified by the calculated IC₅₀ value calculated through a logarithmic function.

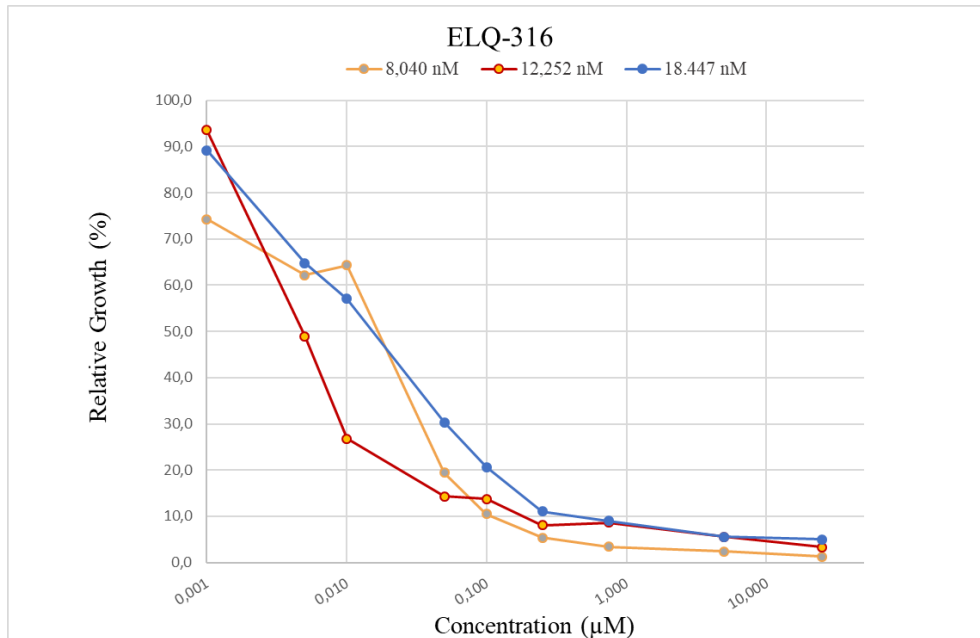


Figure 13. Dose-response curve for ELQ-316 relating the concentration of the compound with the concentration of *B. besnoiti* DNA measured. Each curve is identified by the calculated IC₅₀ value calculated through a logarithmic function.

Table 4. IC₅₀ values for ELQ-316 and ELQ-334 against *B. besnoiti* and *N. caninum*

Compound	Date	IC ₅₀ (nM) for <i>B. besnoiti</i>	X	IC ₅₀ (nM) for <i>N. caninum</i>
ELQ-316	25.09.18	8.040	12.91	0.66
	9.10.18	18.44		
	11.10.18	12.252		
ELQ-334	26.09.18	9.196	44.13	3.33
	12.10.18	66.682		
	18.10.18	56.517		

Table 4. IC₅₀ values calculated for ELQ-316 and its prodrug ELQ-334 against *B. besnoiti* with the corresponding arithmetic mean (X) compared to IC₅₀ values for *N. caninum* assessed by Anghel et al., 2018.

2.3. Discussion and Conclusion

Apicomplexan parasites have a great impact in public health, animal production and welfare. Given that there are no effective agents available to treat bovine besnoitiosis and no vaccines are licensed in Europe, the only strategy to control bovine besnoitiosis is based on herd health management measures (Cortes et al., 2005; Álvarez- García et al., 2013).

The pursuit for an effective treatment against bovine besnoitiosis is not new. Throughout the years, many compounds have been tested against *B. besnoiti in vitro* such as: halofuginone lactate, sulfonamides (Shkap and Pipano, 1987), sulfadiazine (Shkap and Pipano, 1987; Elsheikha and Mansfield, 2004), thiazolides (Cortes et al., 2007), biphenylimidazoazines (Moine et al., 2015), bumped kinase inhibitors (Jiménez-Meléndez et al., 2017), diclazuril and decoquinate (Jiménez-Meléndez et al., 2018), and naphto-quinone buparvaquone (Müller et al., 2019).

Repurposing well-known anticoccidial compounds with proven efficacy against apicomplexan parasites has been used as a viable approach to identify novel therapeutics for

bovine besnoitiosis (Jiménez-Meléndez et al., 2018). Anticoccidial drugs affect the intracellular development of the parasite and many of these compounds can be administrated as food additives or diluted in drinking water, which facilitates the administrations process. However, during the last decades, resistance to anticoccidial drugs has been increasing due to the use in intensive animal production units of anticoccidial commercial compounds for the control of other apicomplexan parasites: *Eimeria* spp., *Sarcocystis* spp., *Cystoisospora* spp. Consequently, the efficacy of prophylactic and therapeutic anticoccidial compounds has decreased in recent years (Ahmad et al., 2016; Cervantes-Valencia et al., 2019). Therefore, the development and use of vaccines and alternative bioactive plant compounds exhibiting natural anticoccidial effects represent a good alternative to synthetic compounds. An interesting study from Cervantes-Valencia et al., 2019 demonstrates the efficacy of curcumin against tachyzoites of *B. besnoiti* *in vitro*. Although the molecular mechanism that confers curcumin antiprotozoal properties is not entirely known, this natural plant-derived compound showed to be active against *B. besnoiti* tachyzoites, with an IC₅₀ value of 5.93µM. Even though the advances and potential compounds active against bovine besnoitiosis, the lack of a suitable *in vivo* model for this disease represents an obstacle for *in vivo* experiments - crucial for further assessments on pharmacokinetics, bioavailability and pharmacodynamics of these options, indispensable for a safe commercialization (Cervantes-Valencia et al., 2019). Potential drug candidates are often evaluated directly in the relevant target host for many veterinary applications (Müller and Hemphill, 2016).

Since only a small number of drugs is available on the market to face a huge number of parasites, it is fair to conclude that the overall supply of treatment options is limited and insufficient. This represents a major concern, particularly in cases where resistance development has taken place, rendering the need for novel and more specific alternative treatment options an urgent issue (Müller and Hemphill, 2016). Based on this concern, it can also be argued that in addition to the need of alternative new therapeutic options, the avoidance of monotherapy could be advantageous on preventing the selection of resistant parasites (Smilkstein et al., 2019).

An effective drug should target the infectious stage of the disease (tachyzoite stage) and affect the dissemination of the parasite into different organs during the acute stage of the disease (Jiménez-Meléndez et al., 2018). For developing antiparasitic drugs, the first step corresponds to an initial screening of compound libraries using suitable *in vitro* culture models (Müller and Hemphill, 2016). As previously reviewed, endochin was initially investigated as an antimalarial drug. Endochin-like quinolones (4-(1H)-quinolone derivatives) exhibit an *in vitro* IC₅₀ value against *Plasmodium falciparum* as low as 0.1 nM, representing selective potent inhibitors of the mitochondrial cytochrome bc1 complex of the parasite (Doggett et al., 2012; Nilsen et al., 2013). Many members of the phylum Apicomplexa have specific biological hallmarks, which allows for cross-species approaches that could be explored for the development of novel therapeutic options (Hemphill et al., 2017).

Doggett et al., 2012 reported the promising efficacy of ELQ-316 against *Toxoplasma gondii*, with an IC₅₀ value of 0.007 nM. In a mouse model, ELQ-316 reduced cyst burden of latent infections by 76-88% (Doggett et al., 2012). ELQ-316 also proved to be active against *Babesia microti*, demonstrating 32% growth inhibition. Moreover, *in vivo* experiments were performed to evaluate the efficacy of its prodrug ELQ-334 against *B. microti*. It was reported that a combination of atovaquone and ELQ-334 treatment resulted in the elimination of parasitaemia with no demonstrable relapse detected in mice followed for up to 95 days after infection (Lawres et al., 2016). *Neospora caninum* also showed to be susceptible to ELQ-316 and ELQ-334, presenting promising IC₅₀ values of 0.66 nM and 3.33 nM respectively (Anghel et al., 2018).

Proliferation inhibition constants are useful to identify potential drug candidates (Müller and Hemphill, 2016). In this assay, *B. besnoiti* tachyzoites were exposed to ELQ-316 and ELQ-334 in nine different concentrations in a 3-day proliferation inhibition assay. Real-Time PCR led to the quantification of the total amount of parasite load for each sample by measuring the accumulation of fluorescent signals. The obtained values were adjusted to achieve the number of tachyzoites per well and then converted in percentage of relative growth. Relative growth in function of the ELQ concentration is shown in Figure 12 and

Figure 13 – as the drug pressure increases, the growth of parasites decreases proving the activity of the compounds against *B. besnoiti*. As previously stated, IC₅₀ values were determined by logit-log transformation and the results are displayed in Table 4. For both compounds, the protocol was repeated three times and the arithmetic mean was calculated - ELQ-316 presented an IC₅₀ value of 12.91nM and ELQ-334 presented an IC₅₀ value of 44.13nM. The obtained values on the present assay are higher than those reported for *T.gondii* and *N. caninum* (Doggett et al., 2012; Anghel et al., 2018). These variations between apicomplexan species could be explained by different individual uptake of drugs and off-target effects species related – resulting in additive or synergistic activity concomitant with cytochrome bc1 inhibition. Variable drug susceptibilities based on slight variations in the molecular target sequences affecting ELQ binding should also be considered as possible causes for IC₅₀ values disparity (Eberhard et al., 2020). It is pertinent to also consider technical deficiencies that may affect the assay's performance. Most relevant obstacles include inadequate storage of samples, mistakes in its preparation, and nucleic acid quality, yielding highly variable results and poor choice of reverse-transcription primers and primers and probes for the PCR, leading to inefficient and less-than-robust assay performance (Bustin et al., 2009).

ELQ-316 and ELQ-334 showed promising activity against *Neospora caninum*, presenting IC₅₀ values of 0.66 µl and 3.33 µl respectively (Anghel et al., 2018). The compounds presented a higher IC₅₀ values when tested against *B. besnoiti* which suggests its efficiency is lower for this parasite. ELQ-316 and its prodrug ELQ-334 are active but less effective against *Besnoitia* than they are against *Neospora*. Hence, it can be concluded that *B. besnoiti* tachyzoites were generally less susceptible to ELQ treatment compared to the closely related *N. caninum* and *T. gondii*.

3. Long Treatment Assay

ELQ-121 showed the lowest IC_{50} value in the primary screening - 0.31nM. In this assay, the compound was evaluated in a prolonged *in vitro* treatment by exposure of infected HFF to ELQ-121 at 2.5 μ M concentration, starting four to five hours after infection. At selected time points (approximately every three days) the compound of two flasks was replaced by medium to stop the treatment. Cultures were further maintained with medium after removal of the drug. The assay had the duration of 20 days (Figure 14).

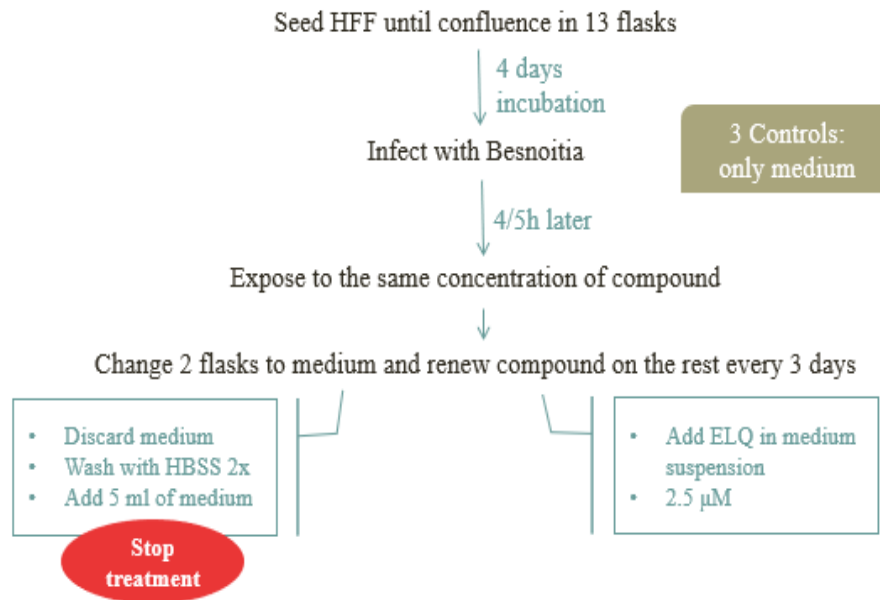


Figure 14. Methods for Long Treatment Experiment. Regrowth of parasites was monitored on daily basis by light microscope for a maximum period of three weeks.

3.1. Methods for Long Treatment Assay

3.1.1. Culture of HFF cells

HFF cells were seeded in 13 T25 tissue culture flasks until confluence following the method described in “2.1.1. Cell culture of human foreskin fibroblasts”. Cells were counted using the Neubauer counting chamber (Figure 8) and 5×10^5 HFF cells were seeded per flask in DMEM. Flasks were then incubated at 37°C and 5% CO₂ for four days. All materials used are specified in the Appendix (2. Materials for Long Treatment Experiment).

3.1.2. Infection of the seeded cells

After four days of incubation, culture tissue flasks were infected with a 5 ml suspension of *Besnoitia besnoiti* strain Bb Lisbon in a ratio of 5×10^5 parasites per flask as described in “2.1.5 Infection of the seeded cells with *B.besnoiti*”.

3.1.3. Positive controls

Three flasks carried the controls. Control cultures were infected with *B. besnoiti* but were not exposed to the compound.

3.1.4. Addition of the compound ELQ-121

For this assay, each flask received the same concentration of the compound (2.5µM) after 4-5 hours of incubation. Incubation time is necessary to allow parasites to infect cells since the compound is added to act intracellularly. The compound ELQ-121 was stored in a stock solution at 10 mM concentration in DMSO at -20°C and diluted in medium DMEM to

a concentration of 2.5 μ M (dilution 1:4000). For a proper handling of the compound, it must be previously heated up to 37°C in a water bath.

Cells were washed with HBSS (Hank's Balanced Salt Solution) twice and the compound was added diluted in 5ml volume of medium. Since control flasks were not treated, only 10 of the 13 flasks received the compound. This corresponds to the day-0 of the experiment, taking place on 11/09/2018. Flasks were incubated at 37°C and 5% CO₂ and parasite growth was observed daily by light microscope.

3.1.5. Renewing the treatment with the compound ELQ-121

Every third day of the experiment, two flasks were withdrawn from treatment and the compound was renewed on the remaining.

To renew the compound medium was discarded, and cells were washed two times with 5ml of HBSS. This washing step removes extracellular parasites on suspension since the aim of the assay is to observe drug-parasite interaction intracellularly. After washing, 5ml of a suspension of medium and ELQ at 2.5 μ M were added to the flasks.

In two flasks, medium (containing the ELQ) was discarded and cells were washed with HBSS twice. To stop each treatment, 5ml of culture medium, without, the compound were added to each flask.

3.1.6. Treatment with increased concentrations of ELQ-121

After nine days of treatment with 2.5 μ M of ELQ, alive parasites were observed on the flasks under light microscope. At this point, it was decided to increase the compound concentration to see parasite's response to a higher drug pressure.

For the effect, ELQ-121 was diluted in DMEM from the stock solution at 10 mM (=10 000 μ M) to the following concentrations: 5 μ M, 7.5 μ M and 10 μ M. On day-9, treatment

was stopped in one flask and the compound was renewed on the remaining in different concentrations as showed in Figure 15.

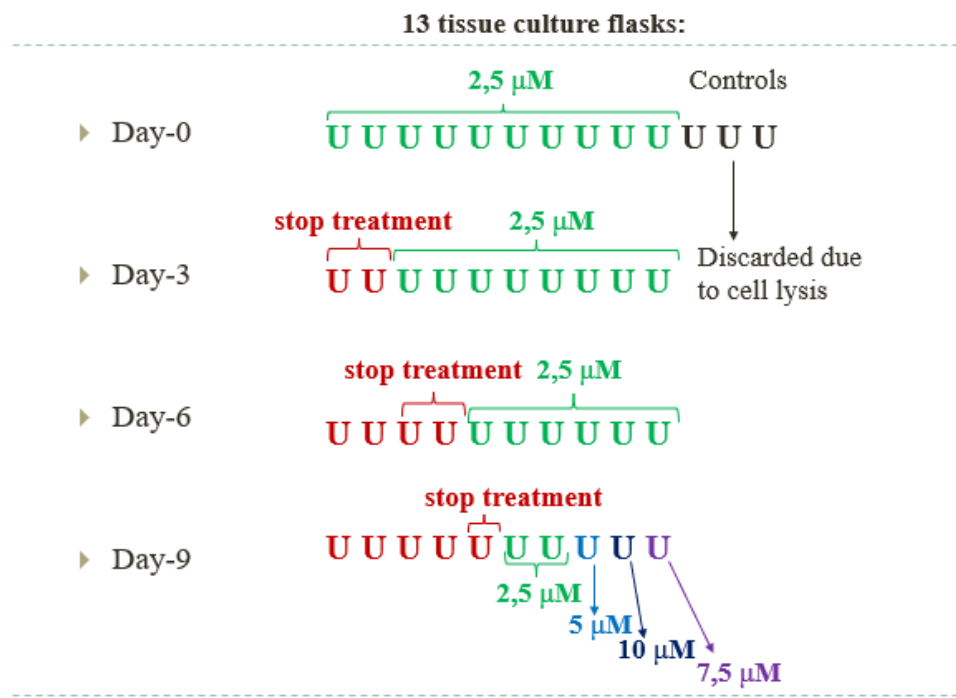


Figure 15. Long treatment experiment since day-0 to day-9. ELQ-121 concentration was increased on day 9; two flasks continued to be exposed to 2.5 μ M of the compound and three flaks were exposed to 5 μ M, 7.5 μ M and 10 μ M.

To renew the compound, medium was discarded and cells were washed two times with 5 ml of HBSS as previously described. The compound was then added at the concentration of 2.5 μ M, 5 μ M, 7.5 μ M and 10 μ M.

3.1.7. Splitting confluent cells

A highly confluent host cell monolayer limits the invasion-surface for parasites, which in turn affects growth conditions. Therefore, upon detection under the light microscope, over confluent cells should be splitted to improve growth conditions.

On day-15 of the experiment, cells were splitted due to their confluence. For splitting the medium was discarded, and cells were washed twice using HBSS. To detach cells, 1.5 ml of trypsin-EDTA were added and the flask was incubated up to 5 min at 37 °C and 5% CO₂. Culture medium was added to stop the trypsin activity after incubation time, in a quantity of at least 1.5 ml. Cells were carefully scraped from the walls and pipetted up and down up to be suspended. Since the parasites were intracellular, cells shouldn't be broken. Infected cells suspension was collected making a volume of at least 3 ml and 1 ml was placed on each one of two flasks, being the last millilitre discarded (splitting 1:3). Medium was added to the flasks: 4 ml per flask, for a final volume of 5 ml. This way, a flask containing confluent cells is splitted in two, allowing parasites to survive and grow.

3.2. Results of long-term treatment with ELQ-121

3.2.1. Day-0 (11.09.18)

Day-0 corresponds to the first day of the experiment. Flasks with seeded HFF cells were infected with *B. besnoiti* and treated using 2.5µM of ELQ-121. Parasite activity was monitored by light microscopy and pictures were taken on approximately every three days (Figures 16 – 24).

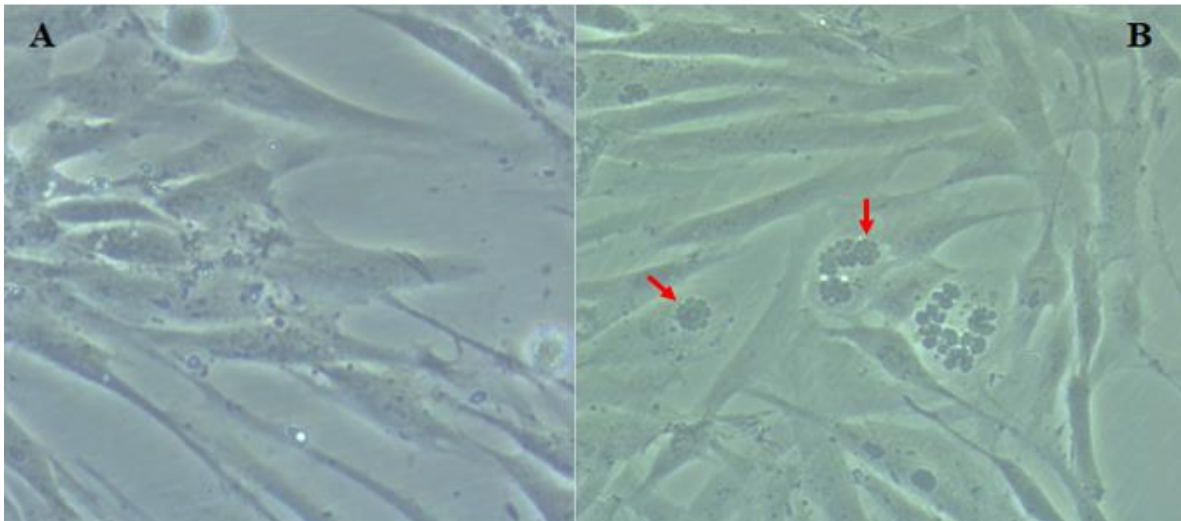


Figure 16. *B. besnoiti* on day-1 (12.09.18). A) ELQ-121 at 2.5 μ M concentration. Extracellular parasites can be observed; B) Control flask, presenting rosette shaped parasitophorous vacuoles (PV)(red arrows).

3.2.2. Day-3 (14.09.18)

Three flasks not exposed to drug pressure were used as control cultures. Parasites proliferated normally on control flasks and the host cell layer was rapidly lysed three to four days post-infection (Figure 17).

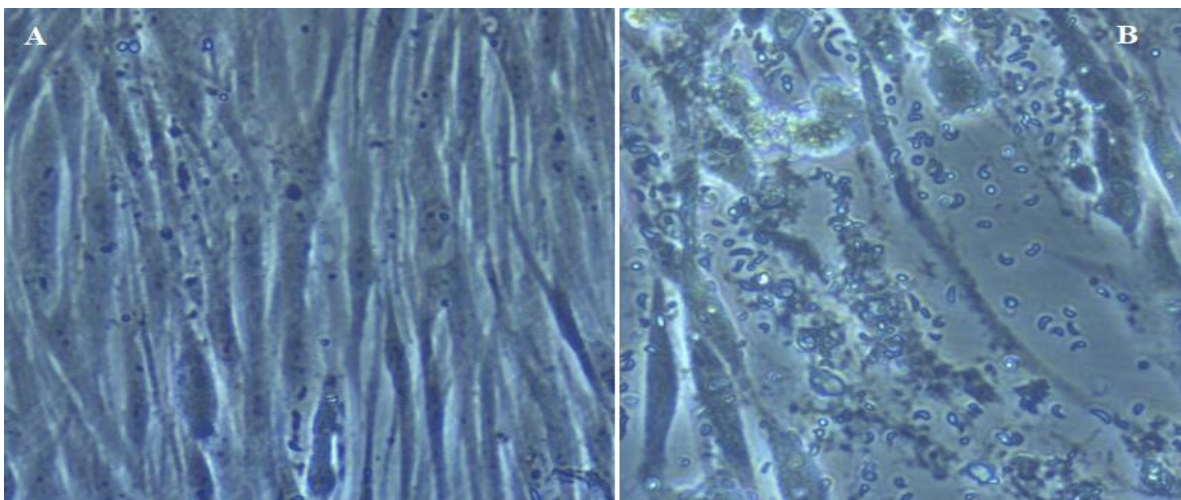


Figure 17. A) *B. besnoiti* after three days of treatment with ELQ-121 at 2.5 μ M concentration with living parasites; B) Control flask, showing big PVs formed by *B. Besnoiti* and lysed cell layer with extracellular parasites.

After three days of treatment tachyzoites presented a rounder shape and proliferation was slowed down when compared to the control. Infected cells not treated on the control showed big parasitophorous vacuoles (PV) and cell lysis due to parasite proliferation at a normal rate. Control flasks were discarded at this time point.

3.2.3. Day-6 (17.09.18)

Abnormal formations such as parasites inside round structures and formations resembling bubbles were detected on day-6 (Figure 18). Nevertheless, morphologically normal PVs were also identified, which indicates that parasites were still proliferating.

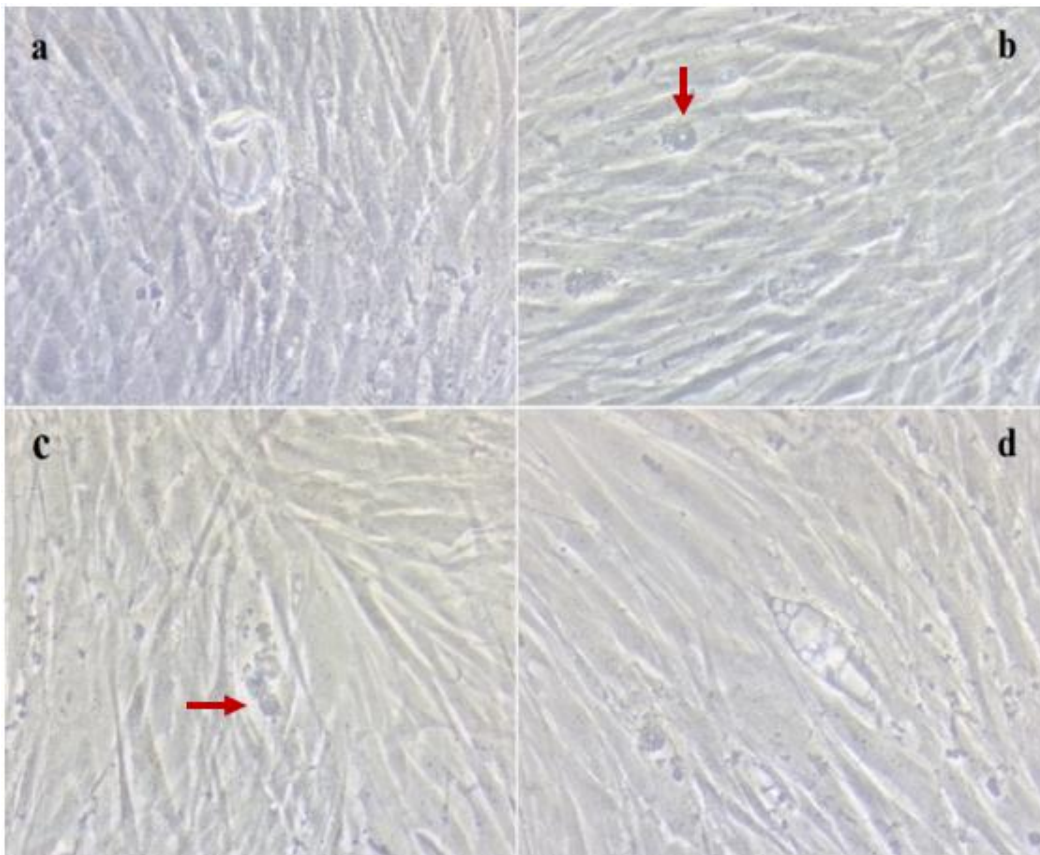


Figure 18. *B. besnoiti* after removal of drug pressure on day-3 (a,b) and after six days of treatment with ELQ-121 at 2.5 μ M. (c,d). a) parasite inside a round structure; b, c) parasitophorous vacuoles with a rosette shape (red arrows); d) abnormal structures resembling bubbles.

3.2.4. Day-9 (20.09.18)

On day-9 of the experiment, some anomalies such as parasites inside round structures and deformed PVs were identified under light microscope, however parasites were still alive and proliferating (Figure 19). At this point, ELQ-121 concentration was increased, thus enhancing drug pressure. The treatment was stopped in one flask and the compound was renewed on the remaining at 5 μM , 7.5 μM and 10 μM .

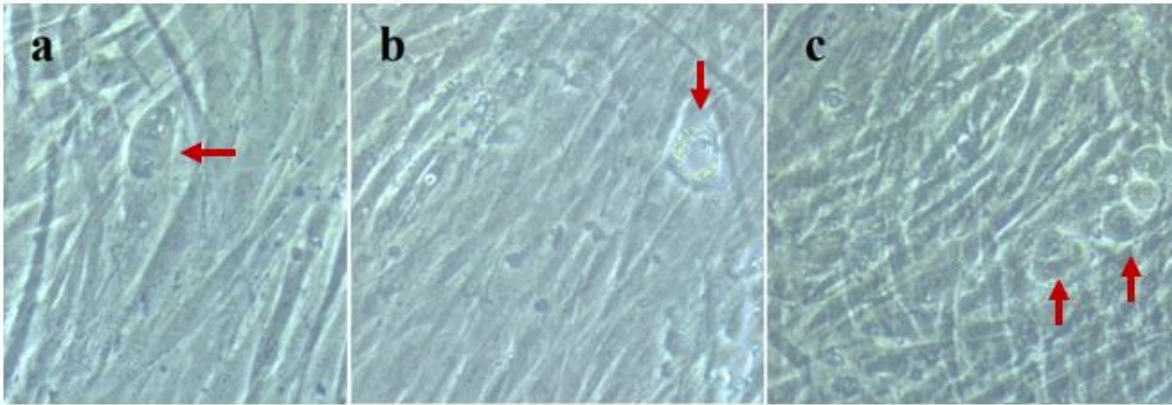


Figure 19. a) *B. besnoiti* after drug removal on day-3. PV (red arrow) and living parasites can be observed; b) *B. besnoiti* after drug removal on day-6. Living parasites and parasites inside a round structure (red arrow) can be observed; c) *B. besnoiti* after nine days of treatment with ELQ-121, 2,5 μM . Living parasites and deformed PVs (red arrows) can be observed.

3.2.5. Day-12 (23.09.18)

Three days after increasing the ELQ concentration, *B. besnoiti* continued to proliferate, invade, and lyse host cells even when exposed to higher concentrations of the compound. Although proliferation rate seems to decrease due to drug pressure, parasites survived and were still able to invade new host cells (Figure 20).

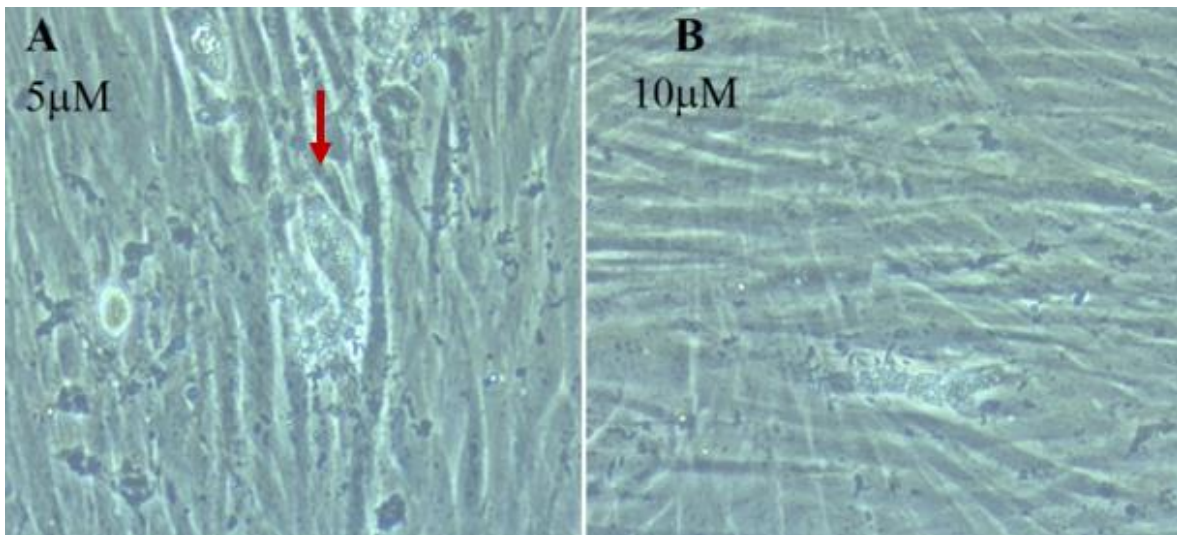


Figure 20. A) *B. besnoiti* treated with ELQ-121 at 5 μM (concentration increased on day-9), a destroyed PV (red arrow) can be observed; B) *B. besnoiti* treated with ELQ-121 at 10 μM (concentration increased on day-9), cell lysis and living parasites were observed.

3.2.6. Day-15 (26.09.18)

After exposure of 2.5 μM ELQ-121 for 15 days, tachyzoites were found alive showing an abnormal shape (looking bigger, swollen and round) and irregular PVs (without the normal rosette shape) were also identified (Figure 21).

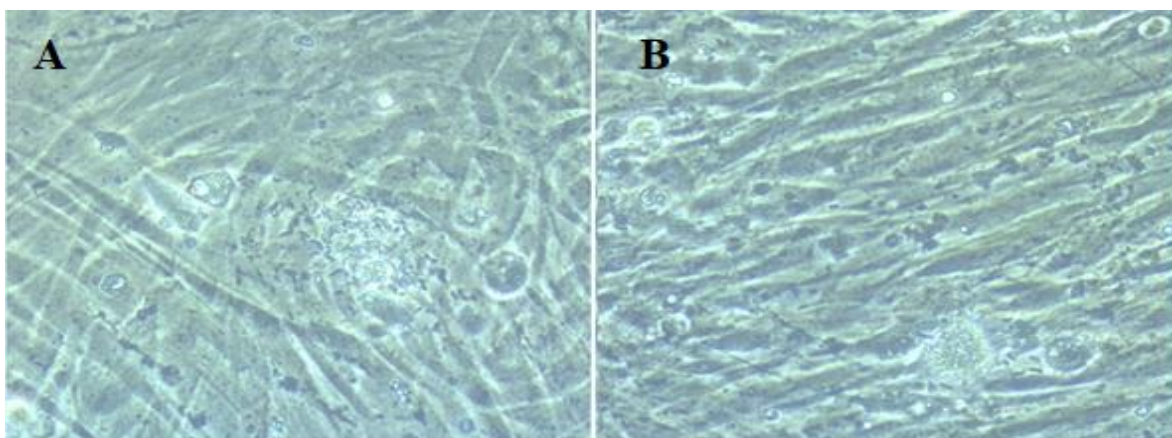


Figure 21. *B. besnoiti* treated with ELQ-121 at 2.5 μM on day-15. A) After 15 days of treatment, parasites still proliferate although some present abnormal shape. B) Several PVs and alive parasites were observed.

3.2.7. Day-20 (01.10.18)

On day-20 of the experiment, parasites were observed alive on flasks treated with ELQ-121 at 2.5 μ M, 5 μ M and 7.5 μ M. The living tachyzoites presented the same previously reported anomalies - a bigger and rounder shape, irregular PVs and abnormal formations similar to bubbles. Parasites appeared very unhealthy but still alive and capable of invading new host cells. At the highest concentration (10 μ M), unhealthy dead parasites were observed (Figure 22).

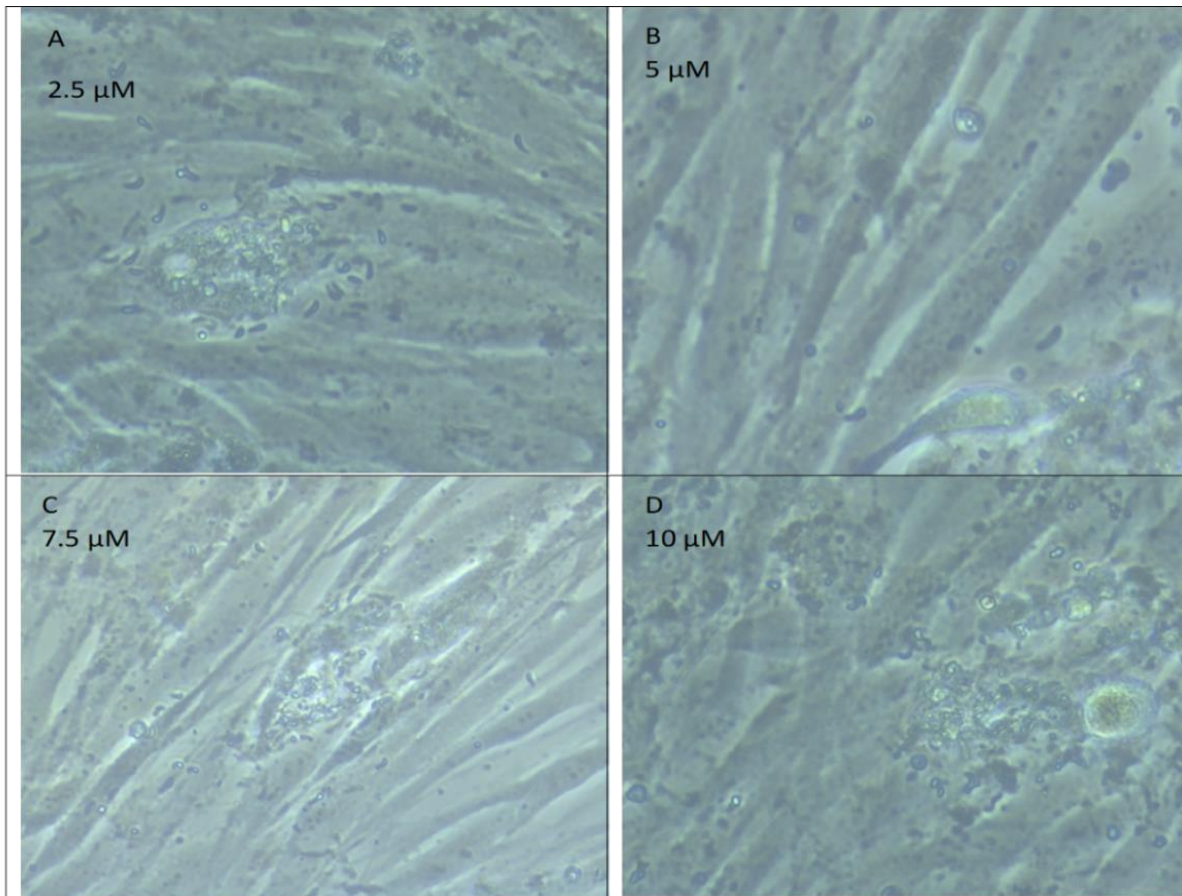


Figure 22. *Besnoitia besnoiti* after 20 days of treatment with ELQ-121 in different concentrations. A, B, C) Living parasites; D - Dead parasites.

Infected cells treated with 2.5 μ M ELQ-121 for three days and removed from treatment showed living and proliferating tachyzoites on day-20. Cells were splitted to allow proliferation of the parasites and assess the effect of the compound after drug release. *B. besnoiti* survived and proliferated on the flask containing splitted cells. Dead parasites were found on the non splitted flask, most likely as result of limiting growth conditions due to the over confluent cell layer (Figure 23).

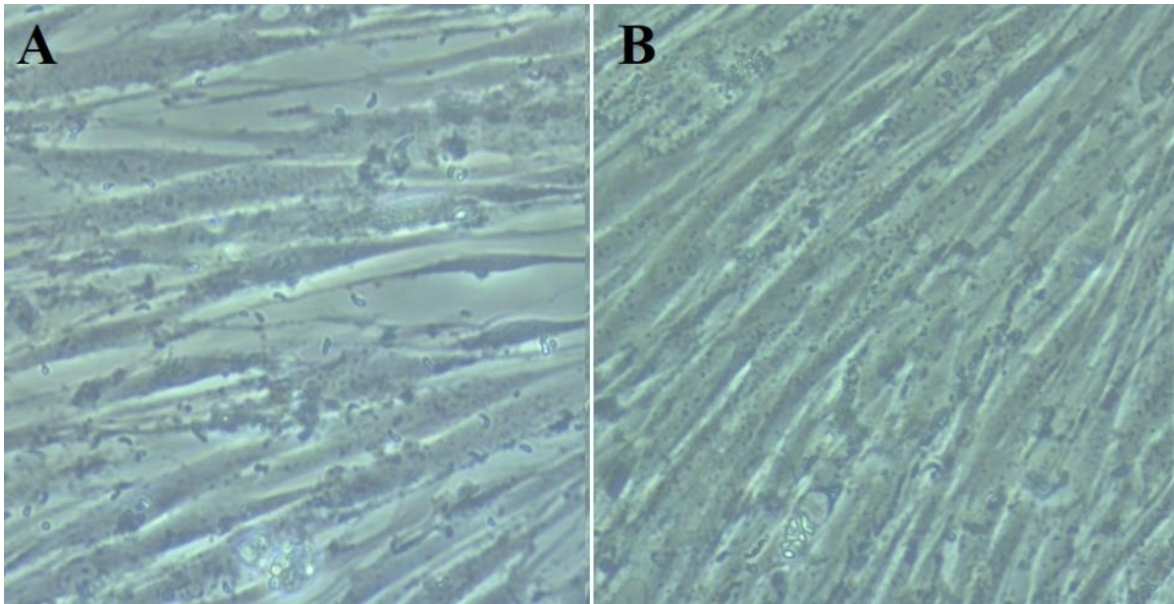


Figure 23. *B. besnoiti* on day-20, treatment with ELQ-121 at 2.5 μ M was interrupted on day-3. A) Non confluent cell layer (flask splitted on day-15) with living parasites. B) Confluent cell layer (non splitted) with living and dead parasites.

After stopping the treatment on day-20, infected cells were kept in culture for 10 days. Past seven days from the withdrawn of the compound (day-27), parasites looked bigger and abnormal PVs could be observed. Figure 24 shows *B. besnoiti* on day-27. Parasites presented anomalies but were still able to proliferate, despite of continuous treatment.

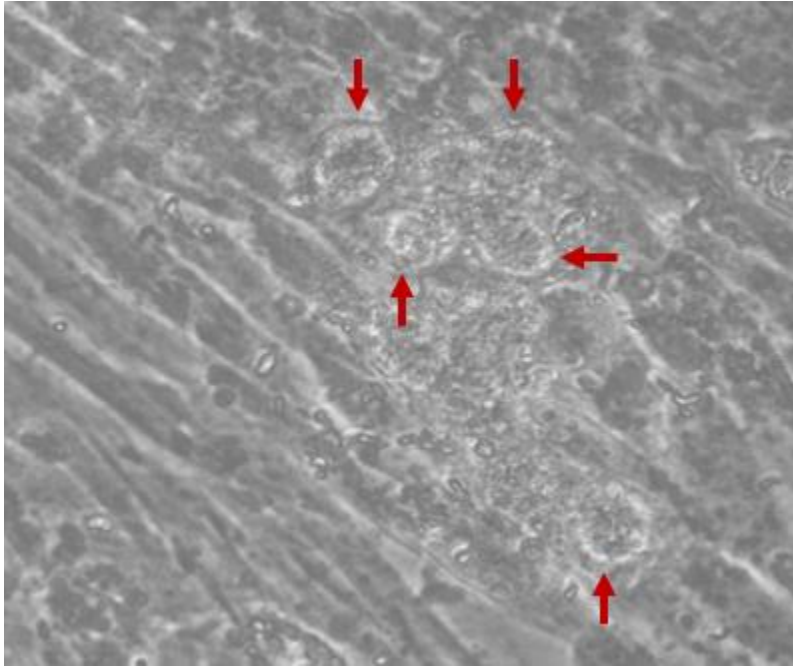


Figure 24. *B. besnoiti* on day-27. Large round parasites and abnormal PVs (red arrows) can be observed.

3.3. Discussion and Conclusion

Long-term assays assume an extraordinary importance on drug development as they allow to assess the activity of a compound through a long period of time. In the Apicomplexa field, long-term assays have been used to study drug sensitivity and adaptation, as well as its prophylactic and parasiticidal potential. Duffy and Avery, 2017, for instance, performed a long-term assay to study the influence of continuous culturing conditions on tolerance and susceptibility of *Plasmodium falciparum* to anti-malarial drugs. It was assessed that different *in vitro* conditions on the same parasite stock could be manifested in transcriptional variation of the parasite and altered tolerance and sensitivity to a range of anti-malarial compounds at different stages of their intra-erythrocytic life cycle (Duffy and Avery, 2017).

As previously reviewed, parasite resistance is a challenging issue to overcome on the development of novel drugs, and long-term trials can represent a method for detection of drug resistance or adaptation. In their work, Kaminsky et al. 1993 evaluate the viability of a long-term assay to detect a single or very small number of hidden resistant parasites in a sensitive population of *Trypanosoma* spp. It was concluded that by employing a long-term assay (7-10 days), sufficient observation time is provided to detect a reduced number of organisms (Kaminsky and Brun, 1993).

In the absence of effective treatment, a reality for many apicomplexans, preventive drugs represent a great option for control of parasitosis. To assess the prophylactic potential of a candidate drug, its effects on the target organism must be effective for a long period of time to assure prolonged protection. Therefore, long-term assays constitute an important method to successfully examine drug distribution, efficacy, and availability *in vivo* over a long period of time. Such method was used to assess the feasibility of ELQ-331 (ELQ-300 prodrug) to achieve duration of protection against malaria, using an altered strain of *Plasmodium yoelii*. Long-term trials were conducted *in vivo* on a mouse model, through injection of the compound and ELQ concentration measurements at a series of timepoints from 6 h to 5½ months after injection. It was demonstrated that the slow distribution of ELQ-

300 in the blood enables its sustained concentration above a minimum fully-protective threshold (60–80 nM), which supports the viability of ELQ-331 to achieve duration of protection against malaria for at least three months (Smilkstein et al., 2019).

Finally, long-term assays are frequently used after determination of proliferation inhibition constants of a compound - such as the IC_{50} - to evaluate its effects on parasites proliferation on a continuous treatment model. The IC_{50} of ELQ-316 and ELQ-334 against *Neospora caninum* tachyzoites was determined by Anghel et al., 2018 as previously reviewed, and thereafter assessed in long-term treatment assay. Infected HFF cells were exposed to the ELQs at a concentration of 0.5 μ M after 3 h of infection and underwent continuous treatment for extended periods of time, ranging from 3 to 17 days. Continuous treatment resulted in decreased proliferation and a delay of host cell lysis, yet it did not have a parasitocidal effect as parasites still survived (Anghel et al., 2018).

ELQ-121 has proven to be an effective inhibitor of *B. besnoiti* tachyzoites growth (Table 1). Therefore, it was selected to be tested in a long-term treatment assay by exposure of infected HFF cells to the compound at an initial concentration of 2.5 μ M. HFF cells are known to present a slower growth rate when compared to other culture cells such as Vero cells. This represents an advantage in long-term assays, as it reduces the frequency of the need to split confluent cells. This assay had the duration of 20 days and was followed by the release of drug pressure. After only three days of treatment (Figure 17), tachyzoites were found presenting a rounder shape and proliferation was slowed down when compared to the control, that showed big healthy parasitophorous vacuoles (PV) and cell lysis due to parasite proliferation at a normal rate. Continuous treatment at the same concentration led to a decrease on parasite proliferation but living parasites and PVs could still be observed after six days. At this point, abnormal formations such as parasites inside round structures were noted, as well as deficient PVs and structures resembling bubbles (Figure 18).

After increasing drug pressure on day-9, *B. besnoiti* continued to proliferate, invade, and lyse host cells (Figure 20). Parasites were still alive on flasks treated with ELQ-121 at 2.5 μ M, 5 μ M and 7.5 μ M on day-20 of the experiment. However, at the highest concentration

(10 μ M) unhealthy and dead parasites could also be observed (Figure 22). Living parasites appeared very unhealthy but still alive and capable of invading new host cells. Ending treatment on all flasks (after 20 days of treatment), infected cultures were kept for 10 more days. Seven days after the withdrawn of the compound (day-27), parasites were alive, displaying the anomalies detected throughout the assay: abnormal PVs with bigger volume were observed. Even after continuous treatment, parasites presented anomalies but were still able to proliferate after drug removal.

Prolonged *in vitro* treatment of *B. besnoiti* tachyzoites with ELQ-121 has shown to be parasitostatic but not parasitocidal. Invasion of host cells and egress seem to be inhibited; however, parasites still survive and proliferate. The available energy inside the parasites for invasion is deficient - but parasites were still able of proliferating at a slower rate. The parasites also continued to proliferate, invade, and lyse host cells after drug pressure ceased.

To further evaluate ultrastructural changes on tachyzoites, samples should be analyzed under the Transmission Electron Microscope (TEM).

4. Transmission Electron Microscopy Assay

Transmission electron microscope (TEM) is a valuable tool to evaluate drug effects on internal organelles of tachyzoites and their host cells. By providing high magnification images of the internal structure of a sample, this technology can provide insights on cellular interactions with new drugs (Marturi, 2015). TEM is a microscopy technique based on the transmission of electron beams through the specimen that produce an image on fluorescent screens (Tizro et al., 2019) (Figure 25).

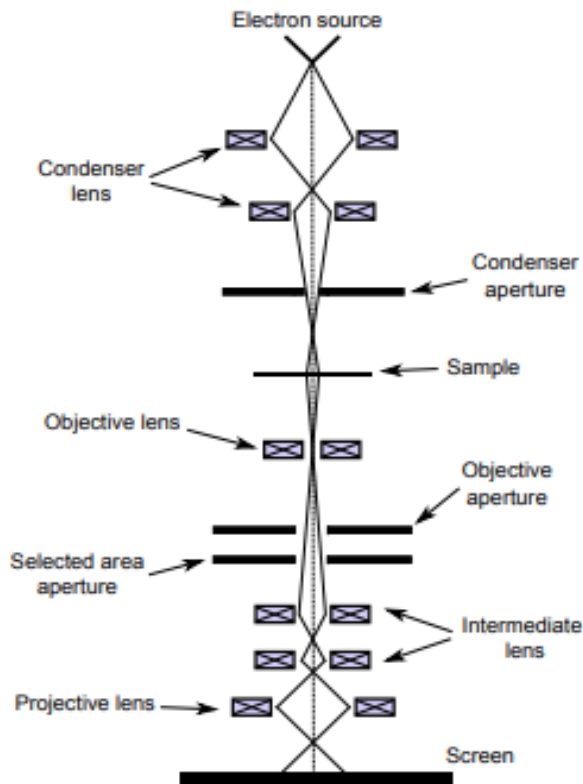


Figure 25. General layout of a TEM describing the path of electron beam. Electrons enter the condenser system, composed by one or two lenses creating a magnetic field that focuses and constricts electrons into a thin beam. The beam of electrons produced is transmitted through the sample and into another series of electromagnetic lenses that focus the electrons onto a fluorescent screen at the bottom of the microscope to create the image. Generally, the images produced by TEM are grey scale: the lighter areas correspond to the higher number of electrons transmitted and the darker areas represent lower number of electrons transmitted - dense areas on the sample. (Marturi, 2015).

In this assay, the effects of ELQ-316 on *Neospora caninum* tachyzoites were analyzed using TEM. Samples of HFF cells infected with *N. caninum* tachyzoites treated with 1µM ELQ-316 after 12 hours, 24h and 48h (as well as a non-treated sample as control) were kindly provided by Nicoleta Anghel.

4.1. Methods for TEM Assay

For a good visualization under TEM, samples must be highly infected and <100 nm thick so that the electrons can pass and stop only where stains delineate objects of interest (Harris et al., 2006). All materials used are listed in the Appendix (3. Materials for Transmission Electron Microscopy Assay).

4.1.1. Embedding samples

EPON embedding is essential to provide a hard support to the samples and protection from the mechanical forces associated with sectioning. *N. caninum* samples used for this assay were already embedded. Nevertheless, a brief review of the process is relevant.

In summary, embedding samples begins with a first fixation using 5 ml of 2% glutaraldehyde in 0.1 M Na-cacodylate buffer for 10 min at room temperature. After scraping the cell layer with a cell scraper, cells were transferred to 15ml falcon tubes and centrifuged for 10 min at 4 °C and 1'200 rpm – followed by overnight incubation at 4°C. Samples were then centrifuged for 5 min, 1200 rpm at 4°C and washed thrice with 0.1 M Na-cacodylate-buffer (being centrifuged at the same conditions between each wash). Osmium tetroxide solution (2% in 0.1 M Na-cacodylate buffer at pH 7.3) was added in the volume of 1ml and samples were incubated for one hour at room temperature (22/24°C). Samples were washed three times using water and centrifuged at 1800 rpm for 5 min, after each wash, at 4°C. Approximately 50µl UranylLess spray were added and samples were incubated for 30 min at room temperature, followed by washing three times with water as previously described. Water was removed and dehydration was performed with increasing

concentrations of ethanol (30%, 50%, 70%, 90%, and 100%). For the effect, 1 ml of ethanol was added, and samples were centrifuged for one minute at 800 rpm, 20°C. To complete the dehydration, ethanol at 100% was added three times, interspersed with incubation and samples were then transferred into Eppendorf tubes. After removing ethanol, Eppendorf tubes were filled with EPON resin and incubated in the water bath (37°C) for 30 min. Tubes were centrifuged at 25°C for a total of 14 min at full speed, and the resin was taken out and renewed. The centrifugation after addition of the resin includes turning the tube 180° in the centrifuge at half time to centrifuge each side of sample and form an even pellet on the ground of the tube. Samples were incubated for one hour in water bath and centrifuged again for 30 min. Resin was renewed and samples were incubated for one to two hours in water bath at 37°C followed by centrifugation for one hour. Resin was let to infiltrate the sample for 24 h at room temperature and samples were finally incubated overnight at 60°C in the oven.

4.1.2. Sectioning of embedded samples in EPON

The process of cutting specimens into ultrathin sections is known as ultramicrotomy (Tizro et al., 2019). The EPON block was initially trimmed in a trapezoid shape using a regular scalpel blade to decrease pressure applied to the section when cut by the ultramicrotome (Figure 26).

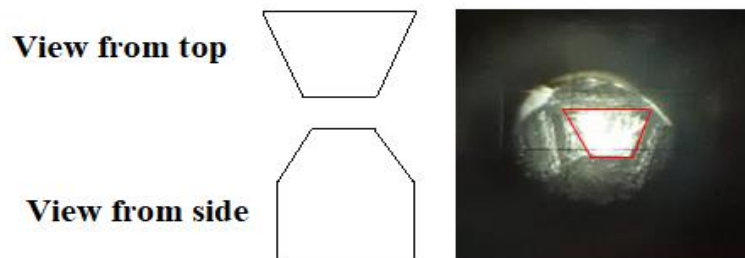


Figure 26. Trapezoid cut on the EPON block.

Once the trapezoid shape was attained, a diamond knife was placed on the ultramicrotome and the base of the trapezoid was aligned to the edge of the knife. The knife basin was filled with water, where ultra-thin sections float after cutting (Figure 27).

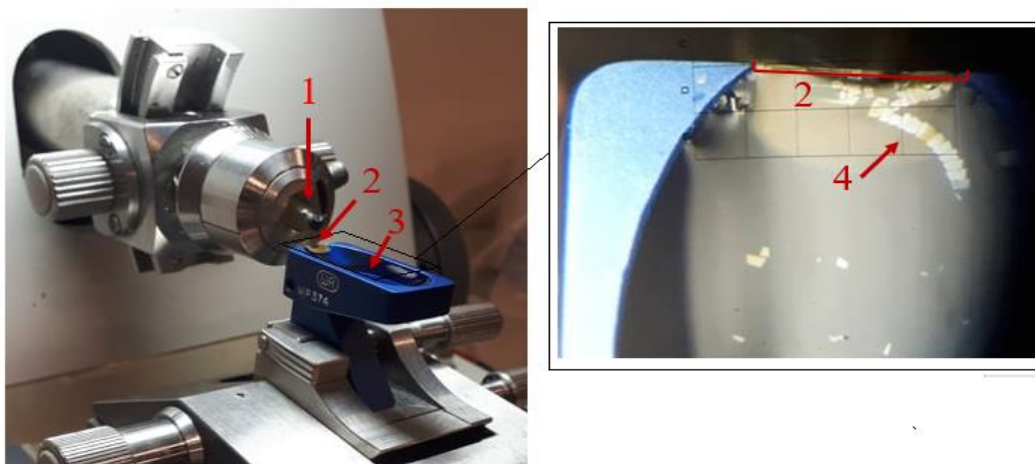


Figure 27. Ultramicrotome. 1) EPON block; 2) Diamond knife; 3) Water; 4) Ultra-thin cut sections. Sections show different colours, since the light reflects in different ways depending on the sample's thickness. The colours corresponding to the aimed thickness are yellow and gold.

4.1.3. Stretching the samples on the surface of the water

Samples must be stretched to alleviate compression and to obtain a better-quality image under TEM. A chloroform impregnated brush was carefully waved over the cut sections to stretch and straighten them. This step facilitates the section collection on the grids and prevents the sections to look wrinkled under the TEM.

4.1.4. Collection of samples to the grids

Using small regular tweezers, yellow and gold coloured sections were carefully collected and transferred to Athene Nickel 300/3.05-mesh copper grids.

4.1.5. Staining of samples for TEM

The classic processing of biological specimens to be analysed under TEM needs fixation, dehydration and a selective staining of structures. Enhancement of structures for TEM was performed with heavy metal salts. To stain the samples, Uranyless EM Stain protocol was followed. Uranyless is a new, commercially available non-radioactive staining reagent that can be used as an alternative to uranyl acetate. It is indicated to biological samples fixed with glutaraldehyde, osmium or ruthenium and embedded in an epoxy type resin.

To perform a classic contrast staining, UranylLess and lead citrate were used. A drop of UranylLess was placed on parafilm, a hydrophobic surface. The grid containing the sample was placed on the drop for one to two minutes, allowing the sections to be in contact with the liquid. The grid was then blotted using filter paper, washed with distilled water, and let to dry. After drying, lead citrate staining was performed by placing the grid on a drop of lead citrate for around three minutes. To prevent contamination of the sections with precipitated stain products, staining with lead citrate should be performed in an environment largely devoid of CO₂ (Reynolds, 1963). Therefore, sodium hydro-carbonate pellets were used aside the samples for this procedure and covered with a plate to achieve an environment with less CO₂. Thereafter the grids were blotted on a filter paper and washed with distilled water.

4.2. Results of TEM evaluation

Samples of *N. caninum* tachyzoites treated with ELQ-316 at 1 µM after 12h, 24h and 48h (as well as a non-treated sample as control) were observed on FEI Tecnai Spirit BioTwin TEM operating at 80 kV. Figures 28 – 32 report the results.

4.2.1. *N. caninum* tachyzoites treated with ELQ-316 after 12h

A non-treated sample of HFF cells infected with *N. caninum* acted as a control -
Figure 28.

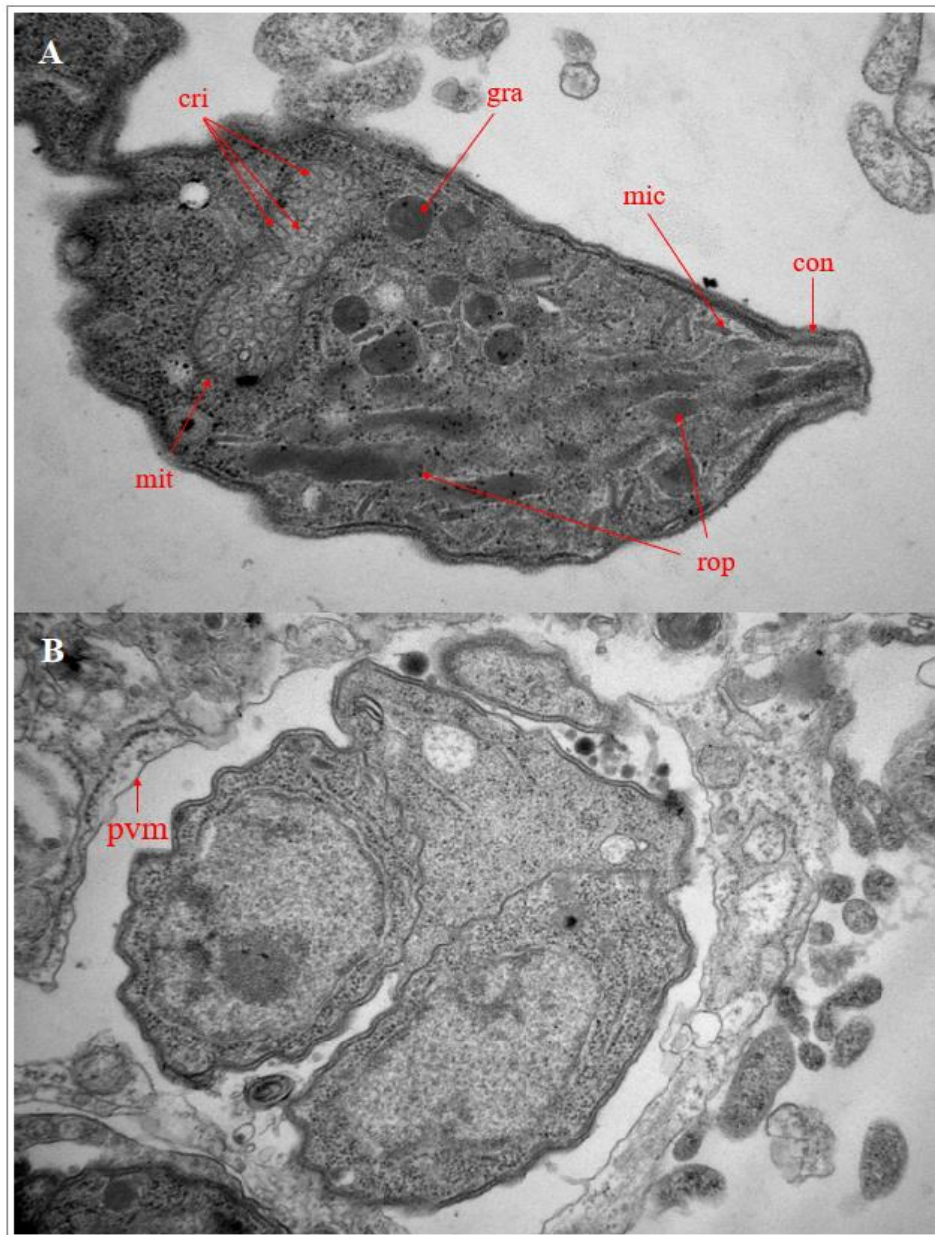


Figure 28. TEM picture of control. A) *N. caninum* tachyzoite non-treated with normal internal structures. cri: cristae; gra: dense granules; mic: micronemes; con: conoid; mit: mitochondria; rop: rhoptries; B) Tachyzoites within a parasitophorous vacuole delineated by a parasitophorous vacuole membrane (pvm).

Without drug pressure, tachyzoites presented normal structures characteristic of apicomplexan parasites such as the apical complex with the conoid, micronemes, rhoptries and dense granules. Structurally intact tachyzoites located within a parasitophorous vacuole enclosed by a parasitophorous vacuole membrane (pvm) could be observed. The mitochondria in the control picture showed normal tubular structure, a dense mitochondrial matrix and structured cristae (folds created by the inner membrane).

After 12h of treatment with ELQ-316 (Figure 29), parasites remained intact, presenting normal structures similar to the control. However, minor alterations regarding the mitochondria were noted in some tachyzoites. Mitochondria presented an abnormal shape and the central matrix was lighter, representing a decreased density when compared to the control. No other organelle registered any alterations.

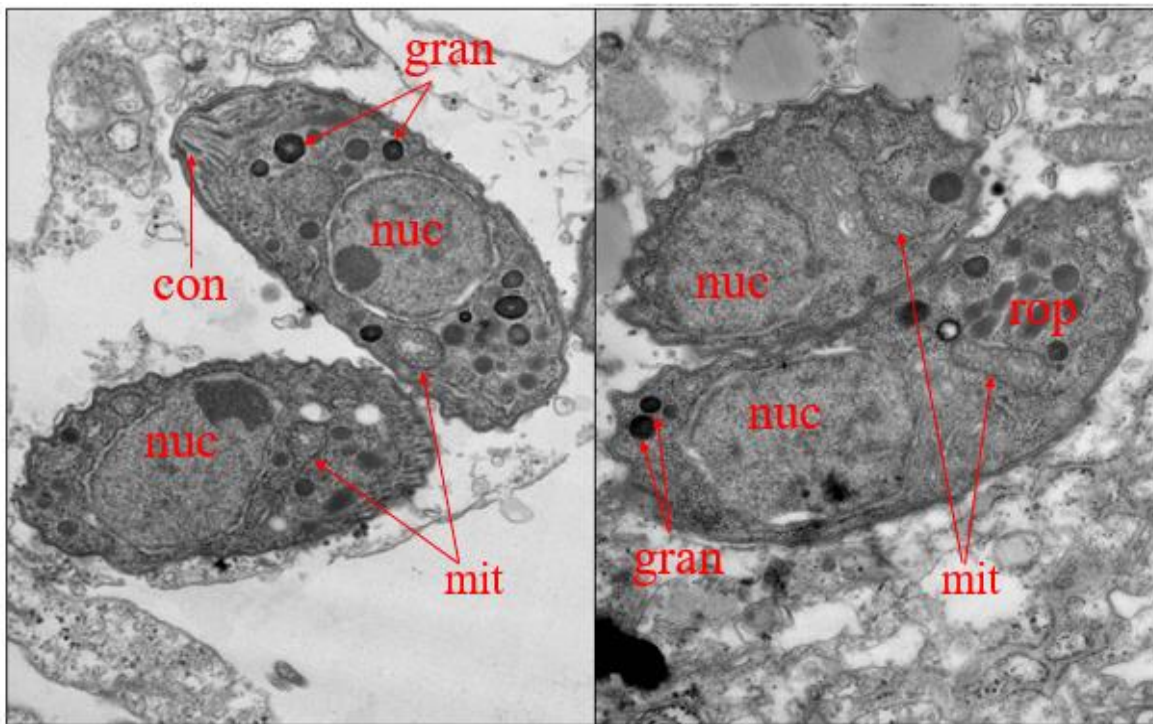


Figure 29. *N. caninum* tachyzoites treated with ELQ-316 at 12h. nuc: nucleous; gran: dense granules; mic: micronemes; con: conoid; mit: mitochondria; rop: rhoptries.

4.2.2. *N. caninum* tachyzoites treated with ELQ-316 after 24h

At this point, mitochondrial alterations were clearly visible. In Figure 30, the mitochondria adopted an abnormal shape and seemed to have an inclusion in the matrix. Intracellular vesicular structures on the tachyzoite cytoplasm possibly corresponding to lipid inclusions were also observed. Figure 31 shows intracellular vesicular structures as well and a damaged increased size mitochondrion with less dense matrix.

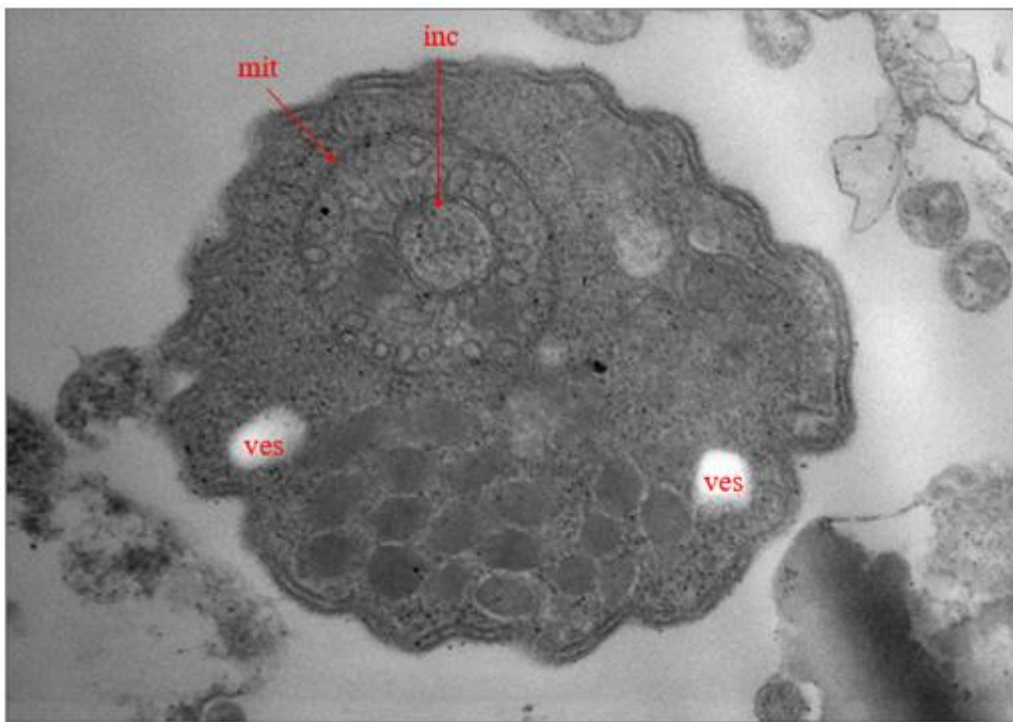


Figure 30. N. caninum tachyzoite treated with ELQ-316 at 24h. mit: mitochondria; inc: inclusion; ves: intracellular vesicular structures.

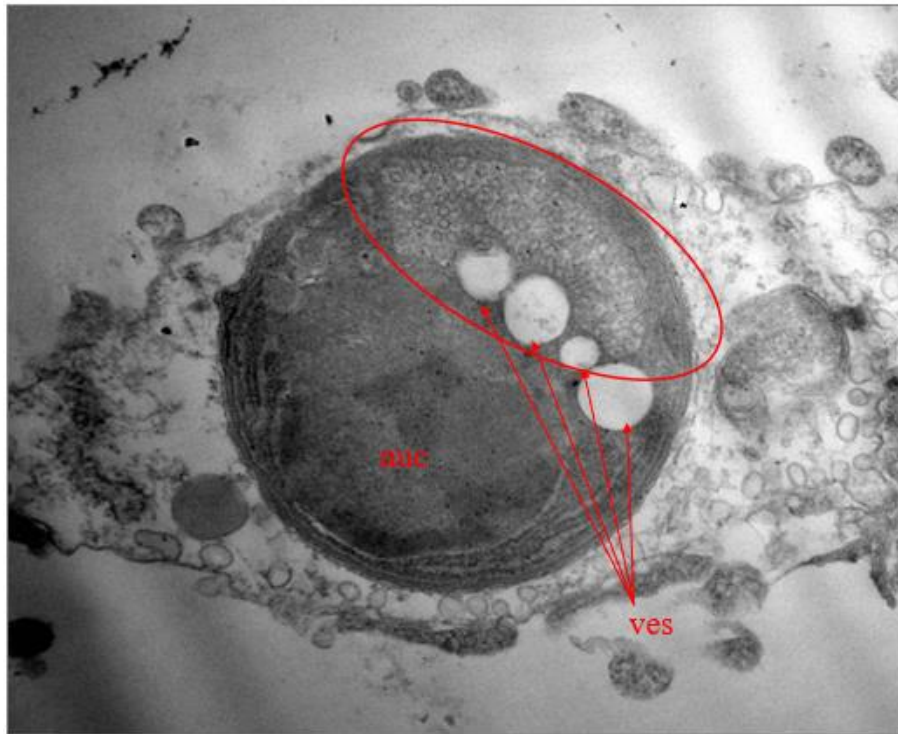


Figure 31. N. caninum tachyzoite treated with ELQ-316 at 24h. The encircled area indicates the mitochondria. inc: inclusion; ves: intracellular vesicular structures; nuc: nucleous.

4.2.3. *N. caninum* tachyzoites treated with ELQ-316 after 48h

Dead parasites could be observed after 48 h of treatment - many of them as extracellular parasites - and the living ones presented severe damage to the mitochondria, although the remaining organelles presented no alterations (Figure 32). The size of the mitochondria was increased, the matrix became lighter and therefore less dense in the central area and cristae seemed to be less structured.

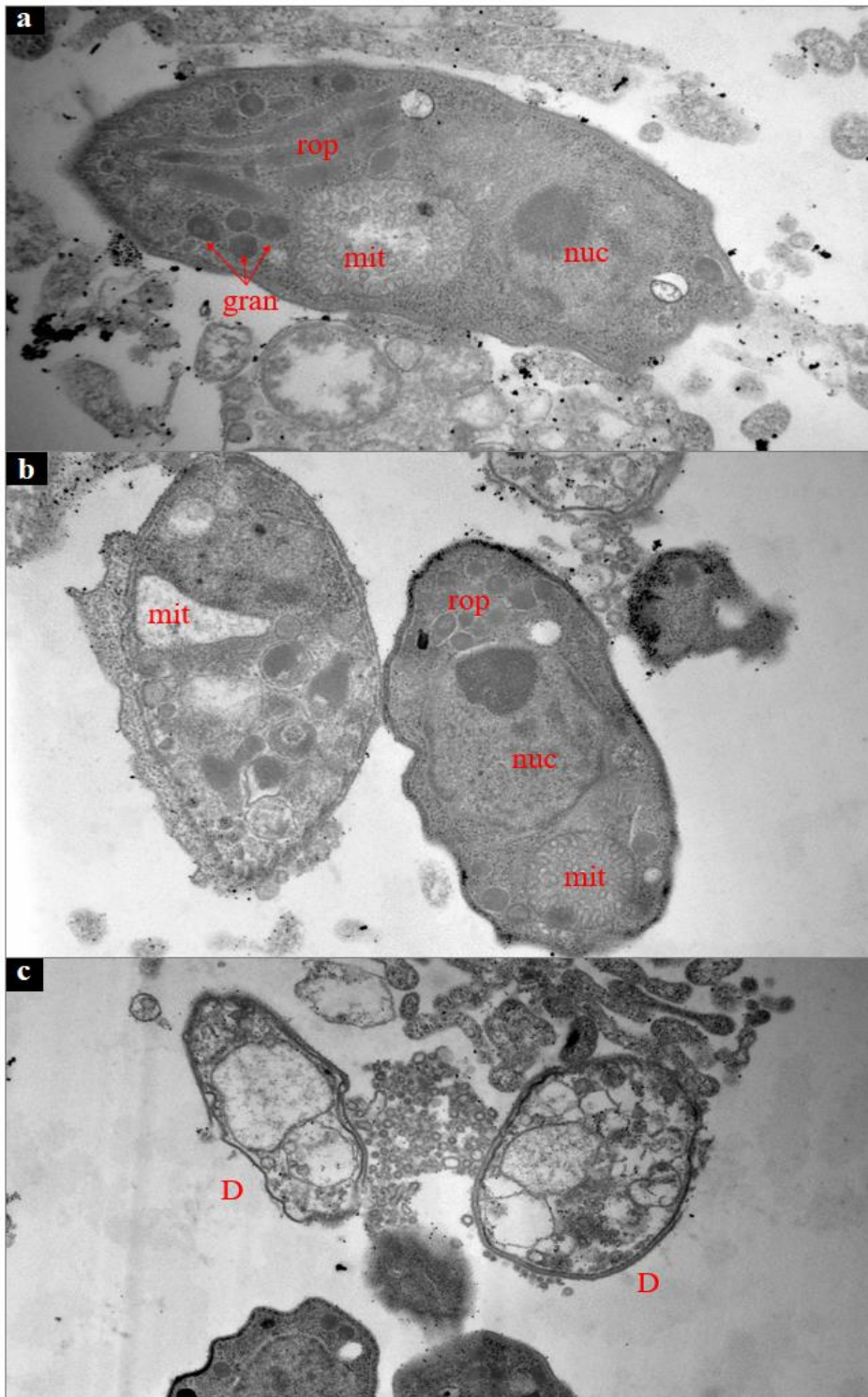


Figure 32. a, b, c) *N. caninum* tachyzoites treated with ELQ-316 at 48h. Alterations in the mitochondria (a,b) and dead parasites (c) can be observed. nuc: nucleus; gran: dense granules; mit: mitochondria; rop: rhoptries; D: dead parasite.

4.3. Discussion and Conclusion

The great potential of TEM is to study individual cells and single events in cell biology, as it allows for a high magnification and an outstanding resolution 10 to 100 times higher than light microscopy. Light microscopy, however, assumes an important role for TEM since in most of the cases its high magnification hinders the search for the cell or event of interest within the sample, like the famous “needle in the haystack”. Therefore, combining light microscopy to identify an area of interest in the sample with TEM has been advantageous. The observed area by light microscopy can then be analysed by electron microscopy at high resolution to define a specific cell and its interactions in a large area. The power of electron microscopy to reveal interactions at the ultrastructural level makes this technology a valuable tool on the research of host-parasite interaction on apicomplexan parasites (Loussert et al., 2012).

The morphological changes on *N. caninum* tachyzoites associated with ELQ-316 treatment were assessed by TEM. The IC_{50} value for this ELQ was determined at 0.66nM and *N. caninum* tachyzoites were exposed to ELQ-316 at 1 μ M. This concentration does not disrupt cell integrity yet applies maximum drug pressure (Anghel et al., 2018; Eberhard et al., 2020). Samples were fixed and prepared for TEM after 12 hours, 24h and 48h of treatment.

Tachyzoites presented classic structures characteristic of apicomplexan parasites on the non-treated control (Figure 28). Intact tachyzoites located within a parasitophorous vacuole (PV) enclosed by a parasitophorous vacuole membrane (pvm) inside the host cell with the distinctive apical complex were observed. The apical complex contains the conoid, micronemes, rhoptries, and dense granules; clearly visible under the high magnification of TEM. The single mitochondrion presented a normal tubular structure, numerous cristae, and an electron dense matrix.

After 12h of treatment with ELQ-316 (Figure 29), minor alterations regarding the mitochondria were noted in some tachyzoites. The mitochondria presented an abnormal shape and the matrix central was lighter when compared to the control, which represents decreased density. At this stage, no other organelle registered any changes, remaining intact.

On figure 30, 24 h post-treatment, mitochondrial alterations seem enhanced. The mitochondria adopted an abnormal form and showed an inclusion in the matrix. Intracellular vesicular structures on the cytoplasm of the tachyzoite possibly corresponding to lipid inclusions were also observed. These round bodies resemble amylopectin granules characteristic of *T. gondii* bradyzoites in tissue cysts. Although the function of these granules storage is not fully understood, amylopectin energy metabolism is hypothesized to be an energy reservoir as a way for the parasitic adaptation to environmental changes (Sugi et al., 2017). Given that ELQs affect the electron transport chain of the mitochondria thus disrupting ATP synthesis, an adaptive survival method could be changing the energy source from oxidative phosphorylation to glycolysis. The mitochondria is the target of ELQ-316 activity; its decrease of matrix density affects the energy production system of the parasite since both characteristic electron dense matrix and cristae are essential for energy production and synthesis of intermediate metabolites such as pyrimidine (Anghel et al., 2018). A damaged increased size mitochondrion with less dense matrix is highlighted in Figure 31.

Structural changes of the mitochondria became even more visible after 48h of treatment (Figure 32). Dead parasites were found at this point, and the living ones presented severe damage to the mitochondria: increased size, matrix became lighter and therefore less dense in the central area and cristae seemed to be less structured. By compromising the ETC, toxic free radicals and ROS can be released. Therefore, in addition to the promotion of glycolysis as the energy source, it seems that discharging of a structurally intact mitochondria is a strategy to prevent adverse effects due to the accumulation of prejudicial metabolites (Eberhard et al., 2020).

Alterations on *N. caninum* tachyzoites can be noticed especially after 24-48h after continued treatment with ELQ-316. The overall internal organization and organelles were

not affected by the drug except for the mitochondria. Unhealthy mitochondria were found, presenting increased size, abnormal form, and internal disorganization. Dead parasites could be observed after 48 h of treatment; however, the drug cannot be considered to have a parasitocidal effect on the tachyzoites.

Therefore, it can be concluded that ELQ-316 affects the mitochondrial integrity but does not induce the rapid death of the parasite, thus having a parasitostatic effect. TEM visualization also revealed the remarkable adaptive potential of the parasite by possibly adopting structural and metabolic alterations to face drug pressure.

III. Monography: “*sag1* gene knock-out on *Neospora caninum* using CRISPR/Cas9”

1. Introduction

1.1. Identification of targets

To successfully discover and develop an effective treatment, the identification of the biological aetiology of a disease as well as potential targets for intervention represent the starting point of a research. Target identification is based on various methods and technologies of genetic manipulation - such as genome sequencing that can provide important information on a pathogen’s molecular biology, and classical transfection allied to gene editing for functional studies (Hemphill et al., 2017).

Apicomplexan research is associated with the maintenance of *in vitro* parasite cultures, the accessibility of complete, well annotated genomes, and functional tools for genetic manipulation. The most used genetic manipulation methods include classic transfections based on the insertion of exogenous DNA applying homologous recombination mechanisms. Recently, the Clustered Regularly Interspaced Short Palindromic Repeats associated with protein Cas9 (CRISPR/Cas9) has proven to be an effective genome editing method (Suarez et al., 2017).

Site-specific alterations of the genome are key in decoding and modifying the genomic information of an organism (Shen et al., 2017). Over the last couple of years, the RNA guided Cas9 nucleases resulting from the prokaryotic type II CRISPR systems have greatly improved the ability of engineering the genomes of a variety of organisms (Shen et al., 2017), being successfully applied to *Cryptosporidium* spp. and *Toxoplasma* spp. (Suarez et al., 2017). In association, CRISPR and Cas9 are able to target and cut almost any DNA *in vivo* and, combined with transfection techniques, they have quickly become valuable as

efficient and specific tools for gene editing (Suarez et al., 2017). CRISPR/Cas9 system-based techniques are already contributing to additional gene function discovery, encouraging the development of new and more effective methods for disease control (Hemphill et al., 2017).

1.1.1. The CRISPR/Cas system

CRISPR is a common adaptive immune system used by bacteria and archaea (Shen et al., 2017). This bacterial host defence system functions analogously to vertebrate adaptive immunity by creating records of previous infections to trigger a prompt and strong response upon reinfection (Wright et al., 2016). CRISPR system provides RNA-mediated immunity against viruses and plasmids based on the ability of copying and specifically cutting exogenous genetic materials (Suarez et al., 2017).

CRISPR *loci* were first identified in *Escherichia coli* in 1987, but only in 2005 it was found that spacers derive from viral genomes and conjugative plasmids. In 2007, it was shown that a spacer genetically matching a phage immunizes the host against the corresponding phage. In addition, it was also revealed that the CRISPR array is expanded by inclusion of new spacers from the phage genome (Wright et al., 2016).

The CRISPR array consists of several repeated sequences of 20–50 nucleic acid base-pair (palindromic repeats), interspaced by unique spacers (Figure 33). These spacers are segments obtained from foreign DNA serving as records of previous infection - providing sequences of specific immunity against foreign DNA elements. A cluster of Cas genes that encode Cas proteins is generally located next to spacer units, flanking the CRISPR arrays. The number of spacer units is variable, differing from just a few to several hundred (Gupta et al., 2019).

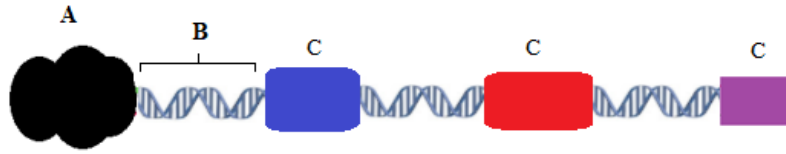


Figure 33. CRISPR/Cas9 System; A – Cluster of Cas genes; B – Short palindromic repeat; C – Spacer: short DNA sequences of exogenous genetic materials.

1.2. Operation and classification of CRISPR systems.

CRISPR immunity operates throughout three stages: spacer acquisition, CRISPR RNA (crRNA) biogenesis, and interference. The first stage – known as spacer acquisition or adaptation – involves the identification of exogenous DNA and its integration into the CRISPR *locus* as a new spacer. Subsequently, CRISPR *locus* is transcribed as a single pre-crRNA to be transformed into crRNAs that contain a spacer - representing the crRNA biogenesis stage, also known as expression. Finally, in the interference stage, the single guide crRNA (sgRNA) produced is used by an effector complex to disable any phage or plasmid with the complementary sequence encoded by crRNA. The specific complement of genes acting on these stages varies. Therefore, CRISPR/Cas systems can be classified into six major types (Figure 34), depending on the presence of “signature genes”, being types I-III best studied whereas types IV-VI were only recently identified (Wright et al., 2016).

Briefly, the signature protein of Type I systems is Cas3. It cleaves foreign DNA that is recognized by the multi-protein-crRNA complex Cascade. Cascade is an interference complex for antiviral defence. It is formed after a spacer is acquired, resulting from the association of crRNA with Cas proteins, being capable of targeting DNA sequences complementing the spacer sequence of the crRNA. In Type II systems, only a single protein is necessary for interference, encoded by the signature Cas9 gene. Finally, Type III systems rely on Cas10, which assembles into a Cascade-like interference complex to target search and elimination (Wright et al., 2016).

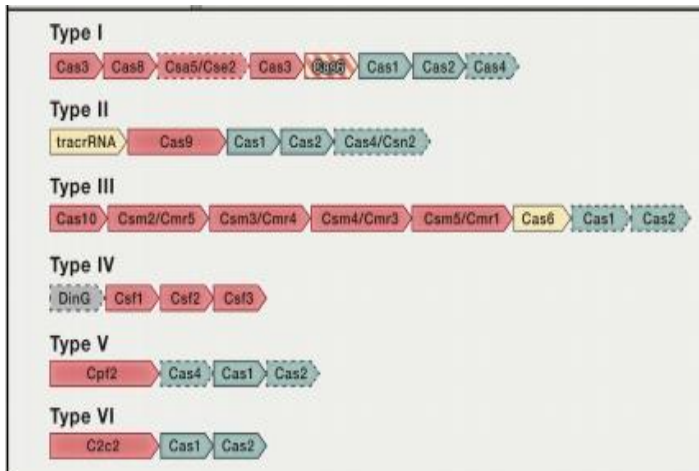


Figure 34. Representative operons for CRISPR System Types. Genes involved in the interference stage are coloured red, genes involved in crRNA biogenesis stage are coloured yellow, and those involved in adaptation are coloured blue (Wright et al., 2016).

1.3. Type II CRISPR/Cas9 System

In 2012, it was discovered that the bacterium *Streptococcus pyogenes* contained a remarkable viral defence system that could be adapted as a programmable system for genome editing (Jinek et al., 2012). The era of CRISPR technology as a promising tool to genome editing in eukaryotic system has emerged from applications of the Type II CRISPR/Cas9 adapted from *Streptococcus pyogenes* (Moon et al., 2019). Given the fact that this system requires only one protein, the RNA-guided endonuclease Cas9, and two small RNA molecules - crRNA and trans-activating RNA (tracrRNA), it is a simple method to work with and easy to customize. Therefore, Type II CRISPR system adapted from *Streptococcus pyogenes* is the most frequently used in research field (Shen et al., 2017).

The CRISPR *locus* can be transcribed into these small RNA molecules capable of recognizing the specific exogenous DNA and guide the nuclease Cas9 to the target DNA causing site-specific double-strand break (DSB) (Shen et al., 2017). The foreign DNA is identified, processed, and included as a new spacer on the CRISPR/Cas9 system acting as an infection memory. This way, upon contact with the same infectious agent, the system has a complementary RNA sequence which recruits the Cas nuclease to cut the exogenous DNA, protecting the organism effectively (Wright et al., 2016). However, having viral genome fragments embedded in CRISPR system can trigger Cas9 to act against endogenous genome.

That is why Protospacer Adjacent Motif (PAM) is critical for immunity, since crRNA guided interference depends on the PAM sequence for foreign DNA identification. PAM has been reported to be the usual position where Cas9 cleaves DNA. Thus, Cas9 only cuts the DNA if an appropriate PAM is placed immediately after the target sequence (Arranz-Solís et al., 2018). The endonuclease Cas9 from *Streptococcus pyogenes* recognizes the PAM sequence 5'-NGG-3' (where “N” can be any nucleotide base) (Shen et al., 2017).

Once exogenous DNA is identified, Cas9 is guided by crRNA to the target sequence that is homologous to the single guide RNA with a PAM sequence and causes site-specific DSB – disabling it in one hand, and on the other hand, being able to introduce mutations or templates on the DNA strand (Shen et al., 2017). These DSBs are repaired by the organism following two pathways: non-homologous end joining (NHEJ) pathway or by homologous direct repair (HDR) – Figure 35.

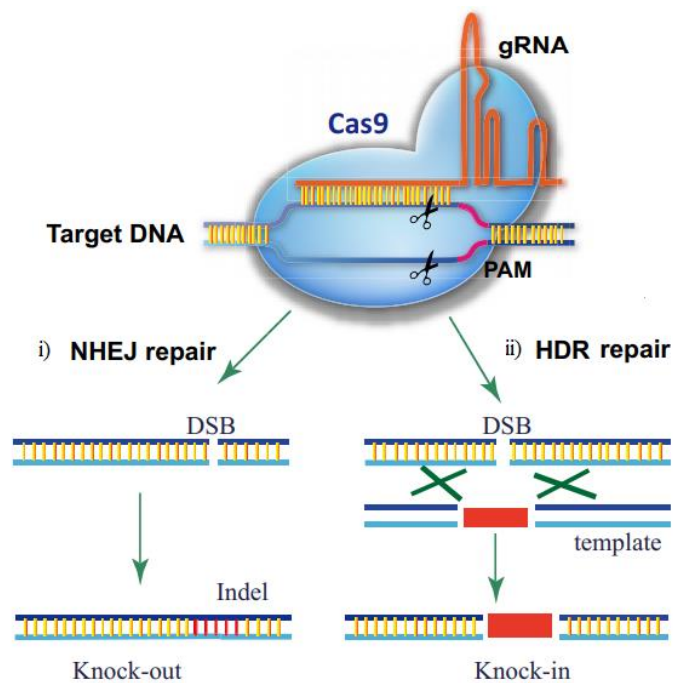


Figure 35. CRISPR-Cas9 mediated gene-editing mechanisms. A guide RNA (gRNA) recognizes a genomic region followed by PAM sequence, recruiting the Cas9 DNA endonuclease. A double stranded break is created, being repaired by (i) non-homologous end joining (NHEJ) or (ii) homology directed repair (HDR) in the presence of a donor template (Ding et al., 2016).

NHEJ is the most active repair mechanism to restore the DNA strand. This mechanism causes small nucleotide insertions or deletions at the DSB site, introducing “indels” on the functional elements – leading to the knock-out (KO) of the gene. The goal is a loss of function mutation within the targeted gene (Ding et al., 2016). On the other hand, HDR allows the integration of foreign DNA fragments to confer new traits to the host. This mechanism acts if a donor template DNA with homology to the flanking sequence is present, performing a knock-in (KI) by integrating the sequence of the donor fragment into the host genome at the DSB site. As a result, this mechanism produces specific nucleotide changes at a targeted site. Nevertheless, its efficiency is generally low– being found to be less efficient than NHEJ (Cribbs and Perera, 2017; Arranz-Solís et al., 2018).

The development of Cas proteins as gene editing tools has been focused on exploring programmable sequence-specific DNA recognition of interference complexes. The ability to sum up Cas9 activity from *S. pyogenes* in a two-component system by fusing the crRNA and tracrRNA into a sgRNA makes it extremely useful in the genome engineering field for its practicality and simplicity (Wright et al., 2016).

1.4. Gene editing on apicomplexan parasites of veterinary importance

Apicomplexan parasites have great impact on animal health worldwide, requiring urgent and effective ways of treatment and control. Because of the remaining difficulties in understanding the biology of these parasites, options for novel control methods are limited (Shen et al., 2017). Only a few species have been studied, and less than half of their genome have been functionally annotated. For this reason, scientists have tried over the years to improve the efficiency and specificity of targeted gene editing (Sidik et al., 2016).

Toxoplasma gondii has been pointed as a model apicomplexan for study purposes due to the facility of being cultured, genetic tractability and high transfection rate. Therefore, methods adapted to analyse gene function in *T. gondii* can be extrapolated to other

apicomplexan parasites. Genetic editing techniques research on *T. gondii* date back to 1993, when reports emerged using methods for transient expression of foreign DNA into parasite cells and targeted gene knock-out and replacement using homologous recombination. In 2016, Sidik et al., adapted the CRISPR/Cas9 system to study the function of each gene from *T. gondii* during infection of human fibroblasts. This method proved to be a unique tool, enabling a rapid identification of genes that mediate infection of human fibroblasts or confer drug sensitivity (Sidik et al., 2016). CRISPR/Cas9 mediated gene manipulation technique was first applied to *T. gondii* and later adapted to other apicomplexan parasites such as *Plasmodium* species and more recently *Cryptosporidium parvum* (Shen et al., 2017). Although a selection of tools has been applied to *T. gondii* – such as selectable markers and genome editing tools – only few of these methods have been applied for *N. caninum* (Suarez et al., 2017).

Genome manipulation on *N. caninum* is limited to a few studies. There are reports of successfully transfected genes from *T. gondii* to an *N. caninum* strain by Howe et al., Beckers et al., and Howe and Sibley dated from 1997 (reviewed in Arranz-Solís et al., 2018). A mutant *N. caninum* strain expressing a foreign gene (*sag1*) from *T. gondii* was constructed using pyrimethamine-resistance and colour marker genes as double selective markers in 2010 (Zhang et al., 2010). Pereira and Yatsuda documented in 2014 the use of the antibiotic chloramphenicol as a selective marker on the development of the first vector for stable expression of proteins using only *N. caninum* promoters (Pereira and Yatsuda, 2014). In the same year, Pereira et al., established a method for stable insertion of genes using pyrimethamine (Pyr) as a selective marker, producing a transgenic *N. caninum* strain resistant to Pyr. For the effect, a mutated Dihydrofolate reductase-thymidylate synthase (*dhfr*) gene was transfected into the strain to confer Pyr resistance. This gene function was initially discovered on *Plasmodium* patients unresponsive to treatment with Pyr, later explained with the presence of point mutations on *dhfr* gene. In Pereira's study, the *dhfr* gene of *N. caninum* was mutated at two points and proven to provide Pyr resistance in a similar way as observed in *Plasmodium* and *T. gondii* (Pereira et al., 2014).

CRISPR/Cas9 system for genome editing on *N. caninum* was first reported by Arranz-Solís et al. in 2018, using plasmids containing the CRISPR/Cas9 elements adapted to the closely related apicomplexan *T. gondii*. The knock-out of a fluorescent protein was successfully performed as well as the disruption of a targeted gene by inserting a pyrimethamine - a standard therapy for human toxoplasmosis (Shen et al., 2017) - resistance fragment. CRISPR/Cas9 technique has proven to be a promising technology for genetic research on *N. caninum* (Arranz-Solís et al., 2018).

The emerging of novel gene editing methods applied to apicomplexan parasites of veterinary interest will accelerate the development of novel and more effective methods for these parasitosis. However, these methods are only possible because of the increasing accessibility of techniques such as *in vitro* culture, transfection, genome sequencing and analysis (Suarez et al., 2017).

2. *Sag1* gene knock-out in *Neospora caninum* using CRISPR/Cas9

Genetic manipulation technology will aid to better understand host-parasite interactions in *N. caninum* and allow promising developments on vaccination and treatment strategies (Arranz-Solís et al., 2018).

In 2017, Shen et al. detailed protocols for performing efficient genetic manipulation using the CRISPR/Cas9 system from *S. pyogenes* in *T. gondii*. Technical details of specific genome editing strategies – such as CRISPR plasmid construction, targeted gene disruption, parasite transfection and positive clone identification - are provided in his work (Shen et al., 2017). One year later, the work of Arranz-Solís et al., 2018, reporting on the first successful use of the CRISPR/Cas9 system in *N. caninum* by transfecting plasmids developed for *Toxoplasma*, demonstrated that (i) CRISPR/Cas9 is an effective tool on gene disruption in *Neospora*; (ii) a selectable marker can be introduced at the DSB site; and (iii) *N. caninum* mutants can be attained by using plasmids adapted from those already described for *T. gondii*.

A targeted gene of interest on *N. caninum* was disrupted by insertion of a pyrimethamine resistance fragment using CRISPR/Cas9 (Arranz-Solís et al., 2018).

The following assay aims to perform a *sag1* gene knock-out by inserting a disrupting pyrimethamine resistance fragment using CRISPR/Cas9. *Sag1* is a surface antigen that has been associated to cell invasion, being also considered homologous between *T. gondii* and *N. caninum* (Mineo, 2006). The goal was to use CRISPR/Cas9 to insert the *dhfr* gene into *sag1* genome, producing a *sag1* knock-out as illustrated on Figure 36.



Figure 36. Illustration of resistance gene *dhfr* Kock-in on *sag1*.

This assay, attempting to produce the knock-out by transfection using CRISPR/Cas9 was conducted at the Institute of Parasitology in 2017. The selection of clones and confirmation of the knock-out took place during the internship, in October 2018. Throughout the following chapter, an overview of the CRISPR/Cas9 targeted knock-out performed is presented and its results are reported and discussed.

To successfully edit genome with CRISPR/Cas9, three elements are required: a Cas9 protein, a gRNA with a guide sequence matching the DNA of the target in one end (5'-end) and a special Cas9 biding site on the other end (3'-end); and a PAM sequence in the genome sequence adjacent to the targeted DNA. This way, any DNA sequence bearing a PAM could theoretically be edited by Cas9 associated with a specific gRNA (Ding et al., 2016).

2.1. *Sag1* as the targeted gene

Sag1 gene has been considered a good candidate for the development of a recombinant vaccine against *T. gondii* infection since it is a great immunodominant antigen, commonly known as *TgSAG1*. It has been demonstrated that a *sag1* homologue was also expressed on *N. caninum*. *TgSAG1* was expressed in *N. caninum*, and the respective transgenic mutant parasite could induce protective immunity against lethal toxoplasmosis in a mouse model. Such results suggest that *N. caninum* may be a valuable tool as a potential live recombinant vector vaccine against toxoplasmosis in animals. As *sag1* is functionally implicated as an important attachment ligand for the host cell, the *sag1* gene represents an interesting gene for the development of new therapies for toxoplasmosis or neosporosis (Zhang et al., 2010).

In this assay, *sag1* was the gene to be knocked out. Functionally, it implies disabling the surface antigen of the parasite which should lead to a reduction in host cell invasion. This conclusion is supported by studies from Dzierszinski et al., 2002 on the disruption of an surface antigen similar to *sag1* (*sag3*) on a *T.gondii* strain that resulted in *sag3* deficient mutants showing attenuated infectivity, with a markedly reduced capacity to cause mortality in mice (Dzierszinski et al., 2002). In the last decade, *sag1* gene disruptions in *Toxoplasma* have been performed not particularly to produce a vaccine but primarily to gain further insight on the function of particular genes. Nevertheless, it has been reported that high *sag1* expression level is related to an increased virulence. Thus, it can also be advantageous for immunization against this and other parasites (Wang and Yin, 2014).

2.2. Construction of the plasmid with repair template

To perform the *sag1* knock-out, CRISPR/Cas9 technology was used to cut a DNA strain on a targeted site encoding *sag1* in the genome of *Neospora* and insert a repair template with a drug selection cassette disrupting the gene. A gene specific CRISPR/Cas9 plasmid

vector must be designed for the gene of interest, co-expressing Cas9 and gRNAs. CRISPR/Cas9 vectors can be acquired from the public plasmid repository of Addgene (available at <http://www.addgene.org/crispr/plant/>). These plasmids co-express an endonuclease like Cas9 and a gRNA specific for the targeted gene. The targeted gene must be a unique sequence compared to the rest of the genome and a PAM sequence must be placed immediately adjacent to the gene of interest. The repository also provides PAM sequences specific for the selected endonuclease.

The pUC19 plasmid (Addgene Plasmid #50005) was used to promote the insertional disruption on *sag1*. Plasmids replicate circular extra-chromosomal DNA autonomously, being able to act as cloning vectors. The pUC19 plasmid is one of a series of cloning vectors designed by Joachim Messing at the University of California, USA. This plasmid contains a lac promoter (*lacZ* gene), the multiple cloning site (MCS) and an ampicillin resistance gene (*ampR*). The MCS holds unique sites for 13 different hexanucleotide-specific restriction endonucleases. These sites allow pieces of foreign DNA to be inserted into the region and later replicated at a high copy number (Norrander et al., 1983).

For the experiment, pUC19 carried Cas9 endonuclease with a *sag1* target specific gRNA and resistance gene coded for dihydrofolate reductase (*dhfr* gene) as repair template, conferring resistance to pyrimethamine – Figure 37.

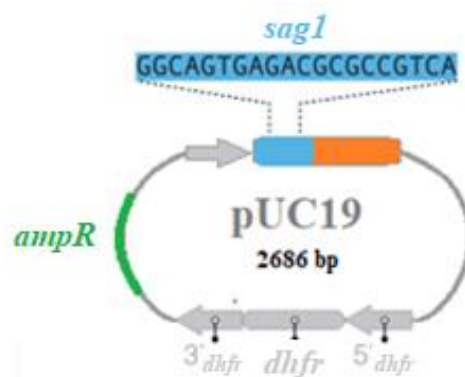


Figure 37. pUC19 plasmid construct with the pyrimethamine-resistance selectable marker (*dhfr*) and an ampicillin resistance gene (*ampR*). The targeting sequence of the *sag1* sgRNA is highlighted. Adapted from Norrander et al., 1983; Sidik et al. 2014.

2.3. Transfection by electroporation

Transfection is the introduction of DNA or RNA into a cell. The transferred nucleic acid, usually DNA, might exist as extra-chromosomal replicating in the nucleus of the transfected cells, or it can also be stably incorporated into chromosomes - usually by homologous recombination mechanisms (Suarez et al., 2017).

Neospora caninum tachyzoites were transfected with pUC19 carrying a *dhfr* gene. Transfection was carried out by electroporation. This transformation technique facilitates the entry of DNA molecules into a cell through electrical discharge that reversibly destabilizes cell membranes and induces the formation of aqueous pathways or transient hydrophobic membrane pores (Kumar et al., 2019).

To generate parasites for transfection, HFF host cells were infected with *N. caninum* on T25 flasks. Parasite load should be enough to induce 75% lysis two days after infection (Shen et al., 2017). Parasites were collected two days p.i. and pipetted to a transfection mix on an electroporation cuvette, after being centrifuged and resuspended in HBSS. Electroporation cuvettes contain a transfection mix with recombinant pUC19 plasmid targeting *sagI*. Parasites were electroporated according to Arranz-Solís et al., 2018.

Following electroporation, parasites were transferred into T25 flasks and incubated at 37°C, 5% CO₂ to allow recovery of the cells and expression of the plasmid. After 24h, individual clones were obtained by performing limiting dilution using 96-well plate culture formats, growing parasites in 200µl/well.

2.4. Pyrimethamine selection

Independently of the specific approach, drug selection is almost always required to obtain clones with the desired genomic changes. A variety of selectable markers such as *dhfr* Pyr resistant gene are available for *T. gondii*. *Dhfr* is known to be one of the strongest selection methods to obtain stable transformants, being highly efficient (Shen et al., 2017). *Neospora* is known to be sensitive to Pyr and this resistance can be achieved by expressing of a mutated version of the *dhfr* gene (Arranz-Solís et al., 2018).

Electroporated parasites should contain the *dhfr* disruptive cassette inserted by HDR. This cassette acts as a selective marker to confirm the success of the electroporation. To select positive clones (meaning parasites resistant to Pyr), 3×10^4 HFF cells per well were seeded in three 24-well plates. Cells were then further expanded in T25 and T75 flasks. They were used to form monolayers in 96-well plates and were infected with transfected parasites and further cultured in 0.2ml medium/well.

2.5. Identification of positive clones

Transfected parasites incubated on the 96-well plates were selected with 12 μ M of Pyr. After plaque development, each well of the 96-well plates was visually checked under light microscope. A positive well contained living parasites, thus transfected with *dhfr*, the Pyr resistant gene. Parasites from positive wells (positive clones) were transferred into 6-well plates and treated again with Pyr. Seventy single clones of pyrimethamine-resistant parasites were isolated. Positive clones were collected for DNA isolation to be verified by PCR to identify the expected gene disruption – *sag1* knock-out.

2.6. PCR confirmation of the knock-out

2.6.1. PCR with primers targeting *sag1*

PCR was used to confirm the efficiency of *sag1* knock-out by verifying if the gene is being expressed. First, primers directed to *sag1* were used to find possible knock-out clones. A possible knock-out is identified by a negative PCR for *sag1* and a positive result for *dhfr*. DNA from 70 clones was isolated for PCR as described on “2.1.6. ii. DNA extraction”. Master mix was produced for 90 samples (Table 5).

Table 5. Master Mix composition

<i>Reagent</i>	<i>Volume per sample (μl)</i>	<i>Volume for 90 samples (μl)</i>
Enhancer	4	360
Buffer	4	360
Primer F (Forward)	0.1	9
Primer R (Reverse)	0.1	9
dnTPs	0.3	27
H ₂ O	11.4	1026
Q5	0.1	9
Total Volume	20	1800

Table 5. Master Mix reagents for PCR composed by an enhancer, buffer, Primers for *sag1* and *dhfr* genes, dnTPs (DNA nucleotides, forming units for new DNA chains formed during PCR reactions), water and DNA polymerase Q5.

PCR reactions were performed in a thermal cycle. The initial step corresponds to a denaturation at 98°C for three minutes in one cycle. The amplification for 10 seconds at 98°C was completed in one cycle and is followed by 20 seconds annealing at 60°C and two seconds extension at 72°C. Subsequently a cycle at 72°C for five minutes was completed to finish replication on all templates on a total of 33 cycles concluded.

The result was analysed using agarose gel electrophoresis. The agarose gel had 24 wells in total and 18 probe wells since each gel also carried three empty wells, a positive control for PCR (original electroporation shut of the plasmid) and two DNA ladders (L). A DNA ladder is a set of DNA fragments, in which each fragment has a different length and molecular weight. DNA ladders (molecular weight markers covering a range from 2000 to 100bp) were used during gel electrophoresis, allowing to estimate the size of the amplified fragment compared to the closest band in the ladder lane.

Possible knock-out of *sagI* was assessed by using primers targeting *sagI*. To study 70 probes, four 1% agarose gels were produced. A 1% agarose gel is composed by agarose and buffer solution on a 1:100 ratio. Four gels were produced with 2 g of agarose to 200ml of buffer solution and stained with 1 µl of ethidium bromide. Gels were loaded as illustrated on Figure 38 and visualized under UV light after electrophoresis (Figures 39-42). Bands of light represent DNA stained with ethidium bromide, a positive result for PCR.

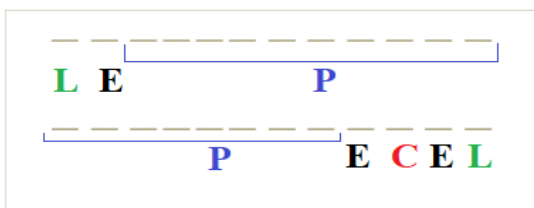


Figure 38. Agarose gel scheme. The gel carries 18 probe wells (P), three empty wells (E) and a positive control well (C).

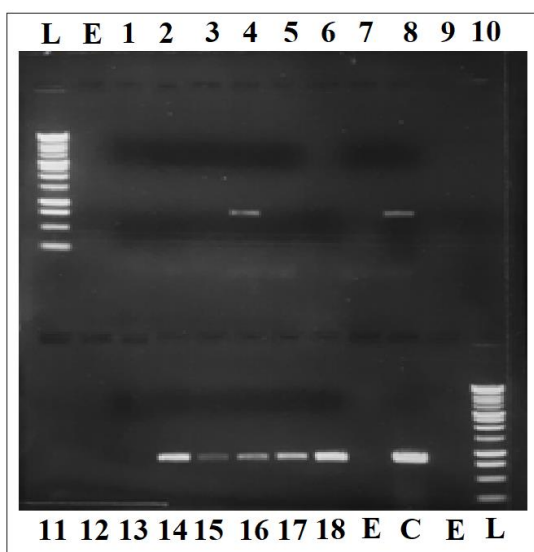


Figure 39. First gel carrying clones 1 – 18, two ladders (L), three empty wells (E) and a positive control (C). Bands of DNA stained with ethidium bromide visualized under UV light represent positive PCR results.

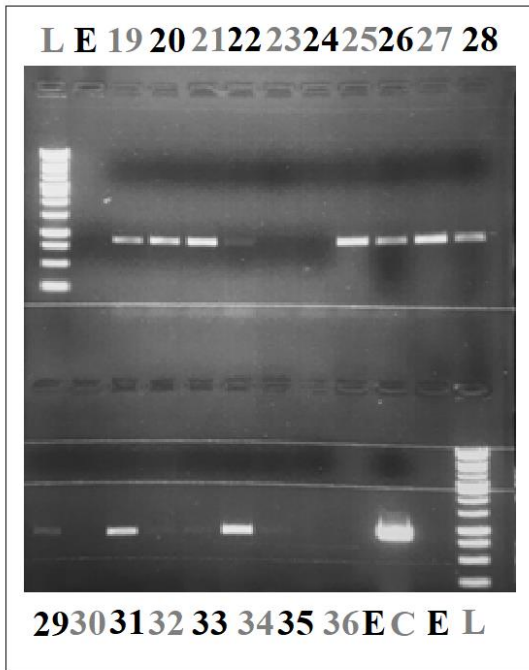


Figure 40. Second gel carrying clones 19 – 36, two ladders (L), three empty wells (E) and a positive control (C).

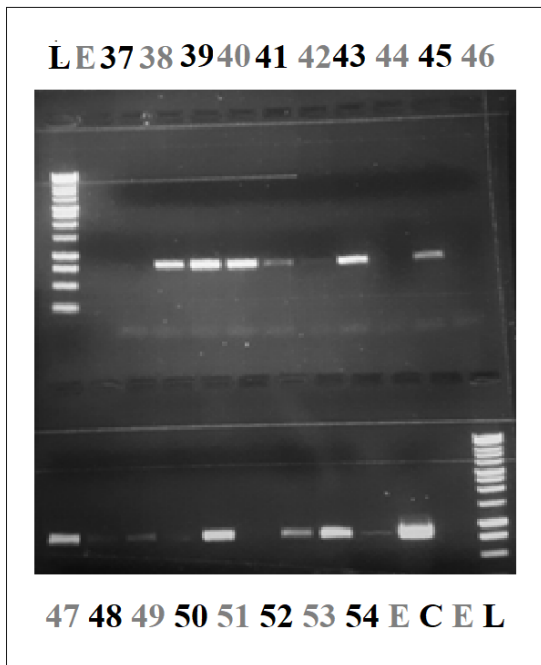


Figure 42. Third gel carrying clones 37 – 54, two ladders (L), three empty wells (E) and a positive control (C).

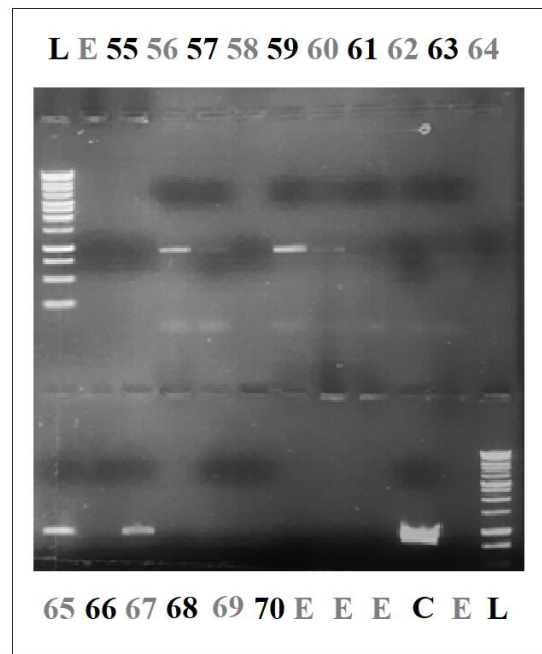


Figure 41. Fourth gel carrying clones 55 – 70, two ladders (L), five empty wells (E) and a positive control (C).

2.6.2. PCR with primers targeting *dhfr* gene

A possible knock-out is translated by a negative PCR for *sagI* and positive result for *dhfr*. Therefore, the previous protocol was repeated using primers targeting *dhfr* to confirm if the gene was inserted on the genome. The result of electrophoresis obtained through PCR reactions is shown on Figure 43.

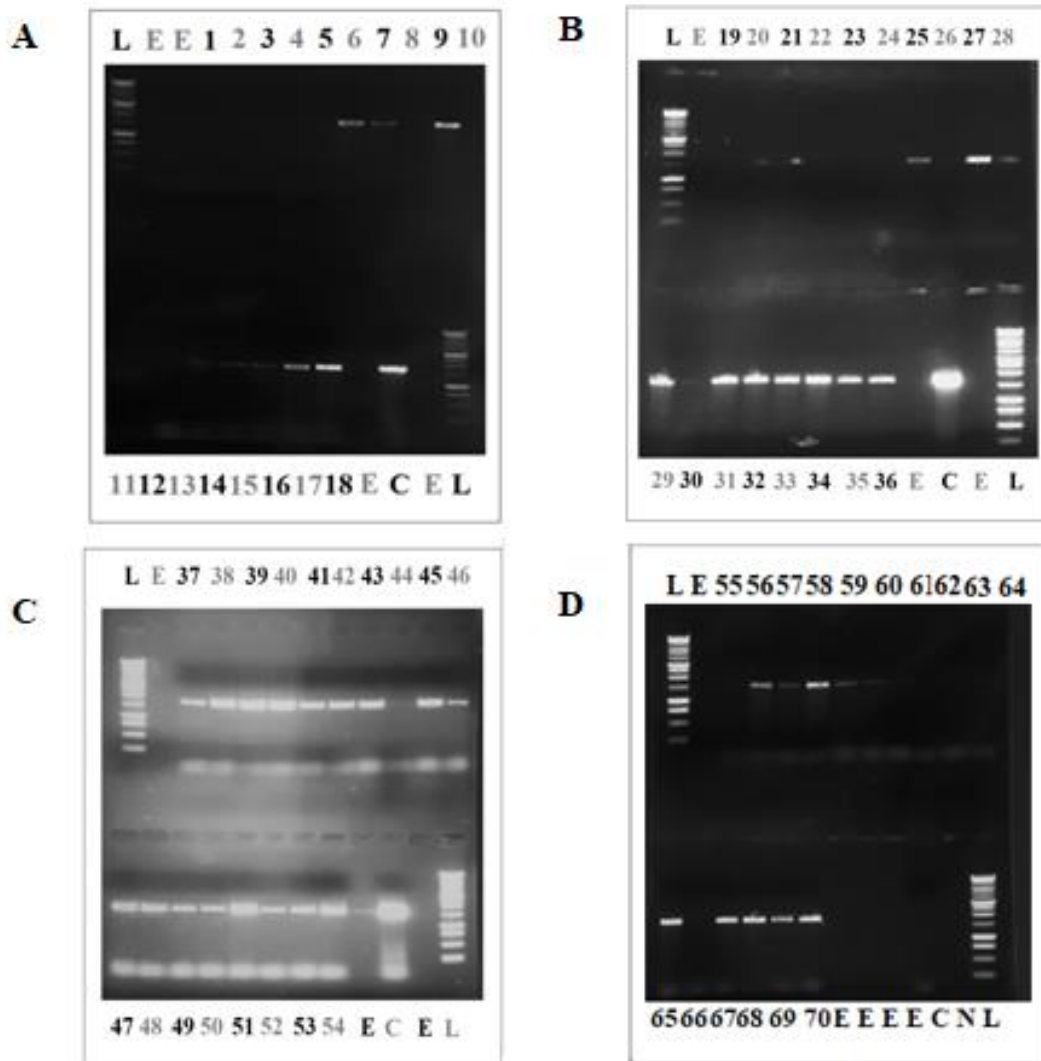


Figure 43. Electrophoresis result. A) First gel, carrying clones 1-18; B) Second gel, carrying clones 19-36; C) Third gel, carrying clones 37-54; D) Fourth gel, carrying clones 55-70; L – Ladder; E – Empty well; C - PCR positive control.

2.6.3. Selection of possible knock-out clones

Results from both PCR reactions using *dhfr* and *sagI* primers were crossed to identify potential knock-out clones – Table 6.

Table 6. Summary of PCR results of 70 clones

Clone	<i>sagI</i>	<i>dhfr</i>	Clone	<i>sagI</i>	<i>dhfr</i>	Clone	<i>sagI</i>	<i>dhfr</i>
1	-	-	26	+	-	51	+	+
2	-	-	27	+	+	52	-	+
3	-	-	28	+	+	53	+	+
4	+	-	29	+	+	54	+	+
5	-	-	30	-	+	55	-	+
6	-	+	31	+	+	56	+	+
7	-	+	32	+	+	57	+	+
8	+	-	33	+	+	58	-	+
9	-	+	34	+	+	59	+	+
10	-	-	35	-	+	60	+	+
11	-	-	36	-	+	61	-	+
12	-	-	37	-	+	62	-	-
13	+	+	38	+	+	63	-	-
14	+	+	39	+	+	64	-	+
15	+	+	40	+	+	65	+	+
16	+	+	41	+	+	66	-	-
17	+	+	42	+	+	67	+	+
18	+	+	43	+	+	68	-	+
19	+	-	44	-	+	69	-	+
20	+	+	45	+	+	70	-	+
21	+	+	46	-	+			
22	+	-	47	+	+			
23	-	-	48	+	+			
24	-	-	49	+	+			
25	+	+	50	+	+			

Table 6. Potential knock-out clones are encircled.

Eight clones (30, 35, 37, 44, 46, 52, 69, 70) showed a negative PCR result for *sagI* primers and a positive PCR for *dhfr*, meaning that these clones have the *dhfr* coding gene integrated into the *sagI*. These clones were selected to further investigate if the *dhfr* gene was inserted on the expected position.

2.6.4. Confirmation of *dhfr* gene's position on clone genome

At this point, it was required to infer the *dhfr* gene's position within the clone genome to confirm if it was successfully inserted and thus disrupted *sagI*. For the effect, four PCRs using primers targeting specific sites on *sagI* and *dhfr* were performed on each clone. Each PCR is numbered according to the used set of primers (Table 7, Figure 44). For a successful knock-out, it was expected the PCR result using *sagI* primers forward and reverse (PCR 1) to be negative, and all PCR 2, PCR 3, and PCR 4 results to be positive.

Table 7. PCR primers for knock-out confirmation

PCR	Primer Forward	Primer Reverse
1	<i>sagI</i>	<i>sagI</i>
2	<i>dhfr</i>	<i>dhfr</i>
3	<i>sagI</i>	<i>dhfr</i>
4	<i>dhfr</i>	<i>sagI</i>

Table 7. Set of primers corresponding to four different PCR reactions.

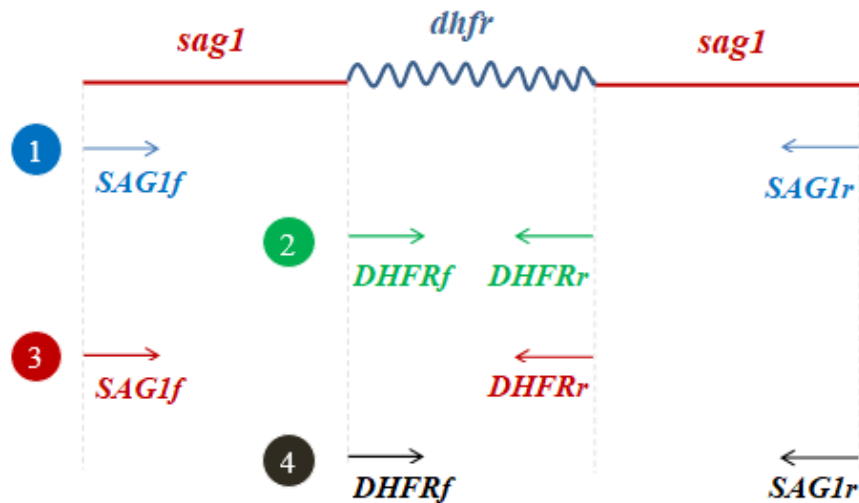


Figure 44. Schematic illustration of target sites for different primers used on PCR 1 – 4.

Three 1% agarose gels were produced - each gel carried two to three clones, ladders, and a control for each PCR. Samples of the same clone were loaded side by side on the gel, following the colour code corresponding to each PCR reaction displayed on Table 7. Reactions were carried as described on “2.6.1 PCR with primers targeting *sagI*”. Results of electrophoresis are shown in Figure 45 and the corresponding PCR results can be found on Table 8.

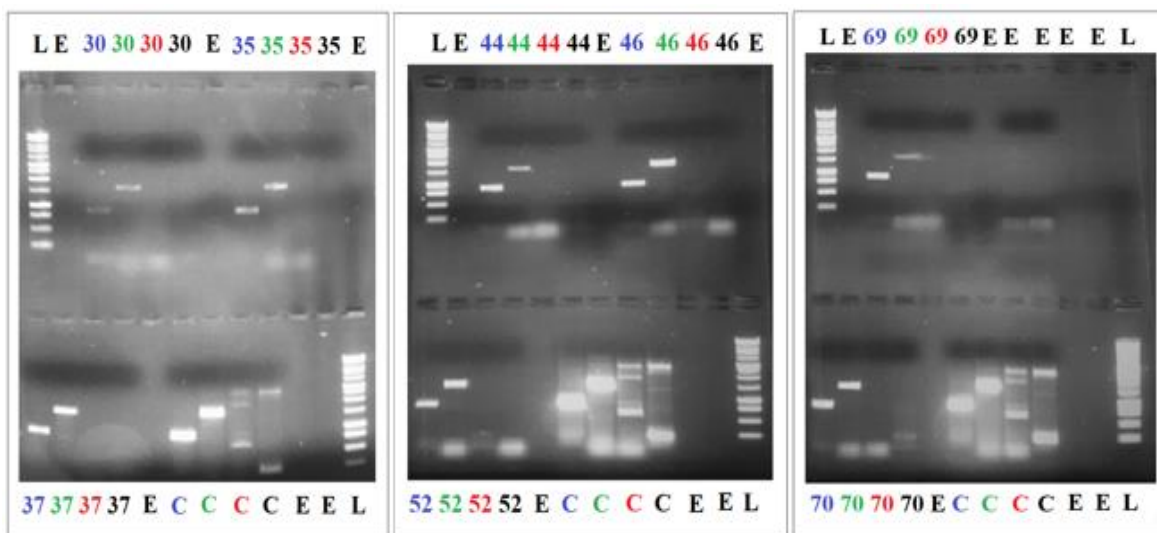


Figure 45. Gel electrophoresis result obtained from four different PCR reactions on clones 30, 35, 37, 44, 46, 52, 69 and 70. L – ladder, E – Empty well, C – PCR positive control.

Table 8. PCR results of possible knock-out clones

Primers	Clones	Clone	Clone	Clone	Clone	Clone	Clone	Clone	
		30	35	37	44	46	52	69	70
PCR 1	SAG1f/SAG1r	+	+	+	+	+	+	+	+
PCR 2	DHFRf/DHFRr	+	+	+	+	+	+	+	+
PCR 3	SAG1f/DHFRr	-	-	-	-	-	-	-	-
PCR 4	DHFRf/SAG1r	-	-	-	-	-	-	-	-

All clones tested expressed *sagI*, therefore the knock-out was not effective. *Dhfr* gene was also expressed on all clones, which suggests that this gene was not placed properly into the *sagI* gene, but at another position in the genome (off-target).

2.6.5. Repetition of PCR with primers targeting *sagI*

The final step of the assay was to repeat PCR reactions with primers targeting *sagI* on clones who were PCR negative for *sagI* on the first trial (Table 7). Reactions were carried as described on “2.6.1 PCR with primers targeting *sagI*”. Two gels were produced to test 35 samples. Results of electrophoresis obtained from PCR reactions are shown in Figure 46.

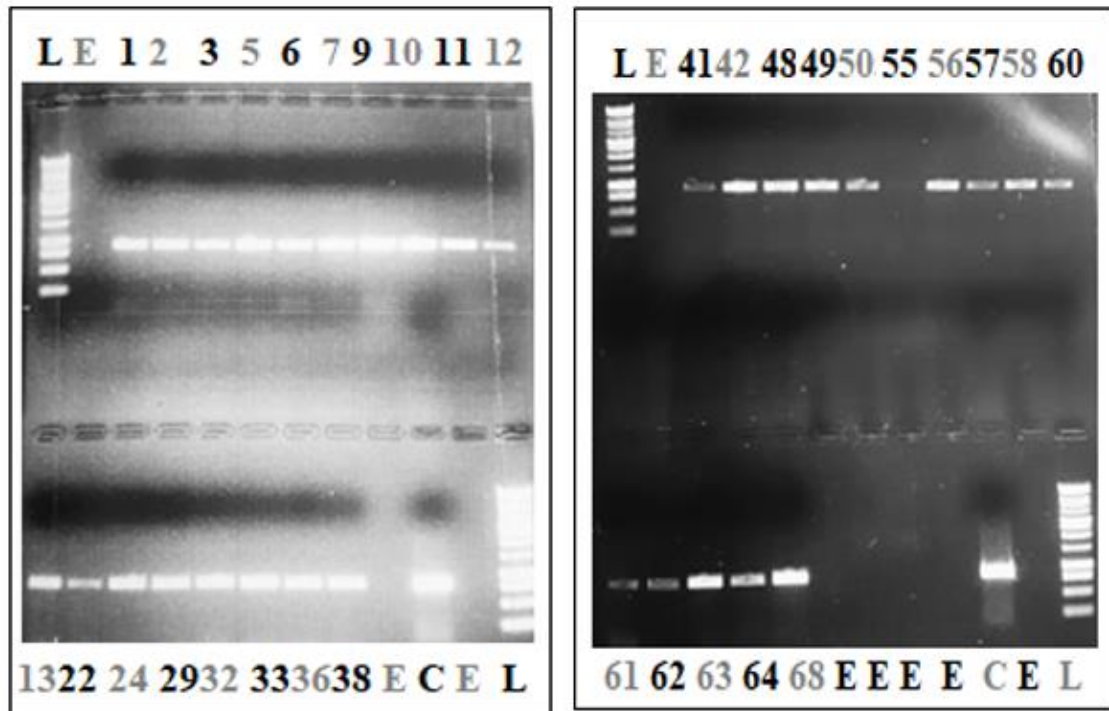


Figure 46. Gel electrophoresis result obtained by PCR reactions using *sagI* primers on PCR negative for *sagI*. L – ladder, E – Empty well, C – PCR positive control.

Additionally, three more samples were tested using the same primers and method (Figure 47). Clones 23 and 66 were also PCR negative for *sagI* on the first test (Table 7); and clone 55 was retested due to its weak result on the repetition test (Figure 45).

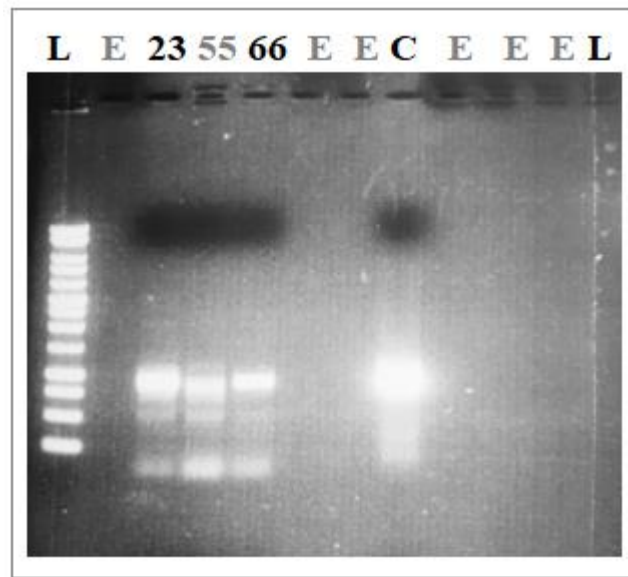


Figure 47. Gel electrophoresis result obtained by PCR reactions using *sagI* primers on three clones. L – ladder, E – Empty well, C – PCR positive control.

The *sagI* gene was expressed in all tested samples. The *sagI* knock-out was thus not successfully performed, even though *dhfr* was transfected to the clones.

3. Discussion

Sag1 was targeted in *Neospora caninum* by the CRISPR/Cas9 system, and a plasmid carrying a Pyr resistant gene was transfected. Selection with Pyr allowed the identification of seventy successfully transfected clones. *N. caninum* can develop resistance to pyrimethamine by expression of the *dhfr* resistance gene described for *Toxoplasma*. *Dhfr* proved to be a very efficient marker for confirmation of transfection. Such results agree with published observations by Arranz-Solís et al., 2018 and Shen et al., 2017.

Expression of the *dhfr* gene implies that CRISPR/Cas9 successfully promoted the integration of this gene into the host genome by DBS. PCR reactions were used to determine whether *dhfr* and *sag1* genes were present in the clones. Results were crossed (Table 6) and eight possible knock-out clones were selected. Selection criteria for possible knock-out clones were PCR results: clones with a positive PCR for *dhfr* and a negative PCR for *sag1* were selected. Four PCR reactions were performed on selected clones using different primers (Table 7). For the expected *sag1* knock-out, PCR 1 should be the only negative result of all four PCR. Table 8 shows that all clones were positive for PCR 1 and PCR 2, confirming the expression of *sag1* and *dhfr* genes. All clones were negative for PCR 3 and PCR 4, which suggests that *dhfr* is not placed into the targeted *sag1*. Lastly, PCR 1 using *sag1* primers was repeated on clones with a negative PCR result for *sag1* on the first test. All clones expressed *sag1* gene – thus, the knock-out was not successful.

It seems plausible that *dhfr* is located on an erratic site. PCR analysis alone cannot exclude the possibility of a donor template being inserted elsewhere in the genome. It is possible that gRNAs have off-target effects (Arranz-Solís et al. 2018). Although highly specific gRNA may be designed in practice, off-target activity of Cas9 reduces the number of targetable sites. The off-target activity of Cas9 is related to the fact that it can edit targeted DNA bearing a small number of mismatches to its gRNA. Off-target effects have been a major concern, having been rigorously analysed by different *in vitro* and *in vivo* approaches. These studies can summarize Cas9/gRNA fidelity as follows: (1) Cas9/gRNA is unable to

recognize a DNA site with more than three mismatches; (2) Cas9/gRNA is unable to recognise and edit targeted DNA if a number of mismatches exist near the PAM sequence; and (3) higher concentration of Cas9/gRNA implies greater potential for off-target effects. Due to these potential effects, gRNA design is essential to reduce Cas9 off-targeting risk. Numerous methods have been developed aiming to increase Cas9 targeting fidelity. Off-target constrains have been addressed by engineering new Cas9 variants that are intolerant to any number of mismatches. These Cas9 variants can recognize a wide range of PAM sequences (including 5'-NAGN-3', 5'-NGCG-3', and 5'-NGNG-3') (Ding et al., 2016).

Although it is relevant to discuss off-target effects, technical errors associated with sample manipulation or pipetting should also be taken into consideration. Corner effects on PCR plaques due to evaporation could have affected the results. In addition, transfected samples were stored for a long period of time before the conclusion of the experiment – it is known that cryopreservation preserves living cells for long term periods, thus a gap of one year is not expected to affect the quality of the sample. Scientific progress requires ongoing critical evaluation of potential errors and constructive solutions. The present assay must be repeated. A review on gRNA construction targeting *sagI* is pertinent, given the potential off-target effects. Also, clone selection and identification should be performed soon after electroporation to avoid eventual deterioration of the sample throughout the storage period.

Although the donor template with *dhfr* was integrated in *N. caninum* genome, the expected knock-out wasn't successfully performed, leading to the conclusion that the disruptive gene was placed on an erratic site.

4. Future prospects

CRISPR/Cas9 system is becoming a revolutionary and flexible tool for genetic manipulation of every branch of science (Ding et al., 2016). The facility of reprogramming these tools makes them easily configurable for a huge range of applications. The discovery of CRISPR/Cas systems provided exciting opportunities for innovation and set the basis for search of potential useful enzymes to implement for improved sensitivity or stability of the current diagnostic tools (Sashital, 2018).

While CRISPR/Cas9 has been extensively used in research, challenges exist with regard to its clinical application. Though achieving targeted cuts has become trivial, directing DNA repair towards homology directed repair rather than non-homologous end joining remains a challenge (Wright et al., 2016). In addition, the potential to standardize tests using this technology for rapid diagnosis would have a great impact on point-of-care settings, such as early detection of viral outbreaks to ensure timely public health response. CRISPR/Cas diagnostic tools are in place to revolutionize the accessibility of rapid, sensitive and accurate diagnosis and treatment of infectious and genetic diseases options in the Veterinary and Human Medicine fields (Sashital, 2018).

5. Ethical issues associated with genome editing

Ethical, legal, and social implications associated with genome editing justify a large social reflection. CRISPR/Cas9 has been a revolution in the genetic manipulation field since its emergence in 2012 due to the facility and practicability of the technique.

The term “bioethics” was introduced by Van Rensselaer Potter in 1970 as the “science of survival”. Potter’s concept of bioethics considers ethical values and biological facts inseparable, arguing that human survival must be assured despite the environmental damage as consequence of human action. This science of survival was perceived as a relationship

between science and ethics to guarantee human survival within a healthy environment (Potter, 1970). Bioethics evolved to be a philosophical moral focused on practical biomedical dilemmas regarding health professionals and research in general such as: genetic manipulation, human and animal experimentation, euthanasia, abortion, and cloning. This brief review will focus on genetic manipulation impact on research and its potential applications.

Genome editing is not a new concept as transgenic mice were successfully used in research in the 1980s, as result of successful gene targeting by homologous recombination in murine embryonic stem cells (Gordon et al., 1980). However, genome editing was considered challenging and presented a low success rate. CRISPR/Cas9 technology made it possible to easily edit any cell in any organism, opening a Pandora's box. In one hand, it can be used on gene manipulation at the germline level to generate *in vivo* animal models to study diseases more effectively, understanding early onset of human diseases using human embryos and preventing or treating disease or disability. On the other hand, CRISPR/Cas9 potential to modify each cell in the human body by altering the germline genome makes it controversial since it can produce intended modifications but also other unforeseeable and irreversible alterations to be passed to the offspring (Cribbs and Perera, 2017).

In short, the main ethical concerns regarding CRISPR/Cas9 are related to its irreversibility and unpredictability. These issues have implications not only on the safety of future generations but also in terms of social values, economy status, individuality, injustices, and accessibility (Cribbs and Perera, 2017). Given the fact that CRISPR/Cas9 germline editing is revolutionary in terms of its ethical implications and potential for human therapy, a distinction can be drawn between the clinical application of germline editing and somatic gene therapy or basic research with CRISPR/ Cas9 (Baumann, 2016).

From an ethical point of view, CRISPR/Cas9 technology should have limitations. An obvious constraint, following Potter's conviction, should be preserving the natural ecosystem and human survival. Therefore, germline modifications remain ethically doubtful while the use of genome editing in somatic cells– not involved in reproduction - with the purpose being

therapeutic interventions is, in general, ethically accepted. Despite of potential unexpected effects regarding the manipulation of somatic cells, its low risk-to-benefit ratio and the presence of informed consent and level of currently available scientific evidence justify the use of gene editing techniques. Due to safety concerns, germline applications for human embryos for implantation may represent a high risk-to-benefit ratio as it may have an unpredictable intolerable effect on future generations. Nevertheless, if this technique evolves to a stage that safety concerns are satisfactory, further discussions will be required to consider the eventual social, legal, and ethical implications to prevent potential misuses of germline editing (Cribbs and Perera, 2017).

The principle of precaution based on the uncertainty of the off-target effects or the potential abuse of this technology is frequently used to disqualify the application of genome manipulation techniques. Scientific progress shouldn't be categorically rejected given these premises but supported and evaluated by an open scientific and ethical debate. The ongoing discussion on the subject leads to a bigger scientific conscience that shouldn't be translated to unreasonable patrolling of the freedom to conduct medical research or unnecessary bureaucratic constraints but understood as a progressive process of evolution and respect for human and animal genetic legacy and ecosystem. The use of genome editing technology must come with ethical responsibility. Even though it shouldn't be limited to a few monopolizing entities but made available for global scientific community, gene editing shouldn't be trivialized into a common and irresponsible practice. Hannah Arendt wrote about the "banality of evil" referring to the Holocaust, defending that trivialization of violence led to one of the most terrible eras in the history of mankind (Arendt, 1963). Along the same lines of reasoning, the "banality of science" - the frivolously use of genome editing technologies without ethical restrains - could also lead to a dangerous future, curiously foreseen in literary dystopias like Huxley's "Brave New World". History brings an important lesson, and it is the responsibility of the scientific community to assure that such error is not repeated.

As a final note, it is relevant to refer that given the complexity of the debate, regulatory organisms such as WHO, UNESCO, and the Declaration on the Human Genome and Human Rights are involved in the current debate on gene editing to establish helpful

guidelines. In addition, legally binding conventions like the “Oviedo Convention” (the Council of Europe Convention for the protection of Human Rights and Dignity of the Human Being with regard to the Application of Biology and Medicine: Convention on Human Rights and Biomedicine) exist to regulate the use of transformative technologies, despite of the discrepancy of policies depending on the legal system (Cribbs and Perera, 2017).

In 1970, Potter argued that ethical values and biological facts couldn't be dissociated when developing solutions for the problems of the world. Therefore, the sustainability of the world ecosystem becomes the ultimate test to the value system (Potter, 1970). In 2020, this idea remains relevant and progressive as it seems that “the survival of the fittest” principle disappointingly persists.

6. Conclusion

Genome editing technology changed research methods in many organisms. Using CRISPR/Cas9, a *dhfr* resistance gene described for *Toxoplasma gondii* was successfully transfected into *N. caninum*. This parasite exhibited resistance to pyrimethamine by expression of *dhfr* as formerly reported by Arranz-Solís et al., 2018. Although CRISPR/Cas9 proved to be effective on producing clones with plasmids available for the closely related parasite *Toxoplasma gondi*, all clones expressed *sag1*. The expected *sag1* knock-out wasn't successful. It is fair to conclude that *dhfr* disruptive cassette was inserted on an erroneous site, not disrupting *sag1*.

CRISPR/Cas9 is undeniably a promising technique with exciting prospects. This work reflects a slight insight on genetic manipulation technologies and a real perception on research work and eventual setbacks. Scientific progress thrives from attempt and error and should serve great purposes to benefit human and animal health, while pondering bioethics.

7. Final considerations

The value of an experience is measured by how much it adds to one's life; as a person, a professional and a potential changing agent in the world. As a final note, a reflection on this internship experience follows the question: "what did I bring home?"

This internship complemented a Veterinary Medicine academic formation at the University of Évora. The study of Veterinary Medicine was a time for the acquisition of strong fundamental scientific basis on areas such as biology, physiology, host/pathogenic agents interaction, pathology and clinical approaches - setting the foundations for a critical spirit and better understanding on animal and public health. The goals of this internship were to obtain more knowledge and experience in science by researching apicomplexan parasites.

This first contact with the world of research can be translated not only in the practical acquirement of technical and scientific knowledge but also in the apprenticeship of the importance of teamwork and scientific debate. It led me to gain experience and improve on important research techniques such as cell culturing, electron microscopy and genetic engineering. Furthermore, having the opportunity of integrating a multidisciplinary team and participating in lab meetings arose the conscience to the benefits of an open and productive scientific debate in a friendly and inclusive work environment.

In terms of conclusion, it is with great pleasure that I conclude that the proposed goals were successfully accomplished. A new and exciting perspective on research field through a great example of scientific excellence and professionalism were "brought home" and will definitely be followed in the future.

IV. References

- Aguado-Martínez A, Basto AP, Leitão A, Hemphill A (2017) *Neospora caninum* in non-pregnant and pregnant mouse models: cross-talk between infection and immunity. *Int. J. Parasitol*, **47**: 723–735.
- Ahmad TA, El-Sayed BA, El-Sayed LH (2016) Development of immunization trials against *Eimeria spp.* *Trials Vaccinol*, **5**: 38–47.
- Álvarez-García G, Frey CF, Mora LMO, Schares G (2013) A century of bovine besnoitiosis: an unknown disease re-emerging in Europe. *Trends Parasitol*, **29**: 407–415.
- Álvarez-García G, García-Lunar P, Gutiérrez-Expósito D, Shkap V, Ortega-Mora LM (2014) Dynamics of *Besnoitia besnoiti* infection in cattle. *Parasitology*, **141**: 1419–1435.
- Anghel N, Balmer V, Müller J, Winzer P, Aguado-Martinez A, Roozbehani M, Pou S, Nilsen A, Riscoe M, Doggett JS, Hemphill A (2018) Endochin-Like Quinolones Exhibit Promising Efficacy Against *Neospora Caninum in vitro* and in Experimentally Infected Pregnant Mice. *Front. Vet. Sci*, **5**: 285.
- Arendt H (1963) *Eichmann in Jerusalem: Um relato sobre a banalidade do mal*. São Paulo, Brasil, Companhia das Letras, 85-7164-962-6.
- Arranz-Solís D, Regidor-Cerrillo, J, Lourido S, Ortega-Mora LM, Saeij JPJ (2018) *Toxoplasma* CRISPR/Cas9 constructs are functional for gene disruption in *Neospora caninum*. *Int. J. Parasitol*, **48**: 597–600.
- Barton V, Fisher N, Biagini GA, Ward SA, O'Neill PM (2010) Inhibiting *Plasmodium* cytochrome bc1: a complex issue. *Curr. Opin. Chem. Biol*, **14**: 440–446.
- Basso W, Lesser M, Grimm F, Hilbe M, Sydler T, Trösch L, Ochs H, Braun U, Deplazes P (2013) Bovine besnoitiosis in Switzerland: Imported cases and local transmission. *Vet. Parasitol*, **198**: 265–273.
- Basso W, Schares G, Gollnick NS, Rütten M, Deplazes P (2011) Exploring the life cycle of *Besnoitia besnoiti*—Experimental infection of putative definitive and intermediate host species. *Vet. Parasitol*, **178**: 223–234.

- Baumann M (2016) CRISPR/Cas9 genome editing – new and old ethical issues arising from a revolutionary technology. *NanoEthics*, **10**: 139–159.
- Belen Cassera M., Zhang, Y, Hazleton K, Schramm V (2011) Purine and Pyrimidine Pathways as Targets in *Plasmodium falciparum*. *Curr. Top. Med. Chem*, **11**: 2103–2115.
- Biagini GA, Fisher N, Shone AE, Mubaraki MA, Srivastava A, Hill A, Antoine T, Warman AJ, Davies J, Pidathala C, Amewu RK, Leung SC, Sharma R, Gibbons P, Hong DW, Pacorel B, Lawrenson AS, Charoensutthivarakul S, Taylor L, Berger O, Mbekeani A, Stocks PA, Nixon GL, Chadwick J, Hemingway J, Delves MJ, Sinden RE, Zeeman AM, Kocken CHM, Berry NG, O’Neill PM, Ward SA (2012) Generation of quinolone antimalarials targeting the *Plasmodium falciparum* mitochondrial respiratory chain for the treatment and prophylaxis of malaria. *Proc. Natl. Acad. Sci*, **109**: 8298–8303.
- Bjerkås I, Mohn SF, Presthus J (1984) Unidentified cyst-forming Sporozoon causing encephalomyelitis and myositis in dogs. *Z. Fur Parasitenkd. Parasitol. Res*, **70**: 271–274.
- Björkman C, McAllister MM, Frössling J, Näslund K, Leung F, Ugglå A (2003) Application of the *Neospora caninum* IgG Avidity ELISA in Assessment of Chronic Reproductive Losses after an Outbreak of Neosporosis in a Herd of Beef Cattle. *J. Vet. Diagn. Invest*, **15**: 3–7.
- Bustin SA, Benes V, Garson JA, Hellemans J, Huggett J, Kubista M, Mueller R, Nolan T, Pfaffl MW, Shipley GL, Vandesompele J, Wittwer CT (2009) The MIQE Guidelines: Minimum Information for Publication of Quantitative Real-Time PCR Experiments. *Clin. Chem*, **55**: 611–622.
- Buxton D, McAllister MM, Dubey JP (2002) The comparative pathogenesis of neosporosis. *Trends Parasitol*, **18**: 546–552.
- Cardoso R, Nolasco S, Gonçalves J, Cortes HC, Leitão A, Soares H (2014) *Besnoitia besnoiti* and *Toxoplasma gondii*: two apicomplexan strategies to manipulate the host cell centrosome and Golgi apparatus. *Parasitology*, **141**: 1436–1454.

- Cervantes-Valencia ME, Hermosilla C, Alcalá-Canto Y, Tapia G, Taubert A, Silva LMR (2019) Antiparasitic Efficacy of Curcumin Against *Besnoitia besnoiti* Tachyzoites in vitro. Doi:10.3389/fvets.2018.00333
- Cortes H, Leitão A, Gottstein B, Hemphill A, (2014) A review on bovine besnoitiosis: a disease with economic impact in herd health management, caused by *Besnoitia besnoiti* (Franco and Borges,). Parasitology, **141**: 1406–1417.
- Cortes H, Leitao A, Vidal R, Vila-Vicosa MJ, Ferreira ML, Caeiro V, Hjerpe CA (2005) Besnoitiosis in bulls in Portugal. Vet. Rec, **157**: 262–264.
- Cortes HCE, Mueller N, Esposito M, Leitão A, Naguleswaran A, Hemphill A (2007) In vitro efficacy of nitro- and bromo-thiazolyl-salicylamide compounds (thiazolides) against *Besnoitia besnoiti* infection in Vero cells. Parasitology, **134**: 975.
- Cribbs AP, Perera SMW (2017) Science and Bioethics of CRISPR-Cas9 Gene Editing: An Analysis Towards Separating Facts and Fiction. The Yale journal of biology and medicine, **90**:625-634.
- Crofts AR (2004) The Cytochrome *bc*₁ Complex: Function in the Context of Structure. Annu. Rev. Physiol. 66: 689–733.
- Ding Y, Li H, Chen LL, Xie K, (2016) Recent Advances in Genome Editing Using CRISPR/Cas9. Front. Plant Sci. 7. Doi:10.3389/fpls.2016.00703
- Doggett JS, Nilsen A, Forquer I, Wegmann KW, Jones-Brando L, Yolken RH, Bordon C, Charman SA, Katneni K, Schultz T, Burrows JN, Hinrichs DJ, Meunier B, Carruthers VB, Riscoe MK (2012) Endochin-like quinolones are highly efficacious against acute and latent experimental toxoplasmosis. Proc. Natl. Acad. Sci, **109**: 15936–15941.
- Dubey JP (2005) Neosporosis in cattle. Vet. Clin. North Am. Food Anim. Pract, **21**: 473–483.
- Dubey JP, Barr BC, Barta JR, Bjerckås I, Björkman C, Blagburn BL, Bowman DD, Buxton D, Ellis JT, Gottstein B, Hemphill A, Hill DE, Howe DK, Jenkins MC, Kobayashi Y, Koudela B, Marsh AE, Mattsson JG, McAllister MM, Modrý D, Omata Y, Sibley LD, Speer CA, Trees AJ, Uggla A, Upton SJ, Williams DJL, Lindsay DS (2002) Redescription of *Neospora caninum* and its differentiation from related coccidia. Int. J. Parasitol, **32**: 929–946.

- Dubey JP, Buxton D, Wouda W (2006) Pathogenesis of Bovine Neosporosis. *J. Comp. Pathol.*, **134**: 267–289.
- Dubey JP, Carpenter JL, Speer CA, Topper MJ, Uggla A (1988) Newly recognized fatal protozoan disease of dogs. *J. Am. Vet. Med. Assoc.*, **192**: 1269–1285.
- Dubey JP, Schares G, Ortega-Mora LM (2007) Epidemiology and Control of Neosporosis and *Neospora caninum*. *Clin. Microbiol. Rev.*, **20**: 323–367.
- Duffy S, Avery VM (2017) *Plasmodium falciparum* in vitro continuous culture conditions: A comparison of parasite susceptibility and tolerance to anti-malarial drugs throughout the asexual intra-erythrocytic life cycle. *Int. J. Parasitol. Drugs Drug Resist.*, **7**: 295–302.
- Dzierszinski F, Mortuaire M, Cesbron-Delauw MF, Tomavo S (2002) Targeted disruption of the glycosylphosphatidylinositol-anchored surface antigen SAG3 gene in *Toxoplasma gondii* decreases host cell adhesion and drastically reduces virulence in mice: *Toxoplasma gondii* SAG3 gene mutants. *Mol. Microbiol.*, **37**: 574–582.
- Eberhard N, Balmer V, Müller J, Müller N, Winter R, Pou S, Nilsen A, Riscoe M, Francisco S, Leitao A, Doggett JS, Hemphill A (2020) Activities of Endochin-Like Quinolones Against in vitro Cultured *Besnoitia besnoiti* Tachyzoites. *Front. Vet. Sci.*, **7**: 96.
- Ellis J, Luton K, Baverstock PR, Brindley PJ, Nimmo KA, Johnson AM (1994) The phylogeny of *Neospora caninum*. Doi: 10.1016/0166-6851(94)00033-6
- Elsheikha M, Mansfield S (2004) Determination of the activity of sulfadiazine against *Besnoitia darlingi* tachyzoites in cultured cells. *Parasitol. Res.* 93.
- Frey CF, Regidor-Cerrillo J, Marreros N, García-Lunar P, Gutiérrez-Expósito D, Schares G, Dubey JP, Gentile A, Jacquiet P, Shkap V, Cortes H, Ortega-Mora LM, Álvarez-García G (2016) *Besnoitia besnoiti* lytic cycle in vitro and differences in invasion and intracellular proliferation among isolates. Doi:10.1186/s13071-016-1405-9
- Gordon JW, Scangos GA, Plotkin DJ, Barbosa JA, Ruddle FH (1980) Genetic transformation of mouse embryos by microinjection of purified DNA. *Proc. Natl. Acad. Sci.*, **77**: 7380–7384.
- Gupta D, Bhattacharjee O, Mandal D, Sen MK, Dey D, Dasgupta A, Kazi TA, Gupta R, Sinharoy S, Acharya K, Chattopadhyay D, Ravichandiran V, Roy S, Ghosh D (2019)

CRISPR-Cas9 system: A new-fangled dawn in gene editing.
Doi:10.1016/j.lfs.2019.116636

- Gutiérrez-Expósito D, Ferre I, Ortega-Mora LM, Álvarez-García G (2017) Advances in the diagnosis of bovine besnoitiosis: current options and applications for control. *Int. J. Parasitol*, **47**: 737–751.
- Harris KM, Perry E, Bourne J, Feinberg M, Ostroff L, Hurlburt J (2006) Uniform Serial Sectioning for Transmission Electron Microscopy. *J. Neurosci.* 26, 12101–12103.
- Hemphill A, Aguado-Martínez A, Müller J (2016) Approaches for the vaccination and treatment of *Neospora caninum* infections in mice and ruminant models. *Parasitology*, **143**: 245–259.
- Hemphill A, Leitão A, Ortega-Mora LM, Cooke BM (2017) ApiCOWplexa 2017 - 4th International Meeting on Apicomplexan Parasites in Farm Animals. *Int. J. Parasitol*, **47**: 697–699.
- Jiménez-Meléndez A, Ojo KK, Wallace AM, Smith TR, Hemphill A, Balmer V, Regidor-Cerrillo J, Ortega-Mora LM, Hehl AB, Fan E, Maly DJ, Van Voorhis WC, Álvarez-García G (2017) *In vitro* efficacy of bumped kinase inhibitors against *Besnoitia besnoiti* tachyzoites. *Int. J. Parasitol*, **47**: 811–821.
- Jiménez-Meléndez A, Rico-San Román, L, Hemphill A, Balmer V, Ortega-Mora LM, Álvarez-García G (2018) Repurposing of commercially available anti-coccidials identifies diclazuril and decoquinate as potential therapeutic candidates against *Besnoitia besnoiti* infection. *Vet. Parasitol*, **261**: 77–85.
- Jinek M, Chylinski K, Fonfara I, Hauer M, Doudna JA, Charpentier E (2012) A Programmable Dual-RNA-Guided DNA Endonuclease in Adaptive Bacterial Immunity. *Science*, **337**: 816–821.
- Kaminsky R, Brun R (1993) *In vitro* assays to determine drug sensitivities of African trypanosomes: a review. *Acta Trop*, **54**: 279–289.
- Kumar P, Nagarajan A, Uchil PD (2019) Electroporation. Doi:10.1101/pdb.top096271
- Lawres LA, Garg A, Kumar V, Bruzual I, Forquer IP, Renard I, Virji AZ, Boulard P, Rodriguez EX, Allen AJ, Pou S, Wegmann KW, Winter RW, Nilsen A, Mao J, Preston DA, Belperron AA, Bockenstedt LK, Hinrichs DJ, Riscoe MK, Doggett JS,

- Ben Mamoun C (2016) Radical cure of experimental babesiosis in immunodeficient mice using a combination of an endochin-like quinolone and atovaquone. *J. Exp. Med.* **213**: 1307–1318.
- Liénard E, Pop L, Prevot F, Grisez C, Mallet V, Raymond-Letron I, Bouhsira É, Franc M, Jacquet P (2015) Experimental infections of rabbits with proliferative and latent stages of *Besnoitia besnoiti*. *Parasitol. Res.* **114**: 3815–3826.
- Loussert C, Forestier CL, Humbel BM (2012) Correlative Light and Electron Microscopy in Parasite Research, in: *Methods in Cell Biology*, Elsevier, pp. 59–73.
- McConnell EV, Bruzual I, Pou S, Winter R, Dodean RA, Smilkstein MJ, Krollenbrock A, Nilsen A, Zakharov LN, Riscoe MK, Doggett JS (2018) Targeted Structure–Activity Analysis of Endochin-like Quinolones Reveals Potent Qi and Qo Site Inhibitors of *Toxoplasma gondii* and *Plasmodium falciparum* Cytochrome *bc*₁ and Identifies ELQ-400 as a Remarkably Effective Compound against Acute Experimental Toxoplasmosis. *ACS Infect. Dis.* **4**: 1574–1584.
- Miley GP, Pou S, Winter R, Nilsen A, Li Y, Kelly JX, Stickles AM, Mather MW, Forquer IP, Pershing AM, White K, Shackelford D, Saunders J, Chen G, Ting LM, Kim K, Zakharov LN, Donini C, Burrows JN, Vaidya AB, Charman SA, Riscoe MK (2015) ELQ-300 Prodrugs for Enhanced Delivery and Single-Dose Cure of Malaria. *Antimicrob. Agents Chemother.* **59**: 5555–5560.
- Mineo DJR (2006). EM CÃES E LOBOS-GUARÁ: SOROEPIDEMIOLOGIA E IMUNODIAGNÓSTICO. Doctoral Degree in Biological Sciences, Federal University of Uberlândia, Brazil.
- Moine E, Denevault-Sabourin C, Debierre-Grockiego F, Silpa L, Gorgette O, Barale JC, Jacquet P, Brossier F, Gueiffier A, Dimier-Poisson I, Enguehard-Gueiffier C (2015) A small-molecule cell-based screen led to the identification of biphenylimidazoazines with highly potent and broad-spectrum anti-apicomplexan activity. *Eur. J. Med. Chem.* **89**: 386–400.
- Monney T, Hemphill A (2014) Vaccines against neosporosis: What can we learn from the past studies? *Exp. Parasitol.* **140**: 52–70.

- Moon SB, Kim DY, Ko J-H, Kim Y-S (2019) Recent advances in the CRISPR genome editing tool set. *Exp. Mol. Med*, **51**: 1–11.
- Morrisette NS, Sibley LD (2002) Cytoskeleton of Apicomplexan Parasites. *Microbiol Mol Biol Rev*, **66**: 21–38.
- Müller J, Aguado A, Laleu B, Balmer V, Ritler D, Hemphill A (2017) In vitro screening of the open source Pathogen Box identifies novel compounds with profound activities against *Neospora caninum*. *Int. J. Parasitol*, **47**: 801–809.
- Müller J, Hemphill A (2016) Drug target identification in protozoan parasites. *Expert Opin. Drug Discov*, **11**: 815–824.
- Müller J, Hemphill A (2013) New Approaches for the Identification of Drug Targets in Protozoan Parasites, in: *International Review of Cell and Molecular Biology*, Elsevier, pp. 359–401.
- Müller J, Manser V, Hemphill A (2019) *In vitro* treatment of *Besnoitia besnoiti* with the naphtho-quinone buparvaquone results in marked inhibition of tachyzoite proliferation, mitochondrial alterations and rapid adaptation of tachyzoites to increased drug concentrations. *Parasitology*, **146**: 112–120.
- Nilsen A, LaCrue AN, White KL, Forquer IP, Cross RM, Marfurt J, Mather MW, Delves MJ, Shackelford DM, Saenz FE, Morrissette JM, Steuten J, Mutka T, Li Y, Wirjanata G, Ryan E, Duffy S, Kelly JX, Sebayang BF, Zeeman A-M, Noviyanti R, Sinden RE, Kocken CHM, Price RN, Avery VM, Angulo-Barturen I, Jimenez-Diaz MB, Ferrer S, Herreros E, Sanz LM, Gamo F-J, Bathurst I, Burrows JN, Siegl P, Guy RK, Winter RW, Vaidya AB, Charman SA, Kyle DE, Manetsch R, Riscoe MK (2013) Quinolone-3-Diarylethers: A New Class of Antimalarial Drug. Doi:10.1126/scitranslmed.3005029
- Norlander J, Kempe T, Messing J (1983) Construction of improved M13 vectors using oligodeoxynucleotide-directed mutagenesis. *Gene*, **26**: 101–106.
- Olias P, Schade B, Mehlhorn H (2011) Molecular pathology, taxonomy and epidemiology of *Besnoitia* species (Protozoa: Sarcocystidae). *Infect. Genet. Evol*, **11**: 1564–1576.
- Ortiz D, Forquer I, Boitz J, Soysa R, Elya C, Fulwiler A, Nilsen A, Polley T, Riscoe MK, Ullman B, Landfear SM (2016) Targeting the Cytochrome *bc*₁ Complex of

- Leishmania* Parasites for Discovery of Novel Drugs. Antimicrob. Agents Chemother, **60**: 4972–4982.
- Pereira LM, Baroni L, Yatsuda AP (2014) A transgenic *Neospora caninum* strain based on mutations of the dihydrofolate reductase-thymidylate synthase gene. Exp. Parasitol, **138**: 40–47.
- Pereira LM, Yatsuda AP (2014) The chloramphenicol acetyltransferase vector as a tool for stable tagging of *Neospora caninum*. Mol. Biochem. Parasitol, **196**, 75–81.
- Peters M, Lütkefels E, Heckerroth AR, Schares G (2001) Immunohistochemical and ultrastructural evidence for *Neospora caninum* tissue cysts in skeletal muscles of naturally infected dogs and cattle. Int. J. Parasitol, **31**: 1144–1148.
- Pols JW (1960) STUDIES ON BOVINE BESNOITIOSIS WITH SPECIAL REFERENCE TO THE AETIOLOGY. Journal of Veterinary Research, **28**, 266-334.
- Potter VR (1970) Bioethics, the Science of Survival. Perspect. Biol. Med. **14**: 127–153.
- Reichel MP, Ayanegui-Alcérreca AM, Gondim LFP, Ellis JT (2013) What is the global economic impact of *Neospora caninum* in cattle – The billion dollar question. Int. J. Parasitol, **43**: 133–142.
- Reichel MP, Ellis JT (2009) *Neospora caninum* – How close are we to development of an efficacious vaccine that prevents abortion in cattle? Int. J. Parasitol. **39**, 1173–1187.
- Reichel MP, Ellis JT, Dubey JP (2007) Neosporosis and hammondiosis in dogs. J. Small Anim. Pract, **48**: 308–312.
- Reynolds ES (1963) THE USE OF LEAD CITRATE AT HIGH pH AS AN ELECTRON-OPAQUE STAIN IN ELECTRON MICROSCOPY. J. Cell Biol. **17**: 208–212.
- Salzer W, Timmler H, Andersag H (1948) Über einen neuen, gegen Vogel malaria wirksamen Verbindungstypus. Chem. Ber, **81**: 12–19.
- Santos JM, Lebrun M, Daher W, Soldati-Favre D, Dubremetz J-F (2009) Apicomplexan cytoskeleton and motors: key regulators in morphogenesis, cell division, transport and motility. Int. J. Parasitol, **39**: 153–62.
- Sashital DG (2018) Pathogen detection in the CRISPR–Cas era. Doi:10.1186/s13073-018-0543-4

- Shen B, Brown K, Long S, Sibley LD (2017) Development of CRISPR/Cas9 for Efficient Genome Editing in *Toxoplasma gondii*, in: Reeves, A. (Ed.), In Vitro Mutagenesis. Springer New York, New York, NY, pp. 79–103.
- Shkap V, Pipano E, Ungar-Waron H (1987) Rev Elev Med Vet Pays Trop. 40(3):259-64.
- Sidik SM, Huet D, Ganesan SM, Huynh M-H, Wang T, Nasamu AS, Thiru P, Saeij JPJ, Carruthers VB, Niles, JC, Lourido S (2016) A Genome-wide CRISPR Screen in *Toxoplasma* Identifies Essential Apicomplexan Genes. Cell **166**: 1423-1435.
- Smilkstein MJ, Pou S, Krollenbrock A, Bleyle LA, Dodean RA, Frueh L, Hinrichs DJ, Li Y, Martinson, T, Munar, MY, Winter RW, Bruzual I, Whiteside S, Nilsen A, Koop DR, Kelly JX, Kappe SHI, Wilder BK, Riscoe MK (2019) ELQ-331 as a prototype for extremely durable chemoprotection against malaria. Doi:10.1186/s12936-019-2921-9
- Stickles AM, de Almeida MJ, Morrisey JM, Sheridan KA, Forquer IP, Nilsen A, Winter RW, Burrows JN, Fidock DA, Vaidya AB, Riscoe MK (2015) Subtle Changes in Endochin-Like Quinolone Structure Alter the Site of Inhibition within the Cytochrome *bc*₁ Complex of *Plasmodium falciparum*. Antimicrob. Agents Chemother, **59**: 1977–1982.
- Suarez CE, Bishop RP, Alzan HF, Poole WA, Cooke BM (2017) Advances in the application of genetic manipulation methods to apicomplexan parasites. Int. J. Parasitol, **47**: 701–710.
- Sugi T, Tu V, Ma Y, Tomita T, Weiss LM (2017) *Toxoplasma gondii* Requires Glycogen Phosphorylase for Balancing Amylopectin Storage and for Efficient Production of Brain Cysts. Doi:10.1128/mBio.01289-17
- Thurmond MC, Hietala SK, Blanchard PC (1999) Predictive Values of Fetal Histopathology and Immunoperoxidase Staining in Diagnosing Bovine Abortion Caused by *Neospora caninum* in a Dairy Herd. J. Vet. Diagn. Invest, **11**: 90–94.
- Tizro P, Choi C, Khanlou N (2019) Sample Preparation for Transmission Electron Microscopy, in: Yong, W.H. (Ed.), Biobanking. Springer New York, New York, NY, pp. 417–424.

- Wang Y, Yin H (2014) Research progress on surface antigen 1 (SAG1) of *Toxoplasma gondii*. *Parasit. Vectors*, **7**: 180.
- Weston JF, Heuer C, Williamson NB (2012) Efficacy of a *Neospora caninum* killed tachyzoite vaccine in preventing abortion and vertical transmission in dairy cattle. *Prev. Vet. Med*, **103**: 136–144.
- Wetzel DM, Schmidt J, Kuhlenschmidt MS, Dubey JP, Sibley LD (2005) Gliding Motility Leads to Active Cellular Invasion by *Cryptosporidium parvum* Sporozoites. *Infect. Immun*, **73**: 5379–5387.
- Winter R, Kelly JX, Smilkstein MJ, Hinrichs D, Koop DR, Riscoe MK (2011) Optimization of endochin-like quinolones for antimalarial activity. *Exp. Parasitol.* 127: 545–551.
- Wright AV, Nuñez JK, Doudna JA (2016) Biology and Applications of CRISPR Systems: Harnessing Nature’s Toolbox for Genome Engineering. *Cell*, **164**: 29–44.
- Zhang G, Huang X, Boldbaatar D, Battur B, Battsetseg B, Zhang H, Yu L, Li Y, Luo Y, Cao S, Goo Y-K, Yamagishi J, Zhou J, Zhang S, Suzuki H, Igarashi I, Mikami T, Nishikawa Y, Xuan X (2010) Construction of *Neospora caninum* stably expressing TgSAG1 and evaluation of its protective effects against *Toxoplasma gondii* infection in mice. *Vaccine*, **28**: 7243–7247.

Appendix

Materials

Unless mentioned differently, chemicals were purchased from Sigma (St. Louis, MO, USA).

1. Materials for IC₅₀ Assay

Bb Lisbon / Bb Lisbon isolate 14	provided by Alexandre Leitão, Instituto de Investigação Científica Tropical, 1600-189 Lisboa (Portugal)
HFF	Human foreskin fibroblasts Normal, Human, Neonatal, ATCC-PCS-201-010, Lot #61728499
ELQ: 100, 121, 127, 136, 271, 300, 316, 334, 400, 433, 434, 435, 436, 437	Health & Science University Department of Medicine in Oregon US. Stock solutions of 5mM or 10mM in dimethyl sulfoxide (DMSO) at -20°C synthesized as previously described in McConnell et al. 2018
Antibiotic-Antimycotic:	Anti-Anti (100X), REF 15240-062 100 mL, Gibco
Camera of light microscope:	THE IMAGINGSOURCE®, DFK 72AUC02, Serial # 26510283, made in Germany

Cell culture flasks:	Sarstedt AG & Co., D-51588 Nümbrecht (Germany)
Cell scraper:	Disposable cell scraper, Sarstedt AG & Co., D-51588 Nümbrecht (Germany)
Centrifuge for conical tubes and plates:	Rotanta 460R, Hettich Zentrifugen (Germany)
Centrifuge for micro tubes:	Centrifuge 5415 R, Vaudaux-Eppendorf, 4124 Schönenbuch (Switzerland)
DMEM for HFF:	High glucose (4.5g/L), HEPES, GlutaMAX™, Phenol Red, without Sodium Pyruvate ThermoFisher (USA) Added 50ml 10% Fetal Calf Serum (FCS), AB/AM
DMSO:	Dimethyl sulfoxide, D4540-100ml, #BCBW5664, ≥99.5% (GC), plant cell culture tested, Sigma-Aldrich (Merck)
Eppendorf Tubes:	Eppendorf 1,5 ml, SafeSeal, 72,706, Sarstedt AG & Co. KG, D-51588 Nümbrecht (Germany)
Falcon Tubes:	Sarstedt AG & Co., D-51588 Nümbrecht (Germany)
Fetal Calf Serum (FCS):	FBS superior standardized by heat-inactivation (30 min at 56°C), tested for virus

and mycoplasma, tested for endotoxin
Biochrom GmbH, 12247 Berlin (Germany)

Flow Bench:	Safe 2020, Thermo Fisher Scientific (USA)
Incubator:	CO ₂ -Incubator C150 (E2), BINDER GmbH, Tuttlingen (Germany)
Light microscope:	Nikon eclipse TS100
Needle:	25G 5/8" 0.5x16mm REF 300600, BD Microlance
Neubauer Counting Chamber:	Zählkammer nach NEUBAUER improved "bright-line", ohne Federklemme, 0.1 mm, LOT: 04 S, BRAND GmbH + CO KG (Germany)
Pipetman:	Pipetman Classic, 1-10 uL, 2-20 uL, 20-200 uL and 100-1000 uL, Gilson (CH)
Pipette filter tips:	Sarstedt AG & CO., D-51588 Nümbrecht (Germany)
Serological pipettes:	aspiration, 2ml, 5ml, 10ml, 25ml, Sarstedt AG & CO., D-51588 Nümbrecht (Germany)
Syringes:	1 ml Norm-Ject® Tuberkulin, nonpyrogenic/ nontoxic, HENKE SASS WOLF, D-78532 Tuttlingen (Germany)

Trypsin-EDTA:	Gibco™ 100 ml Trypsin 0.05% EDTA 0.02% in PBS, w/o Ca ²⁺ and Mg ²⁺ , without Phenol red
Well plates:	Cell culture plate, Greiner Bio-One, 4550 Kremsmünster (Austria)
PBS	1x stock prepared in the lab
Ultrasonic bath	CPX2800H-E, Branson Ultrasonics Corporation, Danbury CT06810, USA
DNA RapidLyse Kit:	NucleoSpin® DNA RapidLyse 250 preps, Machinery-Nahel GmbH & Co. KG, 52355 Düren (Germany)
Thermomixer:	Thermomixer compact, Vaudaux-ependorf, 4124 Schönenbuch (CH)
Capillaries (PCR):	Light cycler capillaries (20 uL), 04, 929, 292, 001, 96 capillaries, ROCHE, Indianapolis, IN, US
Light cycler:	LightCycler™ Instrument, Roche Diagnostic, Basel, (Switzerland)
Primer forward:	SIGMA 1201, SY120525003-002, P-BES-PF1 5'-TGACATTTAATAACAATCAACCCTT 100uM, 16.5 OD, MW = 7572 g/mol

8012517129-000050

HA03666082-001

Primer reverse :

SIGMA 1201, SY120525003-003, P-BES-PR1

5'-GTTTGTATTAACCAATCCGTGA

100uM, 16.6 OD, MW = 7057 g/mol

8012517129-000060

HA03666083-001

RNA free water

Spin down centrifuge

LC Carousel Centrifuge, Roche, Serial-No. 40112073, Roche Diagnostics (Schweiz) AG

2. Materials for Long Treatment Assay

Bb Lisbon / Bb Lisbon isolate 14	provided by Alexandre Leitão, Instituto de Investigação Científica Tropical, 1600-189 Lisboa (Portugal)
HFF	Human foreskin fibroblasts Normal, Human, Neonatal, ATCC-PCS-201-010, Lot #61728499
ELQ-121	Health & Science University Department of Medicine in Oregon US. Stock solutions of 5mM or 10mM in dimethyl sulfoxide (DMSO) at -20°C synthesized as previously described in McConnell et al. 2018
Antibiotic-Antimycotic:	Anti-Anti (100X), REF 15240-062 100 mL, Gibco
Camera of light microscope:	THE IMAGINGSOURCE®, DFK 72AUC02, Serial # 26510283, made in Germany
Cell culture flasks:	Sarstedt AG & Co., D-51588 Nümbrecht (Germany)
Cell scraper:	Disposable cell scraper, Sarstedt AG & Co., D-51588 Nümbrecht (Germany)
DMEM for HFF:	High glucose (4.5g/L), HEPES, GlutaMAX™, Phenol Red, without Sodium Pyruvate ThermoFisher (USA)

	Added 50ml 10% Fetal Calf Serum (FCS), AB/AM
DMSO:	Dimethyl sulfoxide, D4540-100ml, #BCBW5664, $\geq 99.5\%$ (GC), plant cell culture tested, Sigma-Aldrich (Merck)
Eppendorf Tubes:	Eppendorf 1,5 ml, SafeSeal, 72,706, Sarstedt AG & Co. KG, D-51588 Nümbrecht (Germany)
Falcon Tubes:	Sarstedt AG & Co., D-51588 Nümbrecht (Germany)
Fetal Calf Serum (FCS):	FBS superior standardized by heat-inactivation (30 min at 56°C), tested for virus and mycoplasma, tested for endotoxin Biochrom GmbH, 12247 Berlin (Germany)
Flow Bench:	Safe 2020, Thermo Fisher Scientific (USA)
Incubator:	CO ₂ -Incubator C150 (E2), BINDER GmbH, Tuttlingen (Germany)
Light microscope:	Nikon eclipse TS100
Needle:	25G 5/8" 0.5x16mm REF 300600, BD Microlance
Neubauer Counting Chamber:	Zählkammer nach NEUBAUER improved "bright-line", ohne Federklemme, 0.1 mm, LOT: 04 S, BRAND GmbH + CO KG (Germany)

Pipetman:	Pipetman Classic, 1-10 uL, 2-20 uL, 20-200 uL and 100-1000 uL, Gilson (CH)
Pipette filter tips:	Sarstedt AG & CO., D-51588 Nümbrecht (Germany)
Serological pipettes:	aspiration, 2ml, 5ml, 10ml, 25ml, Sarstedt AG & CO., D-51588 Nümbrecht (Germany)
Syringes:	1 ml Norm-Ject® Tuberkulin, nonpyrogenic/nontoxic, HENKE SASS WOLF, D-78532 Tuttlingen (Germany)
Trypsin-EDTA:	Gibco™ 100 ml Trypsin 0.05% EDTA 0.02% in PBS, w/o Ca ²⁺ and Mg ²⁺ , without Phenol red
HBSS	Hank's Balanced Salt Solution modified with sodium bicarbonate, without phenol red, liquid, sterile-filtered, suitable for cell culture, H8261-500 ml, LOT # RNBF9191, SIGMA-Aldrich (Merck)
Ultrasonic bath	CPX2800H-E, Branson Ultrasonics Corporation, Danbury CT06810, USA

3. Materials for Electron Microscopy Assay

Glutaraldehyde:	Glutaraldehyde solution, approx. 50% in water, Fluka Chemie AG, 947 Buchs (Switzerland) 49629
Na-Cacodylate:	Dimethylarinacid Sodiamsalt Trihydrat, Merck KGaA, 64271 Darmstadt (Germany), 8.20670.100
Osmium tetroxide solution:	SIGMA, Osmium tetroxide solution for electron microscopy, 4% in H ₂ O, 75632, Lot #BCBV6384
2% Glutaraldehyde in Na-Cacodylate buffer ¹ :	Glutaraldehyde stock = 50%, to have 2% diluted 1:25 in 0.1 M Na-Cacodylate buffer
Na-Cacodylate buffer (0.1 M) ² :	diluted 0.2 M 1:2 with distilled, deionized water
2% Osmium tetroxide (OsO ₄) ³ :	stock solution = 4%, to have 2% diluted 1:2 in 0.2 M Na-Cacodylate buffer
Na-Cacodylate buffer (0.2 M, pH 7.3) ⁴ :	Sodium Cacodylate 21.4 g; Distilled, deionized water: filled up to 500 ml. Adjusted pH to 7.3 % with 1N HCL
Ethanol:	Ethanol absolute, Merck KGaA, 64271 Darmstadt, Germany)
Cell scraper:	Disposable cell scraper, Sarstedt AG & Co., D-51588 Nümbrecht (Germany)
50 ml Falcon Tubes:	Sarstedt AG & Co., D-51588 Nümbrecht (Germany)

Eppendorf Tubes:	Eppendorf 1,5 ml, SafeSeal, 72,706, Sarstedt AG & Co. KG, D-51588 Nürmbrecht (Germany)
Centrifuge for conical tubes and plates:	Rotanta 460R, Hettich Zentrifugen (Germany)
Centrifuge for micro tubes:	Centrifuge 5415 R, Vaudaux-Eppendorf, 4124 Schönenbuch (Switzerland)
Incubator:	CO2-Incubator C150 (E2), BINDER GmbH, Tuttlingen (Germany)
Ultrasonic bath:	CPX2800H-E, Branson Ultrasonics Corporation, Danbury CT06810, USA
Chloroform:	EMSURE, Index-No. 602-006-00-4, Merck KGaA, 64271 Darmstadt (Germany)
Grids:	Athene Nickel 300/3.05 nm, Plano GmbH, 35578 Wetzlar (Germany)
Lead citrate:	Electron Microscopy Sciences, Hatfield PA, USA Catalog #22410
Resin (EPON):	Epon 812 75ml, DDSA 40ml, MNA 40ml, BDMA 3ml
Sodium hydroxide:	≥98% pellets (anhydrous), lot # SZBF3240V, S5881-1KG, 011-022-00-6, Sigma-Aldrich (Merck)
TEM:	FEI Tecnai Spirit BioTwin Camera: Olympus-SIS Veleta CCD Camera, Objectives: BioTWIN lens Cathode: Tungsten / LaB6
Ultra-microtome:	Reichert-Jung, Ultracut E
UranylLess Spray:	Electron Microscopy Sciences, Hatfield PA, USA Catalog #22409

4. Materials for *sag1* knock-out using CRISPR/Cas9 Assay

Plasmid	Provided by Joachim Messing (Addgene plasmid # 50005 ; http://n2t.net/addgene:50005 ; RRID:Addgene_50005)
gRNA	Sequence provided by PD Dr. Philipp Olias, Animal Pathology, University of Bern
<i>dhfr</i>	Sequence provided by PD Dr. Philipp Olias, Animal Pathology, University of Bern
<i>Neospora caninum</i> strain	<i>N. caninum</i> Nc1 strain. Provided by J.P. Dubey, USDA Beltsville, USA
HFF	Human foreskin fibroblasts Normal, Human, Neonatal, ATCC-PCS-201-010, Lot #61728499
Incubator:	CO ₂ -Incubator C150 (E2), BINDER GmbH, Tuttlingen (Germany)
Antibiotic-Antimycotic:	Anti-Anti (100X), REF 15240-062 100 mL, Gibco
Camera of light microscope:	THE IMAGINGSOURCE®, DFK 72AUC02, Serial # 26510283, made in Germany
Cell culture flasks:	Sarstedt AG & Co., D-51588 Nümbrecht (Germany)
Cell scraper:	Disposable cell scraper, Sarstedt AG & Co., D-51588 Nümbrecht (Germany)

Centrifuge for conical tubes and plates: Rotanta 460R, Hettich Zentrifugen (Germany)

Centrifuge for micro tubes: Centrifuge 5415 R, Vaudaux-Eppendorf, 4124 Schönenbuch (Switzerland)

DMEM for HFF: High glucose (4.5g/L), HEPES, GlutaMAX™, Phenol Red, without Sodium Pyruvate ThermoFisher (USA)
Added 50ml 10% Fetal Calf Serum (FCS), AB/AM

DMSO: Dimethyl sulfoxide, D4540-100ml, #BCBW5664, ≥99.5% (GC), plant cell culture tested, Sigma-Aldrich (Merck)

HBSS Hank's Balanced Salt Solution modified with sodium bicarbonate, without phenol red, liquid, sterile-filtered, suitable for cell culture, H8261-500 ml, LOT # RNBF9191, SIGMA-Aldrich (Merck)

Eppendorf Tubes: Eppendorf 1,5 ml, SafeSeal, 72,706, Sarstedt AG & Co. KG, D-51588 Nümbrecht (Germany)

Falcon Tubes: Sarstedt AG & Co., D-51588 Nümbrecht (Germany)

Flow Bench: Safe 2020, Thermo Fisher Scientific (USA)

Light microscope: Nikon eclipse TS100

Needle:	25G 5/8" 0.5x16mm REF 300600, BD Microlance
Neubauer Counting Chamber:	Zählkammer nach NEUBAUER improved "bright-line", ohne Federklemme, 0.1 mm, LOT: 04 S, BRAND GmbH + CO KG (Germany)
Pipetman:	Pipetman Classic, 1-10 uL, 2-20 uL, 20-200 uL and 100-1000 uL, Gilson (CH)
Pipette filter tips:	Sarstedt AG & CO., D-51588 Nümbrecht (Germany)
Serological pipettes:	Aspiration, 2ml, 5ml, 10ml, 25ml, Sarstedt AG & CO., D-51588 Nümbrecht (Germany)
Syringes:	1 ml Norm-Ject® Tuberkulin, nonpyrogenic/ nontoxic, HENKE SASS WOLF, D-78532 Tuttlingen (Germany)
Trypsin-EDTA:	Gibco™ 100 ml Trypsin 0.05% EDTA 0.02% in PBS, w/o Ca ²⁺ and Mg ²⁺ , without Phenol red
Well plates:	Cell culture plate, Greiner Bio-One, 4550 Kremsmünster (Austria)
Electroporation machine	Gene Pulser Xcell, Bio Rad (Switzerland)
Electroporation cuvettes	Bio Rad (Switzerland)

Pyrimethamine	Sigma Aldrich (Switzerland) BP1227
Agarose for electrophoresis	Merck (Switzerland) A9539
Buffer	Merck Calbiochem (Switzerland) CAS 77-86-1
DNA RapidLyse Kit:	NucleoSpin® DNA RapidLyse 250 preps, Machinery-Nahel GmbH & Co. KG, 52355 Düren (Germany)
Thermomixer:	Thermomixer compact, Vaudaux-eppendorf, 4124 Schönenbuch (CH)
Capillaries (PCR):	Light cycler capillaries (20 uL), 04, 929, 292, 001, 96 capillaries, ROCHE, Indianapolis, IN, US
Light cycler:	LightCycler™ Instrument, Roche Diagnostic, Basel, (Switzerland)
Primer forward:	Microsynth Switzerland
Primer reverse :	Microsynth Switzerland
Ladder:	Sigma, Switzerland, D5042
Spin down centrifuge	LC Carousel Centrifuge, Roche, Serial-No. 40112073, Roche Diagnostics (Schweiz) AG
UV emitter	Lubio-Science, Switzerland